2014

Confinement mechanism of FRP-confined concrete columns

Thong Minh Pham
University of Wollongong

UNIVERSITY OF WOLLONGONG

Confinement Mechanism of FRP-Confined Concrete Columns

By

Thong Minh Pham

BEng

This thesis is submitted in fulfilment of the award of the degree of

Doctor of Philosophy

(Civil Engineering)

School of Civil, Mining and Environmental Engineering

University of Wollongong, Australia

August 2014

DECLARATION

I, Thong Minh Pham, hereby declare that all materials in this thesis, submitted in fulfilment of the requirements of the award of Doctor of Philosophy, in the School of Civil, Mining and Environmental Engineering, University of Wollongong, is wholly my own work unless otherwise referenced or acknowledged. This document has not been submitted for qualification at any other academic institution.

(Signed)

Thong Minh Pham (Student name)

ACKNOWLEDGEMENTS

First and most importantly I would like to give my heartfelt thanks to my supervisor Associate Professor Muhammad N.S. Hadi for his generous support and enlightening guidance throughout my PhD study.

I am grateful to The Vietnamese Government and The University of Wollongong for providing me the full PhD scholarship.

It would have been much more difficult to complete the work without the help and support of all technicians of the High Bay Lab, especially, Messrs Alan Grant, Fernando Escribano, Cameron Neilson, Ritchie McLean and Colin Devenish. I also acknowledge Mr Eric Lume for his advice on casting high strength concrete.

My sincere thanks also go to my friends in the School of Civil, Mining and Environmental Engineering, especially, Drs Ida Bagus Rai Widiarsa, Pezhman Sharafi, Messrs Xu Lei, Tung Minh Tran, Le Viet Doan, and Tan Duy Le. The support from Dr Veysel Yazici for my research proposal is appreciated. I would like express my thanks to Dr Mehmet Eren Uz for the coffees that we had together. He had shown me much useful advice at the beginning of my PhD. I am also grateful to my Vietnamese friends, who supported me at the beginning time in Australia, Dr Thanh Duc Nguyen, Dr Trong Vo Nguyen, Mrs Ha Thi Viet Vu, and Dr Huong Thu Pham.

Lastly, I would like to express my profound gratitude to my parents Pham Chinh and Do Thi Phan, to my sisters and brothers-in-law, to whom this thesis is dedicated. My heartfelt thanks also go to my wife Mrs Huong Vu Quynh Nguyen (Hana). Without her everlasting love, support and encouragement I would never have finished my PhD.

LIST OF PUBLICATIONS

Technical papers are written based on the results of this thesis

Journal papers

[1] **Pham, T. M**. & Hadi, M. N. (2014). “Confinement model for FRP-confined normal- and high-strength concrete circular columns.” *Construction and Building Materials*. Accepted on 23 June 2014. Doi 10.1016/j.conbuildmat.2014.06.036.

[2] **Pham, T. M**. & Hadi, M. N. (2014). “Predicting Stress and Strain of FRP Confined Rectangular/Square Columns Using Artificial Neural Networks.” *Journal of Composites for Construction*. DOI 10.1061/(ASCE)CC.1943-5614.0000477.

[3] **Pham, T.M.,** & Hadi, M.N.S. (2014). "Stress Prediction Model for FRP Confined Rectangular Concrete Columns with Rounded Corners." *Journal of Composites for Construction***,** 18(1), 04013019.

[4] **Pham, T. M**. & Hadi, M. N. (2013). “Strain estimation of CFRP confined concrete columns using energy approach.” *Journal of Composites for Construction*, 17(6), 04013001.

[5] **Pham, T. M**., Doan, L. V., & Hadi, M. N. (2013). “Strengthening square reinforced concrete columns by circularization and FRP confinement.” *Construction and Building Materials*, 49(0), 490-499.

[6] Hadi, M. N., **Pham, T. M**. & Lei, X. (2013). “A new method of strengthening reinforced concrete square columns by circularizing and wrapping with FRP or steel straps.” *Journal of Composites for Construction*, 17(2), 229-238.

[7] **Pham, T.M.**, Hadi, M.N.S., & Tran, T.M. (2014). "Maximum Usable Strain of FRP-Confined Concrete." *Engineering Structures.* (Under review).

Conference papers

[8] **Pham, T. M.**, Doan, L. V., & Hadi, M. N. S. (2013). Strengthening square reinforced concrete columns by shape modification and CFRP. *The 2013 Structures Congress*. Pittsburgh, PA.

[9] **Pham, T. M.** & Hadi, M. N. S. (2013). Retrofitting square RC columns using FRP and precast concrete segments. *First International Conference on Concrete Sustainability, ICCS13*. Tokyo, Japan.

[10] **Pham, T. M**., Lei, X. & Hadi, M. N. S. (2013). Effect of eccentric load on retrofitted reinforced concrete columns confined with FRP. *22nd Australasian Conference on the Mechanics of Structures and Materials (ACMSM22)* (pp. 139-144). London: Taylor & Francis Group.

[11] **Pham, T. M.,** Doan, L. V. & Hadi, M. N.S. (2013). Behaviour of modified RC columns retrofitted with CFRP. *26th Biennial Conference of the Concrete Institute of Australia*. Gold Coast, Queensland, Australia.

[12] Doan, L. V., Lei, X., **Pham, T. M**. & Hadi, M. N.S. (2013). Confinement effect of FRP and transverse steel on retrofitting square concrete columns. *The 4th Asia pacific Conference on FRP in Structures*. Melbourne, Australia.

[13] Lei, X., **Pham, T. M**. & Hadi, M. N. S. (2012). Comparative behaviour of FRP confined square concrete columns under eccentric loading. *6th International Conference on Bridge Maintenance, Safety and Management, IABMAS 2012* (pp. 1207-1214). The Netherlands: CRC Press/Balkema.

[14] Lei, X., **Pham, T. M**. & Hadi, M. N. S. (2012). Behaviour of CFRP wrapped square RC columns under eccentric loading. *Australasian Structural Engineering Conference* (pp. 1-8). Australia: Engineers Australia.

Technical papers written out of the scope of this thesis

Journal papers

[15] Tran, T. M., Hadi, M. N., & **Pham, T. M**. (2014). “A new empirical model for shear strength of reinforced concrete beam-column connections.” *Magazine of Concrete Research*, 66(10), 514-530.

Others

[16] Lei, X., **Pham, T. M**. & Hadi, M. N. (2012). “Behaviour of CFRP wrapped square RC columns under eccentric loading.” *Concrete in Australia*, 38 (3), 45-50.

ABSTRACT

Strengthening concrete columns by externally wrapping fibre reinforced polymer (FRP) around the perimeter of column sections is rapidly growing. This strengthening technique confines the column cores thus increases their carrying loads and ductility. This thesis is concerned with the confinement mechanism of FRP-confined concrete. Particular attention is given to a new technique for strengthening existing concrete columns.

The confinement mechanism of FRP-confined concrete is comprehensively investigated and analysed, which resulted in confinement models for FRP-confined concrete columns. The confinement model for FRP-confined circular concrete columns covers a wide range of unconfined concrete strengths with higher accuracy than other existing models. The confinement model for FRP-confined rectangular concrete columns takes the stress concentration at the corners of sections into account, which has not been done by previous studies. In addition, this study introduces the use of artificial neural network (ANN) to generate analytical equations for calculating the compressive strength and strain of FRP-confined rectangular concrete columns. These equations significantly increase the accuracy compared to existing models.

Additionally, the progressive failure mechanism of FRP-confined concrete that has not been previously investigated is experimentally studied. Experimental results show that the maximum usable strain of 1% recommended by ACI 440.2R (2008) and Concrete Society (2012) is un-conservative for FRP-confined concrete. A new model is then proposed to calculate the residual strength of a concrete core at a given axial strain.

Finally, a new practical method called circularisation technique is proposed to strengthen existing square reinforced concrete columns. The new technique significantly increases the axial capacity of the existing square columns. Through experimental studies, the proposed technique was verified for not only normal strength concrete but also high strength concrete. Two sets of experimental testing proved the viability of the proposed circularization technique.

TABLE OF CONTENTS

LIST OF FIGURES

Chapter 2

Chapter 3

Compressive Strength Model

Compressive Strain Model

Chapter 4

Chapter 5

Chapter 6

Circularization by Normal Strength Concrete

Circularization by High Strength Concrete

LIST OF TABLES

1 INTRODUCTION

1.1 Preamble

The use of fibre reinforced polymer (FRP) in structural engineering has increased in recent years. FRP could be used for new constructions or retrofitting applications. The well-known advantages of FRP have resulted from a wide range of its applications in structural members. These advantages include high strength-to-weight ratio, excellent corrosion resistance and ease of site handling.

FRP used in structural members usually consists of glass, carbon, or aramid fibre encased in a matrix of epoxy, polyester, or vinyl-ester. FRP has been used in a wide range of applications: structural profiles, internal reinforcing bars, and sheets (Bank 2006). Among these applications, strengthening existing concrete columns by externally wrapping with FRP sheets has been attracted to the research society in the last two decades. This strengthening technique challenges material scientists and structural engineers to study structural behaviours. These challenges comprise understanding and prediction of the confinement mechanism of FRP-confined concrete columns.

Confined concrete is a concrete which has closely-spaced transverse reinforcement which restrains the concrete in directions perpendicular to the applied load. Tri-axial compressive stresses delay expansion and damage propagation in concrete by restricting crack growth and decreasing dilation ratio of concrete. When the applied load approaches the uni-axial strength, the concrete becomes confined and commences effects of the transverse reinforcement which then applies a confining reaction to the concrete. Thus confined concrete damaged by a different mode as compared to unconfined concrete. It is well known that confinement effect increases the strength and ductility of concrete (Hadi 2006a; Hadi 2006b; Hadi 2007a; Hadi 2009). FRP confinement is accomplished by wrapping the fibre sheets mainly transverse to the longitudinal axis of the columns providing passive confinement, which is activated once the concrete core starts expanding as a result of Possion’s effect and internal cracking.

The confinement mechanism of FRP-confined circular concrete columns has been investigated experimentally and theoretically by many studies (Toutanji 1999; Lam and Teng 2003a; Matthys et al. 2006; Teng et al. 2007; Wu and Zhou 2010; Hadi et al. 2013; Pham et al. 2013b; Pham and Hadi 2013c). However, there are only a few studies about FRP-confined high-strength concrete. Meanwhile, the confinement effect of non-circular columns is widely accepted to be less efficient than that of circular columns in which the jackets provide circumferentially uniform confining pressure to the column cores. In rectangular or square columns, the confining stress is transmitted to the concrete at the four corners of the section (Bakis et al. 2002; Csuka and Kollár 2012; Pham and Hadi 2014b). This mechanism results in low efficient confinement effect of FRP-confined rectangular or square concrete columns as compared to circular one. Therefore, this study investigates the confinement mechanism of FRP-confined either circular or non-circular concrete columns. The difference in confinement of these types of columns is stated and analysed. These analyses result in a new circularisation technique proposed to strengthen existing square concrete columns with FRP.

1.2 Motivation and Objectives

The confinement mechanism of FRP-confined circular concrete columns has been extensively discussed in the literature. Analytical studies have been proposed to predict the compressive strength and strain of FRP-confined circular columns (Toutanji 1999; Lam and Teng 2003a; Teng et al. 2007; Youssef et al. 2007; Wu and Zhou 2010). Most of these studies have focussed on FRP-confined normal strength concrete. The confinement effects of FRP on high strength concrete have not been comprehensively investigated (Lim and Ozbakkaloglu 2014). Thus, this study proposes a confinement model for FRP-confined normal- and high-strength concrete.

Bisby et al. (2005) stated that existing models for FRP-confined concrete show poor correlation with experimental results. Bisby et al. (2005) revealed that the mean absolute error of strain estimations ranges from 35% to 250% while the error of strength estimation is less than 20%. Thus, it is necessary to develop strain models for FRP-confined concrete.

In addition, most of the existing models for FRP-confined concrete columns based on the confinement mechanism and calibrating test results to predict the compressive stress and strain (Lam and Teng 2003a; Ilki et al. 2008; Wu and Wang 2009; Wu and Wei 2010; Rousakis et al. 2012a; Yazici and Hadi 2012; Pham and Hadi 2013c; Pham and Hadi 2014b). Models developed by this approach provide a good understanding of stress-strain curve of the confined concrete, but their errors in estimating the compressive strength and strain are still remarkable. Ozbakkaloglu et al. (2013) had reviewed 88 existing FRP confinement models for circular columns. That study showed that the average absolute errors of the above models in estimating stress and strain are greater than 10% and 23%, respectively. Thus, it is necessary for the research community to improve the accuracy in estimating both the compressive stress and strain of FRP-confined concrete. This study introduces the use of artificial neural networks (ANN) to predict the compressive strength and strain of FRP-confined concrete columns.

As mentioned above, the difference in the confinement effects of circular and non-circular columns has required much more studies to provide better understanding about the behaviours of FRP-confined rectangular or square columns. Since most of existing models for rectangular sections are quite similar to circular sections except that a shape factor is introduced to account for the non-uniform confinement, this study proposes a model for FRP-confined rectangular columns by focusing on the stress concentration at the corners of the sections.

Experimental studies have shown that the axial strain of FRP-confined concrete varies in a broad range from 0.5% to 8.6% (Ilki et al. 2008; Lee and Hegemier 2009; Teng et al. 2009). However, these studies did not investigate the integrity of the concrete during testing. No study has investigated the precise nature of the progressive failure mechanisms occurring during experimental tests. In other words, the maximum usable strain of 1% recommended by two guidelines (ACI 440.2R-08 2008; Concrete Society 2012) seems small as compared to the experimental results. Therefore, determining the nature of the progressive failure mechanisms and the maximum usable strain of FRP-confined concrete is essentially necessary. This study

conducted experimental tests to investigate the progressive failure mechanisms of FRP-confined concrete at many stages of testing.

Finally, the confinement mechanism of both circular and rectangular sections has been investigated. There is consensus that the efficient confinement is better on circular sections than non-circular sections. So if a non-circular column could be circularised and then wrapped with FRP, the confinement effect could be maximised. Therefore, this study proposes a new technique to strengthen existing square columns by circularisation and FRP confinement. Based on the above analyses, the objectives of this study can be defined as the following:

1. Investigate the effect of the jacket's stiffness on the confinement mechanism of FRP-confined concrete.

2. Develop a confinement model for FRP-confined circular columns in a broad range of unconfined concrete from normal-strength concrete to high-strength concrete.

3. Investigate the mechanism of stress concentration at the corners of column sections in FRP-confined rectangular or square concrete columns.

4. Develop a confinement model for FRP-confined rectangular columns by not using the common method that converts the confinement mechanism of circular columns to rectangular columns.

5. Develop ANN-based confinement models to predict the compressive strength and strain of FRP-confined concrete and to compare with the results from the proposed models above.

6. Investigate the maximum usable strain of FRP-confined concrete and propose a model to calculate the residual compressive strength of a concrete core at a given strain of a FRP-confined concrete column.

7. Propose a new technique to strengthen existing square concrete columns by circularisation and FRP confinement.

1.3 Methodology

To achieve these objectives, theoretical and experimental methods originating not only from civil engineering but also other interdisciplinary fields were employed as follows:

- The energy approach was used to predict the compressive strain of FRP-confined concrete. This study assumes that there is a linear relationship between the energy absorption of the column and the external FRP. Based on this relationship, a strain model was proposed to estimate the compressive strain of FRP-confined concrete.

- The membrane hypothesis was employed to analyse the confinement mechanism of FRP-confined rectangular columns, which is a different approach from existing models for rectangular sections.

- Artificial neural networks (ANN) were used to predict the compressive strength and strain of FRP-confined concrete. Mathematical derivation was developed from the ANN-based models to provide an alternative approach for predicting the ultimate conditions of confined concrete.

- A practical technique was proposed to strengthen existing square columns by circularisation technique and FRP confinement.

Meanwhile, regression analysis has been also employed in this study to obtain the above objectives.

1.4 Thesis Outline

Corresponding to the objectives listed above, the combined experimental and theoretical studies are presented in this thesis in seven chapters, details of which are summarised below:

Chapter 2 proposes a new model for FRP-confined circular concrete columns. The scope of the proposed model covers a broad range of unconfined concrete strength from normal strength concrete to high strength concrete. The stiffness effects of the jacket are taken into account to calculate the compressive strength of confined

concrete. In addition, the compressive strain of confined concrete is estimated based on the energy approach.

Chapter 3 is divided into two sections in which the first section is to calculate the compressive strength and the second section is to predict the compressive strain of FRP-confined rectangular concrete columns. The membrane hypothesis and the stress concentration at the corners of sections were taken into account for calculating the compressive strength. And the energy approach was employed to estimate the compressive strain of confined concrete.

In order to compare with results from the two chapters above, Chapter 4 proposes confined models to calculate the compressive strength and strain of FRP-confined concrete using ANN. Chapter 4 is to focus on two main objectives in which the first objective is to calculate the compressive strength and strain of FRP-confined concrete using ANN that includes two separate models for the strength and strain, respectively. The second objective develops a methodology to generate predictive equations from the two trained ANN-based models above.

Chapter 5 investigates the progressive failure mechanism of FRP-confined concrete. The maximum usable strain of FRP-confined concrete is discussed and a model is proposed to estimate the residual strength of concrete cores at a given strain of the confined concrete.

Chapter 6 is also divided into two parts in which the first part proposes a new technique called “circularisation technique” to strengthen existing square concrete columns. A set of experiments was conducted to prove and verify the efficiency of the proposed technique with normal strength concrete. Additionally, the second part expands the use of the proposed technique for high strength concrete.

In Chapter 7, a summary, concluding remarks and recommendations for future research studies are expressed.

2 MECHANISM OF FRP-CONFINED CIRCULAR CONCRETE COLUMNS

Summary

This study establishes a confinement model for FRP-confined normal- and high-strength concrete circular columns. A new column parameter was suggested for estimating the compressive strength of FRP-confined concrete. The proposed model is able to predict the ultimate condition of FRP-confined concrete columns that have similar unconfined concrete strength and confining pressure but significant differences in the jacket stiffness. The proposed model was then verified using a database of 574 FRP-confined concrete circular columns with different types of FRP. This database covers unconfined concrete strength between 15 MPa and 170 MPa and specimens with a diameter ranging from 51 mm to 406 mm. Furthermore, this database includes specimens with a variety of FRP types: carbon FRP (CFRP), glass FRP, high-modulus carbon FRP, aramid FRP (AFRP), CFRP tube, ultra-high-modulus CFRP tube, and AFRP tube. Finally, the model's prediction fits the experimental results very well by verifying the proposed model with the extensive database.

Citation

This paper was published in Construction and Building Materials with the following citation:

Pham, T.M., and Hadi, M.N.S. (2014). "Confinement Model for FRP-confined Normal- and High-Strength Concrete Circular Columns." *Construction and Building Materials,* accepted on 23 June 2014, DOI 10.1016/j.conbuildmat.2014.06.036.

Construction and Building Materials xxx (2014) xxx–xxx

Contents lists available at ScienceDirect

Construction and Building Materials

journal homepage: www.elsevier.com/locate/conbuildmat

Confinement model for FRP confined normal- and high-strength concrete circular columns

Thong M. Pham [1], Muhammad N.S. Hadi *

School of Civil, Mining and Environmental Engineering, Univ. of Wollongong, Wollongong, NSW 2522, Australia

HIGHLIGHTS

- A confinement model for FRP confined normal- and high-strength concrete is presented.
- Effect of a new column parameter is introduced and discussed.
- The proposed model is verified by an extensive database containing 574 specimens.
- Specimens cover unconfined concrete strength between 15 MPa and 170 MPa.
- Specimens are made of seven different types of FRP.

ARTICLE INFO

Article history:
Received 1 May 2014
Received in revised form 18 June 2014
Accepted 23 June 2014
Available online xxxx

Keywords:
Fiber reinforced polymer
Confinement
Concrete columns
Compressive strength
Strain
High-strength concrete

ABSTRACT

This study establishes a confinement model for FRP confined normal- and high-strength concrete circular columns. A new column parameter was suggested for estimating the compressive strength of FRP confined concrete. The proposed model is able to predict the ultimate condition of FRP confined concrete columns that have similar unconfined concrete strength and confining pressure but significant differences in the jacket stiffness. The proposed model was then verified using a database of 574 FRP confined concrete circular columns with different types of FRP. This database covers unconfined concrete strength between 15 MPa and 170 MPa and specimens with a diameter ranging from 51 mm to 406 mm. Furthermore, this database includes specimens with a variety of FRP types: carbon FRP (CFRP), glass FRP, high-modulus carbon FRP, aramid FRP (AFRP), CFRP tube, ultra-high-modulus CFRP tube, and AFRP tube. Finally, the model's prediction fits the experimental results very well by verifying the proposed model with the extensive database.

1. Introduction

Fiber-reinforced polymer (FRP) has been commonly used in practice as a confining material for concrete columns to enhance significantly their strength and ductility. The use of FRP has been applied to both normal strength concrete (NSC) and high strength concrete (HSC) under both concentric and eccentric loads [1–6]. This use of FRP in industry has required design guidelines for these applications. Many confinement models for FRP confined concrete columns, therefore, were proposed to simulate the behavior of confined concrete columns [7–14]. Most of the existing models is applicable for FRP confined NSC columns with exceptions of models by Mandal et al. [15], Cui and Sheikh [16], Berthet et al. [7], and Xiao et al. [17]. It is noted that the model by Xiao et al. [17] was developed from actively confined HSC. Therefore, it is necessary to develop a model covering a wide range of the unconfined concrete strength from NSC to HSC.

This study first conducts an overview about the existing FRP confined concrete models for circular sections. Column parameters affecting the ultimate condition of FRP confined concrete are discussed. A new column parameter then is suggested to take into account for estimating the compressive strength of FRP confined concrete. The proposed strength model was established based on principles of artificial neural networks (ANN) while the proposed strain model was developed by using the energy approach. This study also collated an extensive database with varied FRP types to calibrate and verify the proposed model.

2. Mechanism of confinement

In this section, key assumptions of existing strength models are studied and discussed. The most popular form for calculating the

* Corresponding author. Tel.: +61 242214762; fax: +61 242213238.
E-mail addresses: mtp027@uowmail.edu.au (T.M. Pham), mhadi@uow.edu.au (M.N.S. Hadi).
[1] Formerly, Faculty of Civil Engineering, HCMC Univ. of Technology, Ho Chi Minh City, Viet Nam.

http://dx.doi.org/10.1016/j.conbuildmat.2014.06.036
0950-0618/

Nomenclature

AAE	average absolute error
d	diameter of circular sections
$d\varepsilon_c$	an increment of the axial strain
E_f	elastic modulus of FRP
f_c	axial stress of concrete
f_f	tensile strength of FRP
f_{fe}	actual tensile stress of FRP
f_l	confining pressure of FRP confined concrete columns
f_{cc}'	confined concrete strength
f_{co}'	unconfined concrete strength
k	proportion coefficient
k_1	confinement effectiveness coefficient
MSE	mean square error
n	experimental coefficient factor
N	total number of the test data
SD	standard deviation
t	thickness of FRP
U_{cc}	additional volumetric strain energy of confined concrete
U_f	volumetric strain energy of FRP
ε_{fe}	actual strain of FRP at rupture
ε_{cc}	ultimate axial strain of confined concrete
ε_{co}	axial strain of the unconfined concrete at the maximum stress
ρ_f	volumetric ratio of FRP
ρ_k	confinement stiffness ratio
$\rho\varepsilon$	strain ratio
ϕ	angle of internal friction of concrete

compressive strength of confined concrete, which was proposed by most of the existing strength models for FRP confined concrete, based on the following form:

$$\frac{f'_{cc}}{f'_{co}} = 1 + k_1 \frac{f_l}{f'_{co}} \tag{1}$$

where f_{cc}' and f_{co}' are the compressive strength of confined concrete and unconfined concrete, respectively, f_l is the lateral confining pressure, and k_1 is the confinement effectiveness coefficient. The above form proposed by Richart et al. [18] based on tests of actively confined concrete with a value of 4.1 for k_1. The confining pressure could be calculated as follows:

$$f_l = \frac{2f_f t}{d} \tag{2}$$

where f_f is the tensile strength of FRP determined from flat coupon tests, t is the thickness of FRP, and d is the section diameter.

In addition, a few of the existing models had proposed a modified format of the above equation in the following form:

$$\frac{f'_{cc}}{f'_{co}} = 1 + k_1 \left(\frac{f_l}{f'_{co}}\right)^n \tag{3}$$

where n is calibrated from a database.

In general, the value of k_1 could be a constant or a function of confinement ratio (f_l/f_{co}'). This coefficient was attained by calibration of a database [7,10–12,19–24]. So, the accuracy of this coefficient depends on the size and reliability of the database used in their calibration. Ozbakkaloglu et al. [25] have conducted an overview of 88 confinement models for FRP confined concrete in circular sections. From that study, it can be seen that majority of equations for calculating the compressive strength of confined concrete was a function of the unconfined concrete strength (f_{co}') and the confining pressure (f_l).

Exceptionally, some other models from the literature presented their models coming up with different forms or approaches. Mander et al. [26] proposed a different form developed from a multiaxial failure surface for estimating the compressive strength of confined concrete as follows:

$$f'_{cc} = f'_{co}\left(-1.254 + 2.254\sqrt{1 + \frac{7.94 f_l}{f'_{co}}} - 2\frac{f_l}{f'_{co}}\right) \tag{4}$$

Mohr-Columb failure criterion was adopted by Shehata et al. [27] and Li et al. [28] to propose the following equation:

$$f'_{cc} = f'_{co} + f_l \tan^2\left(45^\circ + \frac{\phi}{2}\right) \tag{5}$$

where ϕ is the angle of internal friction of concrete.

Wu and Zhou [13] adopted Hoek-Brown failure criterion [29] to propose the following equation for strength estimation:

$$\frac{f'_{cc}}{f'_{co}} = \frac{f_l}{f'_{co}} + \sqrt{\left(\frac{16.7}{(f'_{co})^{0.42}} - \frac{(f'_{co})^{0.42}}{16.7}\right)\frac{f_l}{f'_{co}} + 1} \tag{6}$$

As aforementioned, there are a few approaches to develop an equation for strength estimation of confined concrete. All of the above models assumed that the compressive strength of confined concrete is a function of the unconfined concrete and the confining pressure. In the following sections, this study indicates some specimens, which have been reported in the database and conducted by different researchers, had very similar values of unconfined concrete strength and confining pressure but they had significant difference in the compressive strength of confined concrete.

3. Test database

3.1. General

The test database used in this study contains experimental results of 574 FRP confined circular plain concrete columns. The test database is collated from several experimental tests being conducted over the past few decades [5,8–10,15,17,21,23,27,28,30–60]. Other tests were conducted by Evans et al. (2008), Howie and Karbhari (1994), Ilki et al. (2002), Issa and Karam (2004), Miyauchi et al. (1999), Ongpeng (2006), Owen (1998), Rousakis et al. (2003), Suter and Pinzelli (2001), Comert et al. (2009), Micelli et al. (2001), Rousakis (2001), Chan et al. (2007), Kashyap (2007), and Wang (2008) as cited in Ozbakkaloglu and Lim [61]. The database contains a variety of FRP types: carbon FRP (CFRP, 317 specimens), glass FRP (GFRP, 119 specimens), high-modulus carbon FRP (HM CFRP, 45 specimens), aramid FRP (AFRP, 35 specimens), CFRP tube (28 specimens), ultra-high-modulus CFRP (UHM CFRP, 7 specimens) tube, and AFRP tube (23 specimens). The unconfined concrete strength in the database ranges between 15 MPa and 170 MPa. The diameter of specimens varies between 51 mm and 406 mm. The test database covers a wide range of FRP confinement levels (f_l/f_{co}'). The compressive strength of the most heavily confined specimen and the least lightly confined specimen increased by about 440% and 10%, respectively. All specimens exhibiting a stress–strain curve with a descending branch, which is defined in a subsequent section, and a negligible strength increase were excluded from the database. Specimens damaged by premature rupture of FRP were also excluded from the database.

Please cite this article in press as: Pham TM, Hadi MNS. Confinement model for FRP confined normal- and high-strength concrete circular columns. Constr Build Mater (2014), http://dx.doi.org/10.1016/j.conbuildmat.2014.06.036

3.2. Stress–strain curve

The stress–strain relationship of FRP confined concrete is classified into two types including an ascending branch and a descending branch as shown in Fig. 1. This study only concerns the ascending branch type specimens. There are three key points of the stress–strain curve which are the ultimate strength of unconfined concrete, the transition point, and the ultimate strength of the confined concrete. The stress–strain relationship proposed by Lam and Teng [11] is widely accepted and was adopted by ACI440.2R [62]. So this stress–strain relationship was nominated herein for FRP confined circular plain concrete specimens. It is also commonly accepted that the stress–strain relation is bi-linear. If so, once the ultimate stress/strain is precisely determined, the stress–strain curves should not be much different even though they could be calculated by different models. Therefore, determining the ultimate condition of FRP confined concrete plays an important role in a confinement model.

3.3. Effect of confinement stiffness

As mentioned above, many of the existing models have confirmed that only the unconfined concrete strength and the confining pressure affect significantly the compressive strength of FRP confined concrete. However, Teng et al. [63] indicated that there were specimens with very similar unconfined concrete strength and confining pressure but they yielded different compressive strength of confined concrete. Teng et al. [63] then introduced two new parameters that affect the compressive strength of confined concrete. The two new parameters are the confinement stiffness ratio (ρ_k) and the strain ratio (ρ_ε) as estimated follows:

$$\rho_k = \frac{2E_f t}{\frac{f'_{co}}{\varepsilon_{co}} d} \tag{7}$$

$$\rho_\varepsilon = \frac{\varepsilon_{fe}}{\varepsilon_{co}} \tag{8}$$

where E_f is the elastic modulus of FRP, ε_{co} is the axial strain at peak stress of unconfined concrete, and ε_{fe} is the actual rupture strain of FRP in the hoop direction. The compressive strength of confined concrete was calculated as follows:

$$\frac{f'_{cc}}{f'_{co}} = 1 + 3.5(\rho_k - 0.01)\rho_\varepsilon \tag{9}$$

The equation above is used for specimens having ρ_k greater than 0.01. Table 1 was extracted from the full database to show that even though some specimens had very similar unconfined concrete strength and confining pressure, these specimens had significant difference in the compressive strength of confined concrete. Due to space limitation, only six groups of typical test results are presented in the table. It is noted that the specimens in each group of Table 1 were conducted by different researchers and are named "pseudo-identical specimens". These specimens had different confinement stiffness ratio and strain ratio. As a result, their strengths were different as based on Teng et al.'s model [63]. It means that two new parameters proposed by Teng et al. [63] seem reasonable.

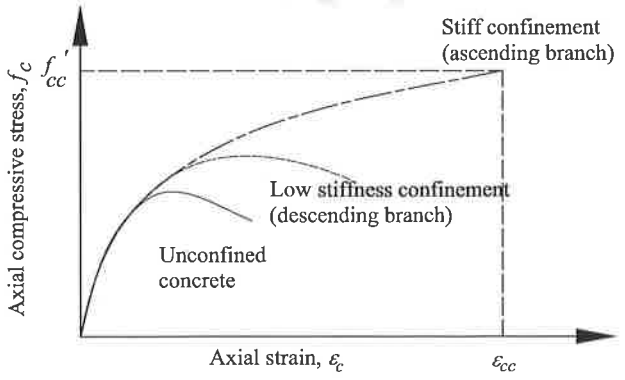

Fig. 1. Stress–strain relationship of FRP confined concrete.

Interestingly, Eq. (9) shows that the compressive strength of confined concrete must be in direct proportion to the value of $(\rho_k - 0.01)\rho_\varepsilon$. It is found in Group 2 of Table 1 that the Columns 2a had the value of $(\rho_k - 0.01)\rho_\varepsilon$ being greater than that of Columns 2b but the value of f_{cc}' of Columns 2a is much smaller than that of Columns 2b. Similarly, the columns in Groups 3 and 6 also have the same indication. It indicates that using the two new parameters may not well predict the compressive strength of confined concrete. In such cases, the FRP thickness ratio (t/d in Table 1) can reflect the difference in these "pseudo-identical specimens" that have the same unconfined concrete strength and confining pressure but different compressive strength of confined concrete. The FRP thickness ratio always is in direct proportion to the compressive strength of confined concrete as confirmed by the database. Furthermore, Pham and Hadi [64] also took the FRP thickness ratio (t/d) into account for calculating the compressive strength of FRP confined rectangular columns. Therefore, this study takes into account the unconfined concrete strength, the confining pressure and the FRP thickness ratio to calculate the compressive strength of confined concrete.

4. Strength model for FRP confined circular concrete columns

4.1. The proposed strength model

In order to calculate the compressive strength of FRP confined concrete columns, this study adopted a method proposed by Pham and Hadi [65] to generate a simple-form equation from a trained ANN. Pham and Hadi [65] concluded that the output could be calculated by multiplying the inputs by a proportional matrix if the proposed ANN is trained and yields good results. The inputs herein are column parameters of FRP confined concrete while the outputs are its compressive strength. It means that the compressive strength of confined concrete could be predicted by multiplying the column parameters by the proportional matrix. The proportional matrix is resulted from multiplying the input weight matrix by the layer weight matrix and normalization process of the inputs and the outputs. Details of this method and definitions of some concepts could be found in the studies by Pham and Hadi [65].

As mentioned above, the ratio between the FRP thickness and the section diameter affects the compressive strength of FRP confined concrete. Thus, three column parameters are considered in this model, which are the unconfined concrete strength f_{co}' (MPa), the confining pressure f_l (MPa), and the ratio between the FRP thickness and the section diameter t/d (%). The compressive strength of FRP confined circular columns could be calculated as follows:

$$f'_{cc} = 0.7f'_{co} + 1.8f_l + 5.7\frac{t}{d} + 13 \tag{10}$$

where the confining pressure f_l is estimated from Eq. (2).

The proposed model could be used to estimate the compressive strength of confined concrete made of a variety of FRP types including CFRP, GFRP, AFRP, HM CFRP, UHM CFRP tube, CFRP tube, and AFRP tube. In addition, it is noted that Eq. (10) covers columns that have parameters in the ranges shown in Table 2.

Please cite this article in press as: Pham TM, Hadi MNS. Confinement model for FRP confined normal- and high-strength concrete circular columns. Constr Build Mater (2014), http://dx.doi.org/10.1016/j.conbuildmat.2014.06.036

Table 1
Pseudo-identical specimens in the database.

No. of group	Sources	d (mm)	f_{co}' (MPa)	f_l (MPa)	t/d (%)	f_{cc}' (MPa)	ρ_k	ρ_v	$(\rho_k - 0.01)\,\rho_v$
1a	Mirmiran et al. [5]	152	29.8	19.5	0.5	63.0	0.04	9.4	0.27
	Mirmiran et al. [5]	152	29.8	19.5	0.5	58.7	0.04	9.4	0.27
	Mirmiran et al. [5]	152	31.2	19.5	0.5	63.1	0.04	9.2	0.25
	Mirmiran et al. [5]	152	31.2	19.5	0.5	65.4	0.04	9.2	0.25
1b	Silva and Rodrigues [55]	150	31.1	19.9	1.7	91.6	0.07	8.3	0.49
	Silva and Rodrigues [55]	150	29.6	19.9	1.7	89.4	0.07	5.0	0.32
	Silva and Rodrigues [55]	150	31.1	19.9	1.7	87.5	0.07	7.9	0.47
	Silva and Rodrigues [55]	150	31.1	19.9	1.7	91.9	0.07	7.8	0.46
	Silva and Rodrigues [55]	150	29.6	19.9	1.7	89.8	0.07	5.0	0.32
	Silva and Rodrigues [55]	150	31.2	19.9	1.7	91.9	0.07	8.0	0.48
2a*	Xiao and Wu [21]	152	33.7	23.7	0.8	82.9	0.09	4.1	0.34
	Xiao and Wu [21]	152	33.7	23.7	0.8	86.2	0.09	4.5	0.38
2b	Lin and Chen [52]	120	32.7	22.3	1.5	101.3	0.06	6.3	0.31
	Lin and Chen [52]	120	32.7	22.3	1.5	104.5	0.06	6.3	0.31
3a	Jiang and Teng [8]	152	45.9	12.3	0.3	64.6	0.03	6.6	0.12
	Jiang and Teng [8]	152	45.9	12.3	0.3	65.9	0.03	8.0	0.15
3b	Youssef et al. [23]	152	44.1	12.5	1.5	80.4	0.03	5.3	0.10
	Youssef et al. [23]	152	44.1	12.5	1.5	80.0	0.03	5.3	0.10
	Youssef et al. [23]	152	44.1	12.5	1.5	81.1	0.03	5.3	0.10
4a	Cui and Sheikh [16]	152	48.1	21.5	1.3	109.4	0.10	4.4	0.41
	Cui and Sheikh [16]	152	48.1	21.5	1.3	126.7	0.10	5.5	0.51
4b	Tamuzs et al. [42]	150	48.8	20.4	0.2	72.1	0.05	1.8	0.08
	Tamuzs et al. [42]	150	48.8	20.4	0.2	72.6	0.05	1.5	0.07
5a	Cui and Sheikh [16]	152	48.1	32.2	2.0	162.7	0.15	5.2	0.76
	Cui and Sheikh [16]	152	48.1	32.2	2.0	153.6	0.15	4.7	0.68
5b	Rousakis et al. (2003)	150	49.2	30.6	0.3	100.6	0.05	6.2	0.28
6a	Aire et al. [30]	150	69	36.5	0.5	156.0	0.08	4.3	0.29
6b	Xiao et al. [17]	152	70.8	36.7	0.7	180.5	0.14	2.0	0.27

Table 2
Statistics of the column parameters for the proposed strength model.

	Max	Min
f_{co}' (MPa)	170	15
f_l (MPa)	109	3
t/d (%)	3.9	0.06
f_{cc}' (MPa)	296	37

4.2. Verification of the strength model

The proposed strength model was verified by the database including seven types of FRP and a wide range of compressive strength of unconfined concrete. Fig. 2 shows 574 data points of the predicted compressive strength of FRP confined concrete versus their experimental results. As can be seen in Fig. 2, the proposed strength model could predict the compressive strength of FRP-confined normal- and high-strength concrete circular columns. The compressive strength of unconfined concrete ranges between 15 MPa and 170 MPa. In addition, the normalized predicted compressive strengths of confined columns versus their normalized experimental results are shown in Fig. 3. Five existing models were studied in this verification [7,12,14,63,66]. The average absolute error (AAE), which is calculated using Eq. (11), of the above models ranges between 11.54% and 15.97%. The proposed model shows the smallest value of AAE (9.88%) among these models.

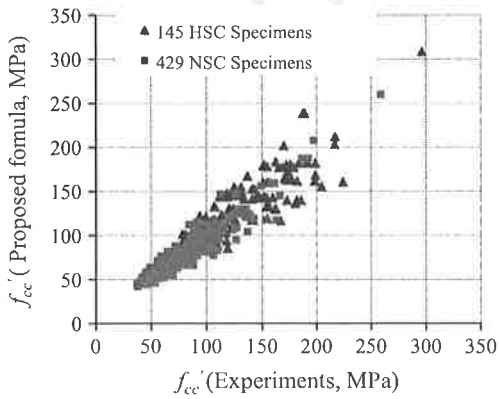

Fig. 2. Performance of the proposed model for both NSC and HSC specimens.

$$AAE = \frac{\sum_1^N \left|\frac{pre_i - exp_i}{exp_i}\right|}{N} \tag{11}$$

where *pre* is the model predictions, *exp* is the experimental results, and N is the total number of specimens. The mean square error (MSE) and the standard deviation (SD) are also calculated to assess the accuracy of the models:

$$MSE = \frac{\sum_1^N \left(\frac{pre_i - exp_i}{exp_i}\right)^2}{N} \tag{12}$$

$$SD = \sqrt{\frac{\sum_1^N \left(\frac{pre_i}{exp_i} - \frac{pre_{avg}}{exp_{avg}}\right)^2}{N-1}} \tag{13}$$

Furthermore, the equation of the best-fit line (in a format of $y = ax$) and the correlation factor (R^2) in each model are reported. The five models above have a correlation factor ranging from 0.76 to 0.79 while that factor of the proposed models is 0.88. The value of "a" of the equation of the best-fit line could depict that the model is conservative ($a < 1$) or vice versa ($a > 1$). As can be easily seen in Fig. 3 that the models by Berthet et al. [7], Teng et al. [63], Wu and Wang [66], and Yazici and Hadi [14] are conservative while the model by Matthys et al. [12] is less-conservative.

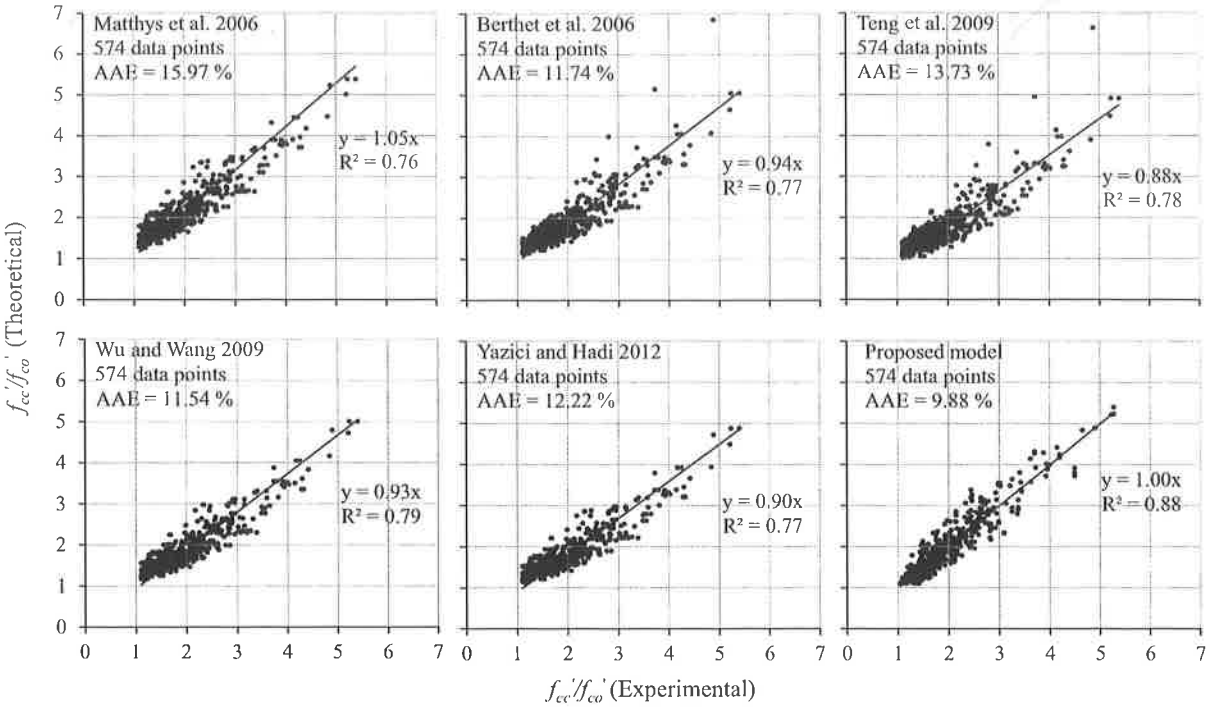

Fig. 3. Comparison of the selected strength models.

Interestingly, the value of "a" of the proposed strength model is equal to 1. In addition, the error of the strength models was statistically verified and presented in Fig. 4.

4.3. Discussion the proposed strength model

Figs. 3 and 4 show that Eq. (10) compares well with the experimental data. However, the constant (value of 13) at the end of the equation may cause a considerable error in estimating the compressive strength of a specimen having low unconfined concrete strength and confining pressure. As a sequence, the following equation is proposed as an approximation:

$$f'_{cc} = 0.91f'_{co} + 1.88f_l + 7.6\frac{t}{d} \quad (14)$$

To verify the performance of Eq. (14) versus the experimental data, Fig. 5 shows the prediction results versus the experimental results. The error calculated from the prediction of Eq. (14) slightly increase as compared to that of Eq. (10). To extend the applicability of the proposed models, larger sizes of specimens which may be available in the future could be used to retrain and test the models. When the proposed model has been properly trained, verified, and tested with a comprehensive experimental database, it can be used with a high degree of confidence.

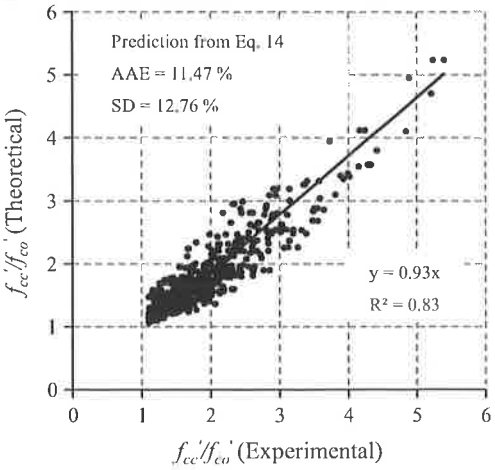

Fig. 5. Performance of the modified proposed model.

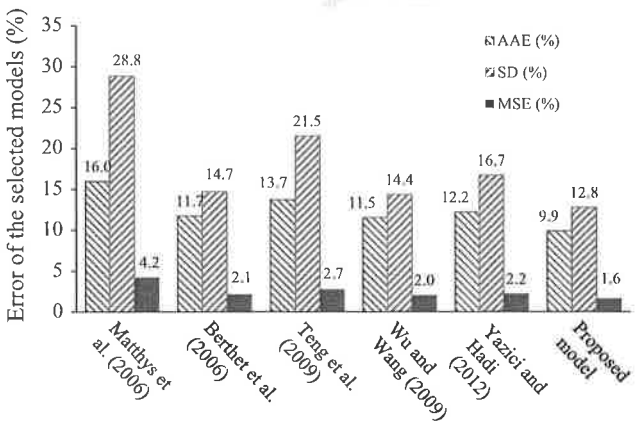

Fig. 4. Accuracy of the selected strength models.

5. Strain model for FRP confined circular concrete columns

5.1. Strain energy absorption

The proposed strain model was developed based on the energy approach that was proposed by Pham and Hadi [67]. Pham and Hadi [67] concluded that there is a linear relationship between the additional volumetric strain energy absorbed by a column core (U_{cc}) and the volumetric strain energy absorbed by FRP (U_f).When the strain of confined concrete is below the peak strain of the corresponding unconfined concrete, the effect of FRP is negligible. Thus, it is assumed that the additional energy in the column core

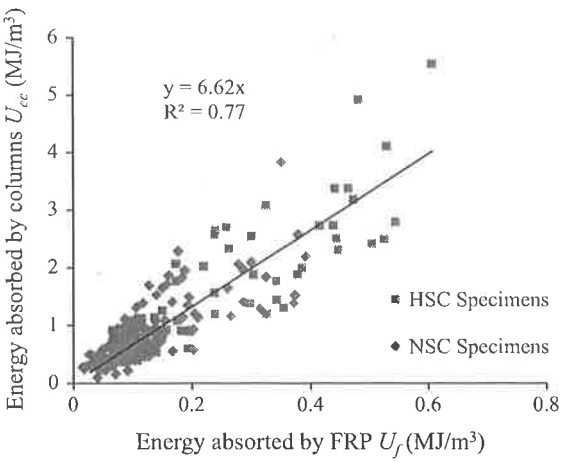

Fig. 6. Energy relationship of FRP confined circular columns.

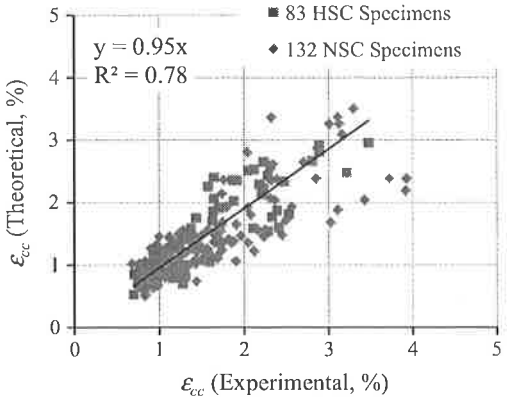

Fig. 7. Performance of the proposed strain model.

equals the area under the experimental stress–strain curves starting from the value of unconfined concrete strain. The additional volumetric strain energy absorbed by a column core (U_{cc}) is calculated as follows:

$$U_{cc} = \int_{\varepsilon_{co}}^{\varepsilon_{cc}} f_c d\varepsilon_c = \frac{(\varepsilon_{cc} - \varepsilon_{co})(f'_{co} + f'_{cc})}{2} \quad (15)$$

where f_c is the axial stress of the concrete, $d\varepsilon_c$ is an increment of the axial strain, U_{cc} is the volumetric strain energy of confined concrete, ε_{cc} is the ultimate strain of confined concrete. The volumetric strain energy absorbed by FRP (U_f) could be determined as follows:

$$U_f = \rho_f \left(\frac{1}{2} f_{fe} \varepsilon_{fe}\right) \quad (16)$$

where ρ_f is the volumetric ratio of FRP and calculated as shown in Eq. (17), U_f is the volumetric strain energy of FRP, and f_{fe} and ε_{fe} are the actual rupture strength and rupture strain of FRP on the columns, respectively.

$$\rho_f = \frac{4t}{d} \quad (17)$$

5.2. The proposed strain model

The proposed strain model requires specimens including the actual rupture strain of FRP reported. Test results of specimens not reporting the actual rupture strain of FRP were excluded from the database. Thus, a new database (215 specimens) extracted from the full database was used to develop the proposed strain model. The new database covers unconfined concrete strength between 24 MPa and 112 MPa, and a variety of FRP types including CFRP, GFRP, AFRP, HM CFRP, CFRP tube, and AFRP tube. The energy absorption of 215 specimens was determined using Eqs. (15) and (16), and the results are presented in Fig. 6. Next, a regression analysis was undertaken to attain the following equation:

$$U_{cc} = 6.62 U_f \quad (18)$$

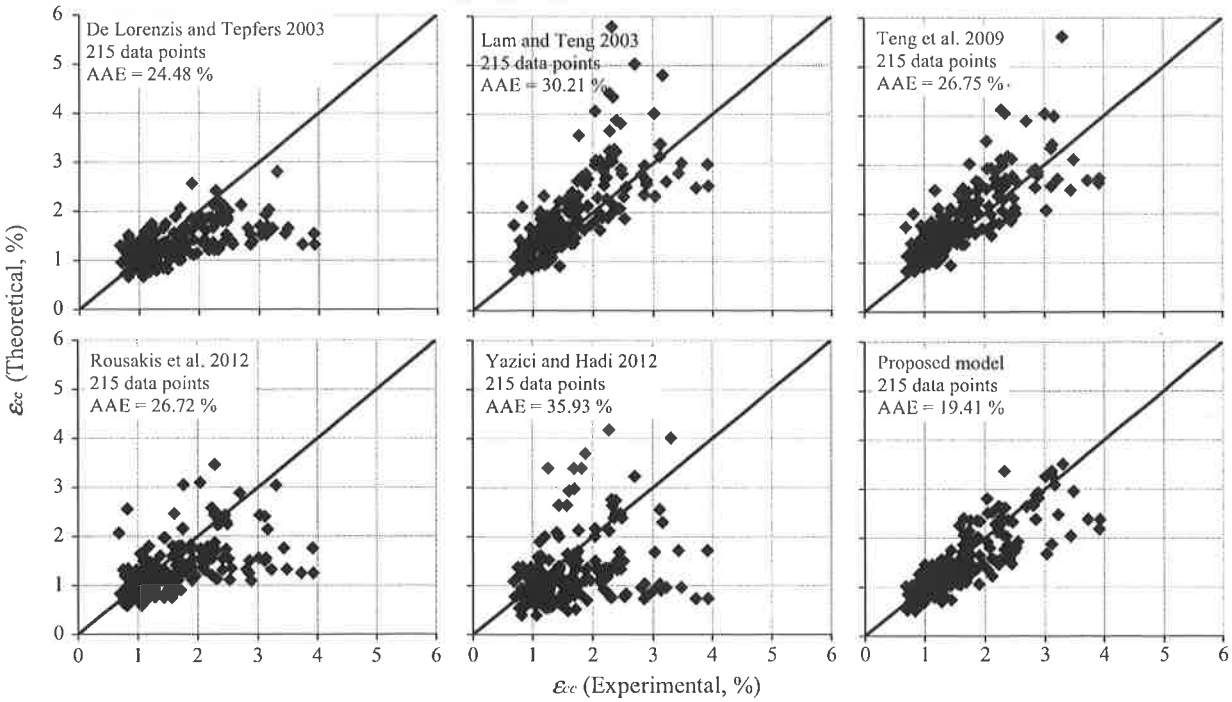

Fig. 8. Comparison of the selected strain models.

Please cite this article in press as: Pham TM, Hadi MNS. Confinement model for FRP confined normal- and high-strength concrete circular columns. Constr Build Mater (2014), http://dx.doi.org/10.1016/j.conbuildmat.2014.06.036

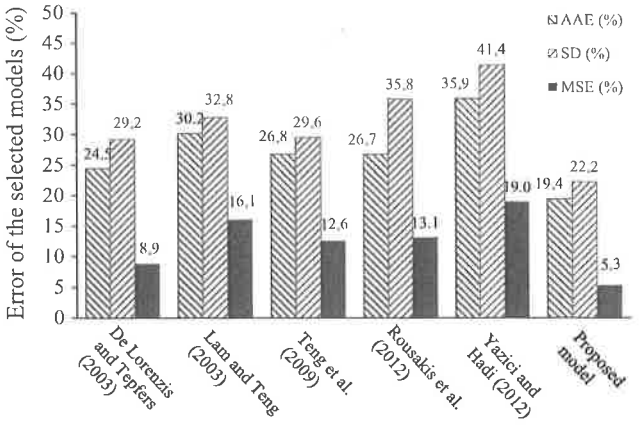

Fig. 9. Accuracy of the selected strain models.

Substituting Eqs. (15) and (16) into Eq. (18), results in the following equation:

$$\varepsilon_{cc} = \varepsilon_{co} + \frac{4ktf_{fe}\varepsilon_{fe}}{d(f'_{co} + f'_{cc})} \tag{19}$$

where the proportion coefficient k is equal to 6.62. This expression could be used to calculate the axial strain of CFRP confined concrete columns in circular sections. Using this calculated strain, any model could be utilized to calculate the confined concrete strength. Lam and Teng model [11]was adopted to express another form of Eq. (19) as follows:

$$\varepsilon_{cc} = \varepsilon_{co} + \frac{2ktf_{fe}\varepsilon_{fe}}{df'_{co} + 3.3f_{fe}t} \tag{20}$$

5.3. Verification of the strain model

Fig. 7 shows theoretical strain versus experimental strain of FRP confined circular columns. This figure depicts that the proposed strain model predicts both the 132 NSC columns and the 83 HSC columns. This figure also shows that the proposed model's prediction of columns with low compressive strain is closer to experimental results than the others. The errors of the model's prediction in a range of high strain could be explained through Fig. 6, which describes that the relationship between the two energies of columns having low energy absorption is more correlative than columns having high energy absorbed.

In addition, a total of 215 data points are plotted in Fig. 8 to assess the performance of existing models and the proposed model. Five strain models were considered in this verification [11,14,63,68,69]. Performance and accuracy of all six models are comparable with the value of AAE ranging from 19% to 36%. Among the above models, the proposed strain model shows the best performance with the AAE of 19%. In general trend, the model by Teng et al. [63] and the proposed model depict good prediction for all ranges of columns' strain. The model by De Lorenzis and Tepfers [68] also shows very good agreement between prediction and experimental results. However, this model is very conservative in a range of columns having high compressive axial strain. In addition, the error of the strain models was statistically verified and presented in Fig. 9.

6. Conclusions

A confinement model was developed for FRP confined normal- and high-strength concrete columns. The predictions of the proposed model fit the experimental results from the extensive database very well. The findings presented in this paper are summarized as follows:

1. In order to calculate the compressive strength of FRP confined circular columns, the ratio between the thickness of FRP and the column diameter should be taken into account. When this parameter is considered, only an unified equation is used to calculate the compressive strength of confined concrete with varied FRP types, which have significant difference in the jacket stiffness.
2. The proposed model could estimate the compressive strength of confined concrete with unconfined concrete strength ranging between 15 MPa and 170 MPa.
3. This study confirms that using energy method could estimate well the compressive strain of FRP confined concrete as compared to experimental results. This study refines the applicability of the energy-based strain model proposed by Pham and Hadi [67] from only CFRP to seven types of FRP.

Finally, this study takes the FRP thickness ratio into account to predict the compressive strength of FRP confined circular concrete columns. This consideration provides an unified equation covering all types of FRP and diminishes the disadvantage of most of existing models that proposed each experimental factor for each FRP type.

Acknowledgement

The first author would like to acknowledge the Vietnamese Government and the University of Wollongong for the support of his full PhD scholarship.

References

[1] Hadi MNS, Li J. External reinforcement of high strength concrete columns. Compos Struct 2004;65(3–4):279–87.
[2] Hadi MNS, Widiarsa IBR. Axial and flexural performance of square RC columns wrapped with CFRP under eccentric loading. J Compos Constr 2012;16(6):640–9.
[3] Hadi MNS, Pham TM, Lei X. New method of strengthening reinforced concrete square columns by circularizing and wrapping with fiber-reinforced polymer or steel straps. J Compos Constr 2013;17(2):229–38.
[4] Hadi MNS. Behaviour of FRP wrapped normal strength concrete columns under eccentric loading. Compos Struct 2006;72(4):503–11.
[5] Mirmiran A, Shahawy M, Samaan M, Echary HE, Mastrapa JC, Pico O. Effect of column parameters on FRP-confined concrete. J Compos Constr 1998;2(4):175–85.
[6] Pham TM, Doan LV, Hadi MNS. Strengthening square reinforced concrete columns by circularisation and FRP confinement. Constr Build Mater 2013;49:490–9.
[7] Berthet JF, Ferrier E, Hamelin P. Compressive behavior of concrete externally confined by composite jackets: Part B: Modeling. Constr Build Mater 2006;20(5):338–47.
[8] Jiang T, Teng JG. Analysis-oriented stress–strain models for FRP-confined concrete. Eng Struct 2007;29(11):2968–86.
[9] Karabinis AI, Rousakis TC. Concrete confined by FRP material: a plasticity approach. Eng Struct 2002;24(7):923–32.
[10] Karbhari VM, Gao Y. Composite jacketed concrete under uniaxial compression verification of simple design equations. J Mater Civ Eng 1997;9(4):185–93.
[11] Lam L, Teng JG. Design-oriented stress–strain model for FRP-confined concrete. Constr Build Mater 2003;17(6–7):471–89.
[12] Matthys S, Toutanji H, Taerwe L. Stress–strain behavior of large-scale circular columns confined with FRP composites. J Struct Eng 2006;132(1):123–33.
[13] Wu YF, Zhou YW. Unified strength model based on Hoek-Brown failure criterion for circular and square concrete columns confined by FRP. J Compos Constr 2010;14(2):175–84.
[14] Yazici V, Hadi MNS. Normalized confinement stiffness approach for modeling FRP-confined concrete. J Compos Constr 2012;16(5):520–8.
[15] Mandal S, Hoskin A, Fam A. Influence of concrete strength on confinement effectiveness of fiber-reinforced polymer circular jackets. ACI Struct J 2005;102(3):383–92.
[16] Cui C, Sheikh SA. Analytical model for circular normal- and high-strength concrete columns confined with FRP. J Compos Constr 2010;14(5):562–72.

Please cite this article in press as: Pham TM, Hadi MNS. Confinement model for FRP confined normal- and high-strength concrete circular columns. Constr Build Mater (2014), http://dx.doi.org/10.1016/j.conbuildmat.2014.06.036

[17] Xiao QG, Teng JG, Yu T. Behavior and modeling of confined high-strength concrete. J Compos Constr 2010;14(3):249–59.
[18] Richart FE, Brandtzaeg A, Brown RL. A study of the failure of concrete under combined compressive stress. Bulletin 1985, Univ. of Illinois Engineering Experimental Station, Champaign, Ill 1928.
[19] Samaan M, Mirmiran A, Shahawy M. Model of concrete confined by fiber composites. J Struct Eng 1998;124(9):1025–31.
[20] Toutanji HA. Stress–strain characteristics of concrete columns externally confined with advanced fiber composite sheets. ACI Mater J 1999;96(3):397–404.
[21] Xiao Y, Wu H. Compressive behavior of concrete confined by carbon fiber composite jackets. J Mater Civ Eng 2000;12(2):139–46.
[22] Bisby LA, Dent AJS, Green MF. Comparison of confinement models for fiber-reinforced polymer-wrapped concrete. ACI Struct J 2005;102(1):62–72.
[23] Youssef MN, Feng MQ, Mosallam AS. Stress–strain model for concrete confined by FRP composites. Composites Part B 2007;38(5):614–28.
[24] Khalili HH, Fardis MN. FRP-encased concrete as a structural material. Mag Concr Res 1982;34(121):191–202.
[25] Ozbakkaloglu T, Lim JC, Vincent T. FRP-confined concrete in circular sections: review and assessment of stress–strain models. Eng Struct 2013;49:1068–88.
[26] Mander JB, Park R, Priestley MJN. Theoretical stress–strain model for confined concrete. J Struct Eng 1988;114(8):1804–26.
[27] Shehata IAEM, Carneiro LAV, Shehata LCD. Strength of short concrete columns confined with CFRP sheets. Mater Struct 2002;35(1):50–8.
[28] Li Y-F, Lin C-T, Sung Y-Y. A constitutive model for concrete confined with carbon fiber reinforced plastics. Mech Mater 2003;35(3):603–19.
[29] Hoek E, Brown ET. Empirical strength criterion for rock masses. J Geotech Eng Div 1980;106:1013–35 (Compendex).
[30] Aire C, Gettu R, Casas JR, Marques S, Marques D. Concrete laterally confined with fibre-reinforced polymers (FRP): experimental study and theoretical model. Mater Constr 2010;60(297):19–31.
[31] Benzaid R, Mesbah H, Chikh NE. FRP-confined concrete cylinders: axial compression experiments and strength model. J Reinforced Plast Compos 2010;29(16):2469–88.
[32] Berthet JF, Ferrier E, Hamelin P. Compressive behavior of concrete externally confined by composite jackets. Part A: Experimental study. Constr Build Mater 2005;19(3):223–32.
[33] Cui C, Sheikh SA. Experimental study of normal- and high-strength concrete confined with fiber-reinforced polymers. J Compos Constr 2010;14(5):553–61.
[34] Green MF, Bisby LA, Fam AZ, Kodur VKR. FRP confined concrete columns: behaviour under extreme conditions. Cem Concr Compos 2006;28(10):928–37.
[35] Lam L, Teng JG. Ultimate condition of fiber reinforced polymer-confined concrete. J Compos Constr 2004;8(6):539–48.
[36] Lam L, Teng JG, Cheung CH, Xiao Y. FRP-confined concrete under axial cyclic compression. Cem Concr Compos 2006;28(10):949–58.
[37] Lee JY, Yi CK, Jeong HS, Kim SW, Kim JK. Compressive response of concrete confined with steel spirals and FRP composites. J Compos Mater 2010;44(4):481–504.
[38] Lin H-J, Liao C-I. Compressive strength of reinforced concrete column confined by composite material. Compos Struct 2004;65(2):239–50.
[39] Matthys S, Toutanji H, Audenaert K, Taerwe L. Axial load behavior of large-scale columns confined with fiber-reinforced polymer composites. ACI Struct J 2005;102(2):258–67.
[40] Rochette P, Labossière P. Axial testing of rectangular column models confined with composites. J Compos Constr 2000;4(3):129–36.
[41] Saenz N, Pantelides C. Short and medium term durability evaluation of FRP-confined circular concrete. J Compos Constr 2006;10(3):244–53.
[42] Tamuzs V, Valdmanis V, Tepfers R, Gylltoft K. Chalmers tekniska h, Department of C, Environmental Engineering SE, Institutionen för bygg- och miljöteknik K, Chalmers University of T. Stability analysis of CFRP-wrapped concrete columns strengthened with external longitudinal CFRP sheets. Mech Compos Mater 2008;44(3):199–208.
[43] Smith ST, Kim SJ, Zhang HW. Behavior and effectiveness of FRP wrap in the confinement of large concrete cylinders. J Compos Constr 2010;14(5):573–82.
[44] Theriault M, Neale KW, Claude S. Fiber-reinforced polymer-confined circular concrete columns: investigation of size and slenderness effects. J Compos Constr 2004;8(4):323–31.
[45] Valdmanis V, De Lorenzis L, Rousakis T, Tepfers R. Behaviour and capacity of CFRP-confined concrete cyliners subjected to monotonic and cyclic axial compressive load. Struct Concr 2007;8(4):187–90.
[46] Wang LM, Wu YF. Effect of corner radius on the performance of CFRP-confined square concrete columns: test. Eng Struct 2008;30(2):493–505.
[47] Yan ZH, Pantelides CP, Reaveley LD. Fiber-reinforced polymer jacketed and shape-modified compression members: I – experimental behavior. ACI Struct J 2006;103(6):885–93.
[48] Zhang S, Ye L, Mai YW. A study on polymer composite strengthening systems for concrete columns. Appl Compos Mater 2000;7(2–3):125–38.
[49] Ahmad SH, Khaloo AR, Irshaid A. Behavior of concrete spirally condined by fiberglass filaments. Mag Concr Res 1991;43(156):143–8.
[50] Almusallam TH. Behavior of normal and high-strength concrete cylinders confined with E-glass/epoxy composite laminates. Composites Part B 2007;38(5):629–39.
[51] Au C, Buyukozturk O. Effect of fiber orientation and ply mix on fiber reinforced polymer-confined concrete. J Compos Constr 2005;9(5):397–407.
[52] Lin HJ, Chen CT. Strength of concrete cylinder confined by composite materials. J Reinforced Plast Compos 2001;20(18):1577–600.
[53] Nanni A, Bradford NM. FRP jacketed concrete under uniaxial compression. Constr Build Mater 1995;9(2):115–24.
[54] Shao Y, Zhu Z, Mirmiran A. Cyclic modeling of FRP-confined concrete with improved ductility. Cem Concr Compos 2006;28(10):959–68.
[55] Silva MAG, Rodrigues CC. Size and relative stiffness effects on compressive failure of concrete columns wrapped with glass FRP. J Mater Civ Eng 2006;18(3):334–42.
[56] Teng JG, Huang YL, Lam L, Ye LP. Theoretical model for fiber-reinforced polymer-confined concrete. J Compos Constr 2007;11(2):201–10.
[57] Wong YL, Yu T, Teng JG, Dong SL. Behavior of FRP-confined concrete in annular section columns. Composites Part B 2008;39(3):451–66.
[58] Wu YF, Liu T, Oehlers DJ. Fundamental principles that govern retrofitting of reinforced concrete columns by steel and FRP jacketing. Adv Struct Eng 2006;9(4):507–33.
[59] Wu G, Wu ZS, Lu ZT, Ando YB. Structural performance of concrete confined with hybrid FRP composites. J Reinforced Plast Compos 2008;27(12):1323–48.
[60] Wu HL, Wang YF, Yu L, Li XR. Experimental and computational studies on high-strength concrete circular columns confined by aramid fiber-reinforced polymer sheets. J Compos Constr 2009;13(2):125–34.
[61] Ozbakkaloglu T, Lim JC. Axial compressive behavior of FRP-confined concrete: experimental test database and a new design-oriented model. Composites Part B 2013;55:607–34.
[62] American Concrete Institute (ACI). Guide for the Design and Construction of Externally Bonded FRP Systems for Strengthening Concrete Structures. 440.2R-08 2008, Farmington Hills, MI.
[63] Teng JG, Jiang T, Lam L, Luo YZ. Refinement of a design-oriented stress–strain model for FRP-confined concrete. J Compos Constr 2009;13(4):269–78.
[64] Pham TM, Hadi MNS. Stress prediction model for FRP confined rectangular concrete columns with rounded corners. J Compos Constr 2009;18(1):04013019.
[65] Pham TM, Hadi MNS. Predicting stress and strain of FRP confined square/rectangular columns using artificial neural networks. J Compos Constr 2014. http://dx.doi.org/10.1061/(ASCE)CC.1943-5614.0000477.
[66] Wu YF, Wang LM. Unified strength model for square and circular concrete columns confined by external jacket. J Struct Eng 2009;135(3):253–61.
[67] Pham TM, Hadi MNS. Strain estimation of CFRP confined concrete columns using energy approach. J Compos Constr 2013;17(6):04013001.
[68] De Lorenzis L, Tepfers R. Comparative study of models on confinement of concrete cylinders with fiber-reinforced polymer composites. J Compos Constr 2003;7(3):219–37.
[69] Rousakis T, Rakitzis T, Karabinis A. Empirical modelling of failure strains of uniformly FRP confined concrete columns. In The 6th International conference on FRP composites in civil engineering – CICE 2012. Rome.

Please cite this article in press as: Pham TM, Hadi MNS. Confinement model for FRP confined normal- and high-strength concrete circular columns. Constr Build Mater (2014), http://dx.doi.org/10.1016/j.conbuildmat.2014.06.036

3 MECHANISM OF FRP-CONFINED SQUARE CONCRETE COLUMNS

3.1 Compressive Strength

Summary

The paper uses the “membrane hypothesis” to formulate the confining behaviour of FRP-confined rectangular columns. A model was developed to calculate the strength of FRP-confined rectangular concrete columns. The model was verified using a database of 190 FRP-confined rectangular concrete columns. The database covers unconfined concrete strength between 18.3 MPa and 55.2 MPa and specimens with dimensions ranging from 79 mm to 305 mm and 100 mm to 305 mm for short and long sides, respectively. The performance of the proposed model shows a very good correlation with the experimental results. In addition, the strain distribution of FRP around the circumference of the rectangular sections was examined to propose an equation for predicting the actual rupture strain of FRP. The minimum corner radius of the sections is also recommended to achieve sufficient confinement.

Citation

This paper was published in Journal of Composites for Construction with the following citation:

Pham, T.M., and Hadi, M.N.S. (2014). "Stress Prediction Model for FRP-confined Rectangular Concrete Columns with Rounded Corners." *Journal of Composites for Construction*, 18(1), 04013019-1-04013019-10.

Stress Prediction Model for FRP Confined Rectangular Concrete Columns with Rounded Corners

Thong M. Pham, S.M.ASCE[1]; and Muhammad N. S. Hadi, M.ASCE[2]

Abstract: The paper uses the membrane hypothesis to formulate the confining behavior of fiber-reinforced polymer (FRP) confined rectangular columns. A model was developed to calculate the strength of FRP confined rectangular concrete columns. The model was verified using a database of 190 FRP confined rectangular concrete columns. The database covers unconfined concrete strength between 18.3 and 55.2 MPa, and specimens with dimensions ranging from 79–305 mm and 100–305 mm for short and long sides, respectively. The performance of the proposed model shows a very good correlation with the experimental results. In addition, the strain distribution of FRP around the circumference of the rectangular sections was examined to propose an equation for predicting the actual rupture strain of FRP. The minimum corner radius of the sections is also recommended to achieve sufficient confinement. **DOI: 10.1061/(ASCE)CC.1943-5614.0000407.**

Author keywords: Rectangular columns; Square columns; Membrane hypothesis.

Introduction

Fiber-reinforced polymers (FRPs) have been commonly used to strengthen existing reinforced concrete (RC) columns. This use of FRP has been proven to increase the strength, stiffness, and ductility of the strengthened columns. The use of FRP in industry has required design guidelines for these applications. Many strength models for FRP confined concrete columns were therefore proposed to simulate the behavior of confined concrete columns (Spoelstra and Monti 1999; Chaallal et al. 2003a; Lam and Teng 2003a; Harajli et al. 2006; Wu and Wang 2009; Cui and Sheikh 2010; Lee et al. 2010; Wu and Zhou 2010; Yazici and Hadi 2012). Most of the existing models based on Richart et al. (1928) are for circular sections causing uniform confining pressure, which can be estimated based on the strength and thickness of the FRP and the diameter of the sections.

There are far fewer models for FRP confined rectangular columns as compared with circular columns (Lam and Teng 2003b; Wu and Wang 2009; Toutanji et al. 2010; Wu and Wei 2010; Wu and Zhou 2010). The confining pressure of a FRP confined rectangular column around its perimeter is not uniform. This nonuniform confining pressure leads to many difficulties to formulate the pressure distribution by a mechanical solution. Most of the existing models for rectangular sections are quite similar to circular sections except that a shape factor is introduced to account for the nonuniform confinement. In addition, the equivalent confining pressure in such cases is calculated based on mechanism analysis of circular sections. The differences between these models are the shape factor and definition of the equivalent diameter of the rectangular sections. Therefore, analyzing the mechanism of FRP confined rectangular columns at the corners to create a model is an interesting concern of the research society. This paper introduces an approach to propose a model by focusing on the stress concentration at the corners of the sections.

This paper first adopts the membrane hypothesis to analyze the behaviors of FRP at the corners of rectangular sections. The confining pressure of the confined columns at the middle of the sides and at the corners of the sections is then examined. Next, the confining pressure at the corners of the section is estimated from the tensile properties of FRP and the corner radius. A model is proposed to estimate the strength of the confined columns, which was evaluated by a database from the literature.

Confining Mechanism

Confining Pressure of Shell Structures

An FRP jacket used in confined concrete columns could be analyzed as a cylindrical shell structure subjected to hydrostatic pressure. In general, the loads are carried in shell structures by a combination of stretching and bending action. However, sometimes the bending effects are rather small when the shell structure is thin enough for eligibility of the membrane hypothesis. For such cases, the equilibrium of an infinitesimal section of the cylindrical shell structure was analyzed by Calladine (1983) [Fig. 1(a)]. The tension force of the shell structure is

$$T = rp \tag{1}$$

where T = tension force in the hoop direction of the shell structure; r = radius of the infinitesimal section; and p = hydrostatic pressure applied on the structure.

This solution is also applicable for a rectangular prism with rounded corners and confined with FRP. The applicability of this solution is for thin shells, which could be expected when the ratio of the round corner and the nominal jacket thickness is greater than 20 ($r/t > 20$) (Calladine 1983). It is assumed that when an axial

[1]Ph.D. Candidate, School of Civil, Mining and Environmental Engineering, Univ. of Wollongong, Wollongong, New South Wales 2522, Australia; formerly, Lecturer, Faculty of Civil Engineering, HCMC Univ. of Technology, Ho Chi Minh City, Vietnam. E-mail: mtp027@uowmail.edu.au

[2]Associate Professor, School of Civil, Mining and Environmental Engineering, Univ. of Wollongong, Wollongong, New South Wales 2522, Australia (corresponding author). E-mail: mhadi@uow.edu.au

Note. This manuscript was submitted on March 20, 2013; approved on June 24, 2013; published online on June 26, 2013. Discussion period open until March 1, 2014; separate discussions must be submitted for individual papers. This paper is part of the ***Journal of Composites for Construction***, © ASCE, ISSN 1090-0268/04013019(10)/$25.00.

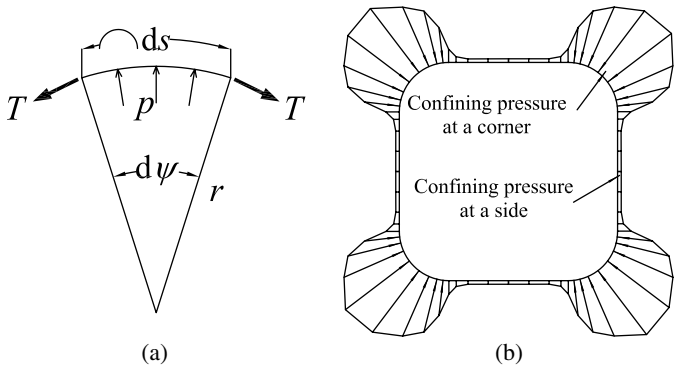

Fig. 1. Confinement behavior at the corner of the section: (a) mechanism of the tension force; (b) distribution of confining stress

load is applied on a FRP confined rectangular concrete column, the confining pressure concentrates only at the corners of the section. The confining pressure at middle of the section sides is rather small, which could be negligible. For simplicity, the term rectangular columns, used in this paper, is used for rectangular columns with round corners.

Confining Pressure of FRP Confined Rectangular Concrete Columns

When a FRP confined rectangular concrete column is subjected to an axial load, the concrete laterally expands and is confined by the FRP. The tension force of the jacket at the rupture state is

$$f_{fe} = E_f \varepsilon_{fe} \tag{2}$$

where f_{fe} = actual tensile stress of FRP; E_f = elastic modulus of FRP; and ε_{fe} = actual strain of FRP at rupture.

Substituting Eq. (2) into Eq. (1), the confining pressure of the FRP confined rectangular concrete column at the corners is identical to that for a circular section

$$f_l = \frac{ntE_f \varepsilon_{fe}}{r} \tag{3}$$

where f_l = nominal confining pressure of the confined column; t = nominal thickness of FRP; n = number of FRP layers; and r = corner radius.

It is assumed that the radius of the curvature at middle of the section sides (as the column is bulging under an axial load) is much greater than that at the corners. As a result, from Eq. (3), the confining pressure of the column at the middle of the sides is rather small and could be negligible. Therefore, the appropriate confining stress of a FRP confined rectangular column should be at the corners. Bakis et al. (2002) similarly concluded that the confining stress is transmitted to the concrete at the four corners of the section. The actual rupture strain of FRP at the corners of the columns should be considered and recorded, which was recommended by Wang et al. (2012). Csuka and Kollár (2012) analytically proved that the distribution of the confining pressure of the FRP confined square columns is concentrated at the section corners [Fig. 1(b)].

Experimental Behavior of FRP Confined Rectangular Columns

Test Database

The number of specimens for an acceptable database was investigated before collating data of tested specimens. Table 1 summarizes the number of specimens of a few published models from the literature. Several experimental studies have been conducted on FRP confined rectangular or square concrete columns by researchers over the past few decades. The research described in this paper collated a test database of 190 FRP confined rectangular concrete columns (Table 2), reported by Rochette and Labossière (2000), Shehata et al. (2002), Lam and Teng (2003b), Ilki and Kumbasar (2003), Masia et al. (2004), Harajli et al. (2006), Rousakis et al. (2007), Al-Salloum (2007), Wang and Wu (2008), Tao et al. (2008), Wu and Wei (2010), and Wang et al. (2012). The database covers unconfined concrete compressive strength between 18.3 and 55.2 MPa. Different types of FRP were tested in the previously noted experiments, namely carbon FRP (CFRP), aramid FRP (AFRP), and glass FRP (GFRP). The majority of specimens were plain concrete except the reinforced specimens reported by Harajli et al. (2006) and Wang et al. (2012). The effect of reinforcing-bars in confining the concrete was deducted when calculating the FRP confined concrete strength. The dimensions of the specimens range from 79–305 mm and 100–305 mm for shorter and longer sides, respectively. The aspect ratio of the specimens ranged from 1–2.7, among them 1 (138 specimens), 1.3 (16 specimens), 1.5 (12 specimens), 1.7 (12 specimens), 2 (6 specimens), and 2.7 (6 specimens).

In the previously noted studies, reported FRP hoop strains were the average values from strain gages at the critical regions or were taken to be the same as lateral strains deduced from measurement of LVDTs at the midheight of the specimens. Only the hoop strains measured by strain gages were utilized in creating a model for estimating the actual rupture strain of FRP. Other strains deduced from the LVDTs are average values and do not represent the hoop strains at the critical points. The FRP hoop strains of those specimens were excluded from the database, whereas other results were still used in the verification.

For most specimens, the physical properties of FRP were determined from flat coupon tensile tests by the researchers themselves with the exception of those by Masia et al. (2004), Harajli et al. (2006), and Rousakis et al. (2007). However, the FRP properties provided by manufacturers in these studies are quite similar to the tensile properties of FRP tested by the other researchers. Those test results also fit very well with the selected models such that they were included in this database.

Table 1. Summary of Published Models

Papers	Square specimens	Rectangular specimens	Total number of specimens
Chaallal et al. (2003a)	19	—	19
Lam and Teng (2003b)	60	10	70
Al-Salloum (2007)	16	—	16
Youssef et al. (2007)	—	38	38
Wu and Wang (2009)	170	—	170
Wu and Wei (2010)	22	60	82
Toutanji et al. (2010)	59	—	59
Proposed model	138	52	190

Table 2. Test Results of FRP Confined Rectangular Specimens

Number	Branches[a]	Specimens b (mm)	h (mm)	r (mm)	Concrete f'_{co} (MPa)	Fiber-reinforced polymer Type[b]	Number of layers	t (mm)	f_f (MPa)	ε_{fu} (%)	E_f (GPa)	ε_{fe} (%)	f'_{cc} (MPa)
					Rochette and Labossière (2000)								
1	A	152	152	38	42.0	C	3	0.30	1,265	1.50	83	0.71	47.5
2	A	152	152	25	43.9	C	4	0.30	1,265	1.50	83	0.59	50.9
3	D	152	152	25	43.9	C	5	0.30	1,265	1.50	83	0.51	47.9
4	A	152	152	25	35.8	C	4	0.30	1,265	1.50	83	0.70	52.3
5	A	152	152	25	35.8	C	5	0.30	1,265	1.50	83	0.65	57.6
6	A	152	152	38	35.8	C	4	0.30	1,265	1.50	83	0.89	59.4
7	A	152	152	38	35.8	C	5	0.30	1,265	1.50	83	0.86	68.7
8	D	152	203	5	43.0	A	3	0.42	230	1.69	14	0.79	50.7
9	D	152	203	5	43.0	A	6	0.42	230	1.69	14	1.30	51.6
10	D	152	203	5	43.0	A	9	0.42	230	1.69	14	1.48	53.8
11	D	152	203	5	43.0	A	12	0.42	230	1.69	14	0.90	54.2
12	D	152	203	25	43.0	A	3	0.42	230	1.69	14	1.12	51.2
13	D	152	203	25	43.0	A	6	0.42	230	1.69	14	1.27	51.2
14	D	152	203	25	43.0	A	9	0.42	230	1.69	14	0.94	53.3
15	A	152	203	25	43.0	A	12	0.42	230	1.69	14	1.04	55.0
16	D	152	203	38	43.0	A	6	0.42	230	1.69	14	1.05	50.7
17	A	152	203	38	43.0	A	9	0.42	230	1.69	14	0.97	52.9
					Harajli et al. (2006)								
18	A	132	132	15	18.3	C	1	0.13	3,500	1.50	230	—	28.9
19	A	132	132	15	18.3	C	2	0.13	3,500	1.50	230	—	40.0
20	A	132	132	15	18.3	C	3	0.13	3,500	1.50	230	—	43.1
21	A	132	132	15	18.3	C	1	0.13	3,500	1.50	230	—	25.4
22	A	132	132	15	18.3	C	2	0.13	3,500	1.50	230	—	36.8
23	A	132	132	15	18.3	C	3	0.13	3,500	1.50	230	—	47.0
24	A	102	176	15	18.3	C	1	0.13	3,500	1.50	230	—	23.5
25	A	102	176	15	18.3	C	2	0.13	3,500	1.50	230	—	31.0
26	A	102	176	15	18.3	C	3	0.13	3,500	1.50	230	—	36.5
27	A	102	176	15	18.3	C	1	0.13	3,500	1.50	230	—	21.5
28	A	102	176	15	18.3	C	2	0.13	3,500	1.50	230	—	27.8
29	A	102	176	15	18.3	C	3	0.13	3,500	1.50	230	—	36.4
30	D	79	214	15	18.3	C	1	0.13	3,500	1.50	230	—	27.8
31	D	79	214	15	18.3	C	2	0.13	3,500	1.50	230	—	28.4
32	D	79	214	15	18.3	C	3	0.13	3,500	1.50	230	—	30.4
33	D	79	214	15	18.3	C	1	0.13	3,500	1.50	230	—	18.5
34	A	79	214	15	18.3	C	2	0.13	3,500	1.50	230	—	22.0
35	A	79	214	15	18.3	C	3	0.13	3,500	1.50	230	—	28.9
					Rousakis et al. (2007)								
36	D	200	200	30	33.0	C	1	0.12	3,720	1.55	240	—	38.4
37	A	200	200	30	33.0	C	3	0.12	3,720	1.55	240	—	45.9
38	A	200	200	30	33.0	C	5	0.12	3,720	1.55	240	—	55.6
39	D	200	200	30	33.0	G	3	0.14	1,820	2.80	65	—	42.6
40	A	200	200	30	33.0	G	6	0.14	1,820	2.80	65	—	44.4
41	A	200	200	30	33.0	G	9	0.14	1,820	2.80	65	—	51.9
42	D	200	200	30	34.0	C	1	0.12	3,720	1.55	240	—	42.2
43	D	200	200	30	34.0	C	3	0.12	3,720	1.55	240	—	45.2
44	A	200	200	30	34.0	C	5	0.12	3,720	1.55	240	—	54.6
45	D	200	200	30	38.0	G	6	0.14	1,820	2.80	65	—	52.8
46	D	200	200	30	38.0	G	9	0.14	1,820	2.80	65	—	59.8
47	D	200	200	30	40.0	G	6	0.14	1,820	2.80	65	—	54.2
48	D	200	200	30	40.0	G	9	0.14	1,820	2.80	65	—	59.5
					Lam and Teng (2003b)								
49	D	150	150	15	33.7	C	1	0.17	4,519	1.76	257	—	35.0
50	A	150	150	25	33.7	C	1	0.17	4,519	1.76	257	—	39.4
51	A	150	150	15	33.7	C	2	0.17	4,519	1.76	257	—	50.4
52	A	150	150	25	33.7	C	2	0.17	4,519	1.76	257	—	61.9
53	A	150	150	15	24.0	C	3	0.17	4,519	1.76	257	—	61.6
54	A	150	150	25	24.0	C	3	0.17	4,519	1.76	257	—	66.0
					Masia et al. (2004)								
55	A	100	100	25	25.5	C	2	0.13	3,500	1.50	230	—	55.9
56	A	100	100	25	22.8	C	2	0.13	3,500	1.50	230	—	48.7
57	A	100	100	25	25.1	C	2	0.13	3,500	1.50	230	—	45.7

Table 2. (*Continued*.)

Number	Branches[a]	Specimens			Concrete	Fiber-reinforced polymer							
		b (mm)	h (mm)	r (mm)	f'_{co} (MPa)	Type[b]	Number of layers	t (mm)	f_f (MPa)	ε_{fu} (%)	E_f (GPa)	ε_{fe} (%)	f'_{cc} (MPa)
						Masia et al. (2004)							
58	A	100	100	25	23.8	C	2	0.13	3,500	1.50	230	—	50.7
59	A	100	100	25	21.7	C	2	0.13	3,500	1.50	230	—	56.2
60	A	125	125	25	23.7	C	2	0.13	3,500	1.50	230	—	45.0
61	A	125	125	25	22.9	C	2	0.13	3,500	1.50	230	—	39.9
62	A	125	125	25	25.7	C	2	0.13	3,500	1.50	230	—	42.1
63	A	125	125	25	25.5	C	2	0.13	3,500	1.50	230	—	35.5
64	A	125	125	25	24.3	C	2	0.13	3,500	1.50	230	—	40.2
65	A	150	150	25	24.5	C	2	0.13	3,500	1.50	230	—	35.7
66	A	150	150	25	21.3	C	2	0.13	3,500	1.50	230	—	36.2
67	A	150	150	25	24.8	C	2	0.13	3,500	1.50	230	—	36.6
68	A	150	150	25	23.6	C	2	0.13	3,500	1.50	230	—	36.5
69	A	150	150	25	25.3	C	2	0.13	3,500	1.50	230	—	36.0
						Wang and Wu (2008)							
70	D	150	150	15	32.9	C	1	0.17	4,364	1.99	219	1.39	38.8
71	D	150	150	15	32.2	C	1	0.17	4,364	1.99	219	1.39	31.0
72	D	150	150	15	30.7	C	1	0.17	4,364	1.99	219	1.39	30.8
73	A	150	150	15	32.9	C	2	0.17	4,364	1.99	219	1.16	40.5
74	A	150	150	15	32.2	C	2	0.17	4,364	1.99	219	1.16	43.6
75	A	150	150	15	30.7	C	2	0.17	4,364	1.99	219	1.16	42.4
76	A	150	150	30	32.6	C	1	0.17	4,364	1.99	219	1.11	43.4
77	A	150	150	30	31.1	C	1	0.17	4,364	1.99	219	1.11	38.8
78	A	150	150	30	33.1	C	1	0.17	4,364	1.99	219	1.11	37.1
79	A	150	150	30	32.6	C	2	0.17	4,364	1.99	219	1.28	58.1
80	A	150	150	30	31.1	C	2	0.17	4,364	1.99	219	1.28	57.5
81	A	150	150	30	33.1	C	2	0.17	4,364	1.99	219	1.28	53.8
82	A	150	150	45	30.1	C	1	0.17	4,364	1.99	219	1.27	48.3
83	A	150	150	45	32.6	C	1	0.17	4,364	1.99	219	1.27	42.1
84	A	150	150	45	29.3	C	1	0.17	4,364	1.99	219	1.27	40.8
85	A	150	150	45	30.1	C	2	0.17	4,364	1.99	219	1.68	64.6
86	A	150	150	45	32.6	C	2	0.17	4,364	1.99	219	1.68	69.4
87	A	150	150	45	29.3	C	2	0.17	4,364	1.99	219	1.68	70.1
88	A	150	150	60	30.9	C	1	0.17	4,364	1.99	219	1.37	50.9
89	A	150	150	60	31.1	C	1	0.17	4,364	1.99	219	1.37	51.7
90	A	150	150	60	33.5	C	1	0.17	4,364	1.99	219	1.37	47.3
91	A	150	150	60	30.9	C	2	0.17	4,364	1.99	219	1.75	81.1
92	A	150	150	60	31.1	C	2	0.17	4,364	1.99	219	1.75	73.6
93	A	150	150	60	33.5	C	2	0.17	4,364	1.99	219	1.75	82.1
94	D	150	150	15	54.7	C	1	0.17	3,788	1.92	226	1.01	55.0
95	D	150	150	15	55.2	C	1	0.17	3,788	1.92	226	1.01	56.1
96	D	150	150	15	52.5	C	1	0.17	3,788	1.92	226	1.01	56.2
97	D	150	150	15	54.7	C	2	0.17	3,788	1.92	226	0.62	59.6
98	D	150	150	15	55.2	C	2	0.17	3,788	1.92	226	0.62	59.6
99	D	150	150	15	52.5	C	2	0.17	3,788	1.92	226	0.62	59.0
100	D	150	150	30	53.5	C	1	0.17	3,788	1.92	226	1.10	56.2
101	D	150	150	30	53.1	C	1	0.17	3,788	1.92	226	1.10	55.5
102	D	150	150	30	49.4	C	1	0.17	3,788	1.92	226	1.10	56.0
103	D	150	150	30	53.5	C	2	0.17	3,788	1.92	226	1.17	65.2
104	D	150	150	30	53.1	C	2	0.17	3,788	1.92	226	1.17	61.4
105	D	150	150	30	49.4	C	2	0.17	3,788	1.92	226	1.17	62.5
106	D	150	150	45	53.2	C	1	0.17	3,788	1.92	226	1.34	56.4
107	D	150	150	45	51.5	C	1	0.17	3,788	1.92	226	1.34	58.4
108	D	150	150	45	53.3	C	1	0.17	3,788	1.92	226	1.34	57.9
						Wang and Wu (2008)							
109	A	150	150	45	53.2	C	2	0.17	3,788	1.92	226	1.27	81.3
110	A	150	150	45	51.5	C	2	0.17	3,788	1.92	226	1.27	78.8
111	A	150	150	45	53.3	C	2	0.17	3,788	1.92	226	1.27	80.9
112	A	150	150	60	53.9	C	1	0.17	3,788	1.92	226	1.39	62.4
113	A	150	150	60	52.0	C	1	0.17	3,788	1.92	226	1.39	62.7
114	A	150	150	60	52.3	C	1	0.17	3,788	1.92	226	1.39	62.8
115	A	150	150	60	53.9	C	2	0.17	3,788	1.92	226	1.38	87.9
116	A	150	150	60	52.0	C	2	0.17	3,788	1.92	226	1.38	90.9
117	A	150	150	60	52.3	C	2	0.17	3,788	1.92	226	1.38	90.4

Table 2. (*Continued*.)

Number	Branches[a]	Specimens			Concrete	Fiber-reinforced polymer							
		b (mm)	h (mm)	r (mm)	f'_{co} (MPa)	Type[b]	Number of layers	t (mm)	f_f (MPa)	ε_{fu} (%)	E_f (GPa)	ε_{fe} (%)	f'_{cc} (MPa)
						Wu and Wei (2010)							
118	A	150	150	30	35.3	C	1	0.17	4,192	1.84	229	1.84	40.5
119	A	150	150	30	35.3	C	1	0.17	4,192	1.84	229	1.84	40.7
120	A	150	150	30	35.3	C	1	0.17	4,192	1.84	229	1.84	42.5
121	A	150	150	30	35.3	C	2	0.17	4,192	1.84	229	1.21	59.2
122	A	150	150	30	35.3	C	2	0.17	4,192	1.84	229	1.21	59.6
123	A	150	150	30	35.3	C	2	0.17	4,192	1.84	229	1.21	62.3
124	D	150	188	30	35.3	C	1	0.17	4,192	1.84	229	1.46	38.0
125	D	150	188	30	35.3	C	1	0.17	4,192	1.84	229	1.46	38.9
126	D	150	188	30	35.3	C	1	0.17	4,192	1.84	229	1.46	39.4
127	A	150	188	30	35.3	C	2	0.17	4,192	1.84	229	1.33	48.8
128	A	150	188	30	35.3	C	2	0.17	4,192	1.84	229	1.33	51.9
129	A	150	188	30	35.3	C	2	0.17	4,192	1.84	229	1.33	53.3
130	D	150	225	30	35.3	C	1	0.17	4,192	1.84	229	1.58	37.6
131	D	150	225	30	35.3	C	1	0.17	4,192	1.84	229	1.58	35.6
132	D	150	225	30	35.3	C	1	0.17	4,192	1.84	229	1.58	39.2
133	A	150	225	30	35.3	C	2	0.17	4,192	1.84	229	1.44	43.0
134	A	150	225	30	35.3	C	2	0.17	4,192	1.84	229	1.44	45.2
135	A	150	225	30	35.3	C	2	0.17	4,192	1.84	229	1.44	43.4
136	D	150	260	30	35.3	C	1	0.17	4,192	1.84	229	1.31	35.2
137	D	150	260	30	35.3	C	1	0.17	4,192	1.84	229	1.31	37.8
138	D	150	260	30	35.3	C	1	0.17	4,192	1.84	229	1.31	37.6
139	D	150	260	30	35.3	C	2	0.17	4,192	1.84	229	1.72	38.9
140	D	150	260	30	35.3	C	2	0.17	4,192	1.84	229	1.72	41.4
141	D	150	260	30	35.3	C	2	0.17	4,192	1.84	229	1.72	41.3
142	D	150	300	30	35.3	C	1	0.17	4,192	1.84	229	1.15	36.6
143	D	150	300	30	35.3	C	1	0.17	4,192	1.84	229	1.15	37.7
144	D	150	300	30	35.3	C	1	0.17	4,192	1.84	229	1.15	38.0
145	D	150	300	30	35.3	C	2	0.17	4,192	1.84	229	1.37	38.6
						Wu and Wei (2010)							
146	D	150	300	30	35.3	C	2	0.17	4,192	1.84	229	1.37	39.1
147	D	150	300	30	35.3	C	2	0.17	4,192	1.84	229	1.37	39.3
						Wang et al. (2012)							
148	D	305	305	30	25.5	C	1	0.17	4,340	1.81	240	0.88	17.2
149	D	305	305	30	25.5	C	2	0.17	4,340	1.81	240	0.70	24.4
150	D	305	305	30	25.5	C	1	0.17	4,340	1.81	240	0.37	19.4
151	D	305	305	30	25.5	C	2	0.17	4,340	1.81	240	0.28	26.0
152	D	305	305	30	25.5	C	3	0.17	4,340	1.81	240	0.60	29.2
153	D	305	305	30	25.5	C	1	0.17	4,340	1.81	240	—	24.9
154	D	305	305	30	25.5	C	2	0.17	4,340	1.81	240	0.33	26.2
155	D	305	305	30	25.5	C	3	0.17	4,340	1.81	240	1.24	31.1
156	D	204	305	20	25.5	C	1	0.17	4,340	1.81	240	0.86	25.0
157	A	204	305	20	25.5	C	2	0.17	4,340	1.81	240	0.62	31.4
158	D	204	305	20	25.5	C	1	0.17	4,340	1.81	240	—	29.7
159	A	204	305	20	25.5	C	2	0.17	4,340	1.81	240	—	35.3
160	D	204	305	20	25.5	C	1	0.17	4,340	1.81	240	—	26.9
161	A	204	305	20	25.5	C	2	0.17	4,340	1.81	240	1.42	36.1
						Shehata et al. (2002)							
162	D	150	150	10	23.7	C	1	0.17	3,550	1.50	235	—	27.4
163	D	150	150	10	23.7	C	2	0.17	3,550	1.50	235	—	36.5
164	D	150	150	10	29.5	C	1	0.17	3,550	1.50	235	—	40.4
165	D	150	150	10	29.5	C	2	0.17	3,550	1.50	235	—	43.7
						Ilki and Kumbasar (2003)							
166	D	250	250	40	32.8	C	1	0.17	3,430	1.50	230	—	32.7
167	D	250	250	40	32.8	C	1	0.17	3,430	1.50	230	—	32.3
168	A	250	250	40	32.8	C	3	0.17	3,430	1.50	230	—	41.4
169	A	250	250	40	32.8	C	3	0.17	3,430	1.50	230	—	40.6
170	A	250	250	40	32.8	C	5	0.17	3,430	1.50	230	—	56.7
171	A	250	250	40	32.8	C	5	0.17	3,430	1.50	230	—	53.6

Table 2. (*Continued*.)

Number	Branches[a]	Specimens b (mm)	h (mm)	r (mm)	Concrete f'_{co} (MPa)	Fiber-reinforced polymer Type[b]	Number of layers	t (mm)	f_f (MPa)	ε_{fu} (%)	E_f (GPa)	ε_{fe} (%)	f'_{cc} (MPa)
					Al-Salloum (2007)								
172	D	150	150	5	28.7	C	1	1.20	935	1.25	75	—	41.2
173	D	150	150	5	30.9	C	1	1.20	935	1.25	75	—	42.5
174	A	150	150	25	31.8	C	1	1.20	935	1.25	75	—	48.3
175	A	150	150	25	28.5	C	1	1.20	935	1.25	75	—	45.6
176	A	150	150	38	27.7	C	1	1.20	935	1.25	75	—	57.0
177	A	150	150	38	30.3	C	1	1.20	935	1.25	75	—	55.0
178	A	150	150	50	26.7	C	1	1.20	935	1.25	75	—	61.7
179	A	150	150	50	28.3	C	1	1.20	935	1.25	75	—	63.7
					Tao et al. (2008)								
180	A	150	150	20	22.0	C	1	0.17	4,470	1.87	239	—	33.5
181	A	150	150	20	22.0	C	2	0.17	4,470	1.87	239	—	49.6
182	A	150	150	20	19.5	C	2	0.17	4,470	1.87	239	—	47.2
183	A	150	150	35	22.0	C	2	0.17	4,470	1.87	239	—	64.8
184	A	150	150	35	19.5	C	2	0.17	4,470	1.87	239	—	58.7
185	A	150	150	50	22.0	C	2	0.17	4,470	1.87	239	—	76.6
186	A	150	150	50	19.5	C	2	0.17	4,470	1.87	239	—	63.6
187	D	150	150	20	49.5	C	1	0.17	4,470	1.87	239	—	54.2
188	A	150	150	20	49.5	C	2	0.17	4,470	1.87	239	—	61.4
189	A	150	150	35	49.5	C	2	0.17	4,470	1.87	239	—	84.9
190	A	150	150	50	49.5	C	2	0.17	4,470	1.87	239	—	86.1

[a]A and D stand for ascending and descending branches of stress-strain diagrams, respectively.
[b]Type of FRP (i.e., C, A, and G) stands for carbon FRP, aramid FRP, and glass FRP, respectively.

Failure Modes and Distribution of FRP Strain

The specimens in Table 2 failed suddenly by tensile rupture of the FRP wrap within the midheight region. The rupture position was experimentally confirmed at or near the corners of the sections (Rochette and Labossiére 2000; Chaallal et al. 2003b; Wang et al. 2012; Hadi et al. 2013). Thus, the mechanism of the FRP confined rectangular columns should focus on the FRP hoop strain at the corners.

The distribution of FRP hoop strain is not uniform around the perimeter of the columns. The rupture of FRP always happens at the corner regions such that the hoop strain of FRP was expected to have the highest value at these zones. A few studies investigated the FRP hoop strain at the middle of the sides and at the corners. The FRP hoop strain at the middle of the sides is always greater than at the corners (Rochette and Labossiére 2000; Smith et al. 2010; Wang et al. 2012). As a result, the mean value of all the hoop strains (including the strains at the middle of the sides and at the corners) overestimates the rupture strain and the confinement effectiveness of FRP. In addition, the confinement is assumed to be available at the high-curvature locations (e.g., corners of the sections) [Eq. (1)]. Confinement is therefore only appropriate at the corners of the sections. For convenience, the phrase rupture strain of FRP stands for the rupture strain of FRP at the corners of the sections.

Rupture Strain of FRP in Rectangular Sections

Wang and Wu (2008) conducted experiments to investigate the effect of corner radius on the rupture strain of FRP. They showed that when the radius of the corners increases, the rupture strain of FRP generally increases. An investigation was also conducted in the database reported in this paper to yield the same result. It is assumed that the FRP rupture strain is dependent on the ratio of the corner radius and the side length, which could be $2r/b$ or $2r/h$. In addition, Wu and Wei (2010) investigated the effects of the aspect ratio (h/b) on the rupture strain of FRP. They depicted that when the aspect ratio (h/b) ranged from 1–2, the FRP rupture strains at corners of rectangular sections were identical or close together. This indicates that the FRP rupture strain maintained at a certain value as tested columns had different long-side length of sections but the same short-side length of section and material properties (unconfined concrete strength, number of FRP layers, and corners radius). In such cases, these columns had the same ratio of the corner radius and the short-side length ($2r/b$). Therefore, the writers assumed that the actual rupture strain of FRP is a function of the ratio of the corner radius and the shorter-side length ($2r/b$).

Furthermore, an investigation was conducted on the database to show the dependence of the actual rupture strain of FRP on the confinement stiffness ratios R_s (Rochette and Labossiére 2000; Wang and Wu 2008; Wang et al. 2012). The confinement stiffness ratio (R_s) was defined by Teng et al. (2009)

$$R_s = \frac{2ntE_f}{\left(\frac{f'_{co}}{\varepsilon_{co}}\right)D} \tag{4}$$

where f'_{co} = unconfined concrete strength (MPa); ε_{co} = its corresponding strain; and D = diameter of circular sections.

As this paper deals with rectangular sections, Eq. (4) was modified by replacing $D/2$ with r, which is the corner radius of rectangular sections

$$R_s = \frac{ntE_f}{\left(\frac{f'_{co}}{\varepsilon_{co}}\right)r} \tag{5}$$

To use Eq. (5), when the value of ε_{co} was not specified by the database, it was calculated in accordance with Tasdemir et al. (1998)

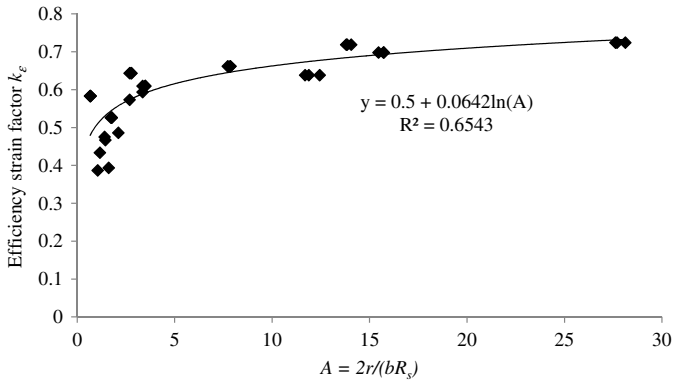

Fig. 2. Relationship between factor A and FRP strain-efficiency factor k_ε

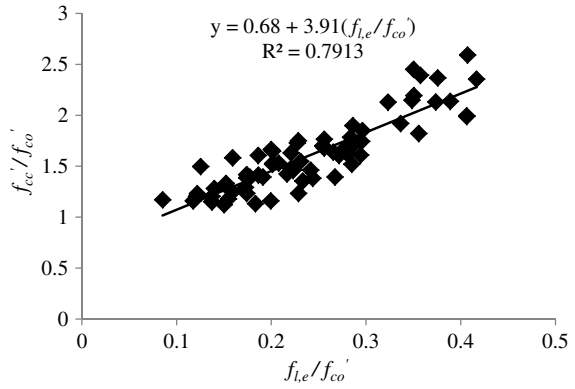

Fig. 3. Relationship between normalized confining stress and normalized confined strength (strength equation)

$$\varepsilon_{co} = (-0.067f_{co}'^2 + 29.9f_{co}' + 1{,}053)10^{-6} \quad (6)$$

In conclusion, it is assumed that the actual rupture strain of FRP is a function of the ratio of the corner radius and the shorter-side length ($2r/b$) in addition to the confinement stiffness ratio (R_s). Fig. 2 shows the relationship between the FRP strain efficiency factor (k_ε), which is the ratio of the actual rupture strain of FRP and the ultimate strain of FRP from flat coupon tensile tests, and the factor A

$$A = \frac{2r}{bR_s} \quad (7)$$

where b = shorter-side length of the column section. In accordance with linear regression analysis, the value of the FRP strain efficiency factor (k_ε) was obtained for FRP confined rectangular columns

$$k_\varepsilon = 0.5 + 0.0642\ \ln(A) \quad (8)$$

To generate Eq. (8), the rupture strain of FRP at the corners of sections needs to be reported. Only a few specimens in Table 2 reported the FRP rupture strain at the corners of sections. Thus, the database used to generate Eq. (8) is smaller than the database used to verify the proposed model. Based on Fig. 2, the FRP strain efficiency factor varied between 0.4 and 0.7. It is conservatively recommended that the FRP strain efficiency factor be neither less than 0.4 nor greater than 0.7.

Proposed Model

Equation for Confined Concrete Strength

As noted previously, the confining pressure of a FRP confined rectangular column is not uniform around the perimeter of the sections. Thus, the FRP confinement herein is only to account for the confinement effect at the corners. The corner effect ratio (k_c) introduced by Pham and Hadi (2013) was utilized to calculate the effective confining pressure ($f_{l,e}$). The corner effect ratio is the ratio of the total length of the four round corners and the circumference of the section

$$f_{l,e} = f_l k_c \quad (9)$$

$$k_c = \frac{\pi r}{b + h - r(4 - \pi)} \quad (10)$$

where f_l = nominal confining pressure, which was calculated from Eq. (3); and b and h = short and long sides of the column section, respectively.

The experimental stress-strain curves show two typical types, as follows: (1) ascending branches, and (2) descending branches. In most cases, a FRP confined concrete column is expected to provide an ascending-type curve that exhibits the well-known bilinear shape. This curve ends with the rupture of the confining jacket at the ultimate point defined by the compressive strength f_{cc}' and the ultimate axial strain ε_{cc}. Based on the results of the ascending-type specimens in the database, the relationship between the normalized compressive strength and the normalized confining pressure is linear (Fig. 3). Eq. (11) formulates the previously noted linear relationship

$$\frac{f_{cc}'}{f_{co}'} = 0.68 + 3.91\frac{f_{l,e}}{f_{co}'} \quad (11)$$

In brief, Eq. (11) was used to calculate the compressive strength of confined concrete for specimens that have sufficient confinement. In such cases, the effective confining pressure ($f_{l,e}$) of specimens needs to be greater than a certain value estimated from Eq. (12), to be presented in the next section.

Minimum Amount of FRP for Sufficient Confinement

A FRP confined concrete column that exhibits the ascending-type curve is defined as the sufficient confinement. In such a case, a significant improvement of the compressive strength and strain of a FRP confined concrete column could be expected. Otherwise, FRP confined concrete with a stress-strain curve of the descending type illustrates a concrete stress at the ultimate strain less than the compressive strength of unconfined concrete. A confined column needs a minimum amount of FRP to obtain sufficient confinement. Fig. 4 shows the relationship between the normalized compressive strength and the normalized effective confining pressure. From Fig. 4, to avoid the descending-type specimens, the normalized effective confining pressure should not be less than 0.15

$$\frac{f_{l,e}}{f_{co}'} \geq 0.15 \quad (12)$$

Briefly, the proposed model is summarized by the following steps: (1) the FRP strain efficiency factor (k_ε) is estimated using Eq. 8, (2) the effective confining pressure ($f_{l,e}$) is calculated using Eqs. (3), 9), and (10) the compressive strength of confined concrete (f_{cc}') is computed as recommended in Eq. (11).

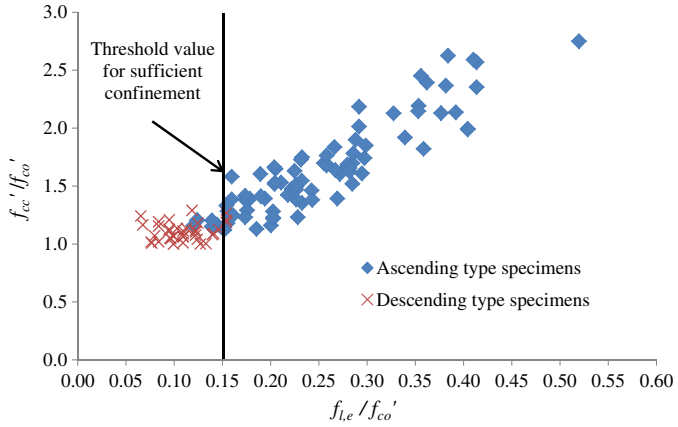

Fig. 4. Relationship between normalized confining stress and normalized confined strength (minimum amount of FRP for sufficient confinement)

Verification of the Proposed Model

The model performance was tested by using three statistical indicators, as follows: (1) mean square error (MSE), (2) average absolute error (AAE), and (3) standard deviation (SD), as determined by Eqs. (13)–(15)

$$\text{MSE} = \frac{\sum_1^N \left(\frac{\text{pre}_i - \text{exp}_i}{exp_i}\right)^2}{N} \tag{13}$$

$$\text{AAE} = \frac{\sum_1^N \left|\frac{\text{pre}_i - \text{exp}_i}{\text{exp}_i}\right|}{N} \tag{14}$$

$$\text{SD} = \sqrt{\frac{\sum_1^N \left(\frac{\text{pre}_i}{\text{exp}_i} - \frac{\text{pre}_{\text{avg}}}{\text{exp}_{\text{avg}}}\right)^2}{N-1}} \tag{15}$$

where pre = model predictions; exp = experimental results; the subscript avg indicates the average value; and N = total number of the test data. In general, the mean square error shows the errors to be more significant compared with the average absolute error such that it was used to emphasize the precision of the selected models.

Fig. 5 shows 104 data points (ascending-type specimens) to assess the performance of the existing models and the proposed model. Five existing models were studied in this verification (Chaallal et al. 2003a; Lam and Teng 2003b; Wu and Wang 2009; Toutanji et al. 2010; Wu and Wei 2010). The comparison between the predictions and test results (Fig. 5) shows the improvement of the selected models in calculating the strength of FRP confined rectangular columns for a decade. Among the presented models, the proposed model has the largest general correlation ($R^2 = 89\%$) for a linear trend between the predictions and test results. In addition, the error of the models was statistically verified (Fig. 6).

Although the establishment of the proposed model was based on the database of the ascending-type specimens, the proposed model was also validated with the full database (including the descending-type specimens) to verify its applicability to the descending-type specimens. Fig. 7 illustrates that the proposed model predicts very well the compressive strength of FRP confined rectangular columns for both the ascending-type and descending-type of specimens (190 data points). The linear trend between the predictions and test results has the general correlation factor of 0.82 ($R^2 = 82\%$), which is a small decrease compared with Fig. 5.

As noted previously, the behavior of the FRP jacket comply with the membrane hypothesis, in which the ratio of the round corners (r) and nominal jacket thickness (t) should be greater than 20 ($r/t > 20$). Four specimens had the dimensions of 152×203 mm^2 and corner radius of 5 mm (Rochette and Labossiére 2000). These specimens were wrapped with a number of FRP layers to have a thickness of 1.2, 2.4, 3.6, and 4.8 mm (the r/t ratios ranges between 4.2 and 1), respectively. Two specimens presented in the study of Al-Salloum (2007) also had a corner radius of 5 mm (the r/t ratio was 4.2). Therefore, the predictions of the proposed

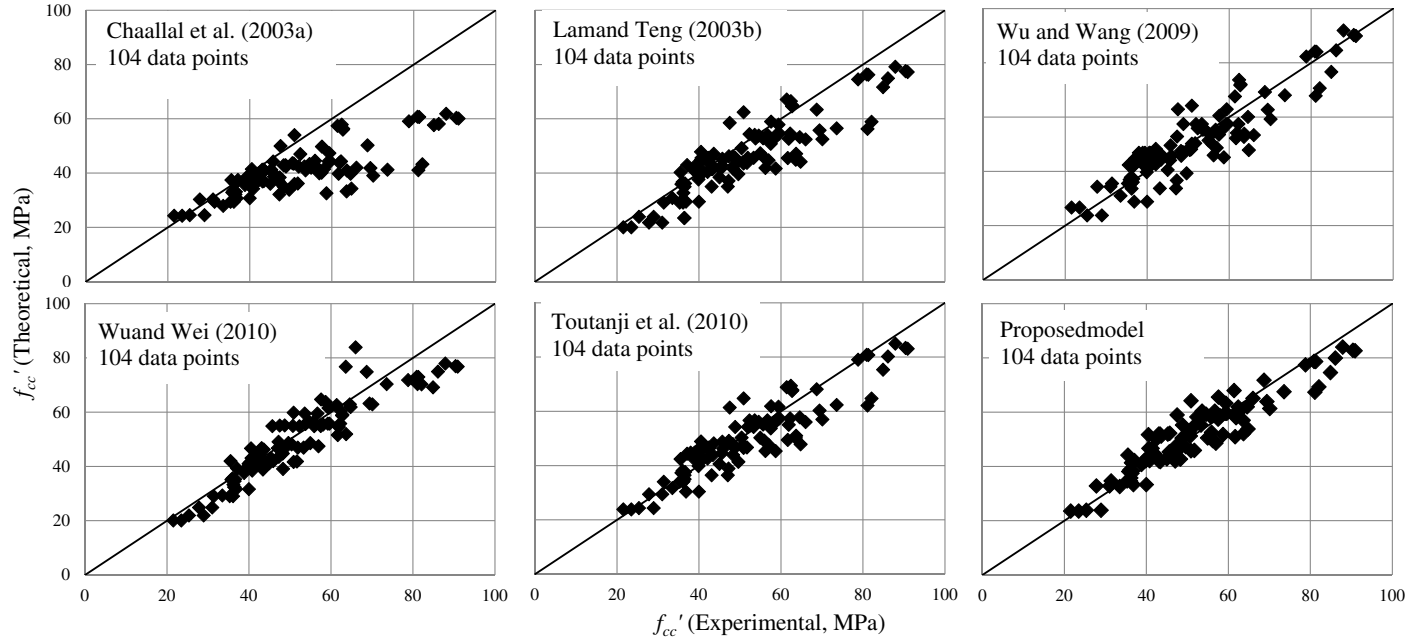

Fig. 5. Performance of the selected models (ascending-type specimens)

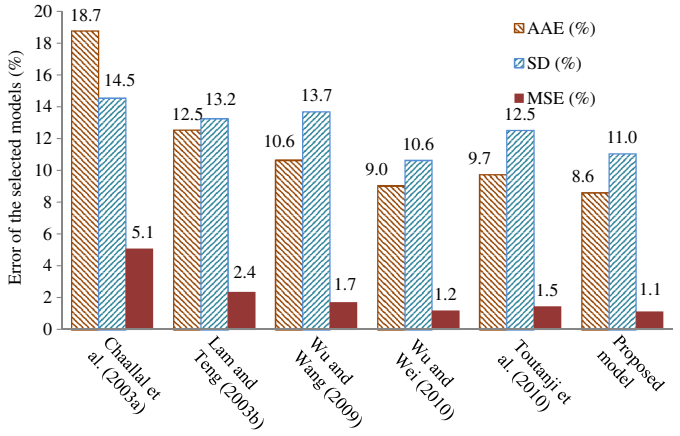

Fig. 6. Accuracy of the selected models

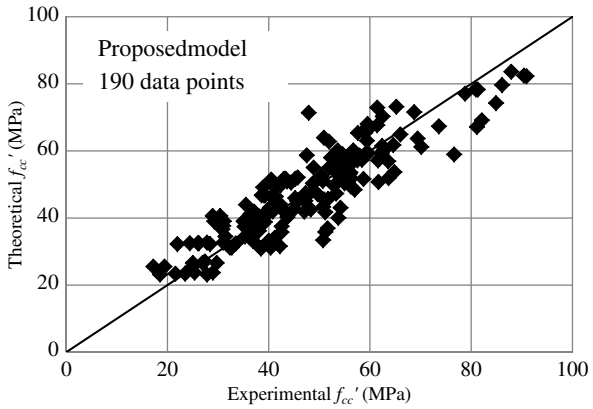

Fig. 7. Performance of the proposed models (ascending-type and descending-type specimens)

model on the strength of six specimens are not accurate ($f'_{cc(\text{pre})}/f'_{cc(\text{exp})} \approx 0.75$). It is recommended that FRP confined rectangular columns should be round to have a ratio of r/t greater than 20.

Conclusions

A model was proposed to calculate the strength of FRP confined rectangular columns. The predictions of the proposed model fit very well with the experimental results. The research reported in this paper addresses the approach to analyze the mechanism of FRP confined rectangular columns, the actual rupture strain of FRP at the corners of specimens, and the minimum amount of FRP to obtain sufficient confinement. The findings presented in this paper are summarized as follows:

- The membrane hypothesis was utilized to analyze the behavior of FRP confined rectangular columns. The confining pressure of confined columns is concentrated at the corners of the section only. To comply with the membrane hypothesis, the corner of the sections should be rounded to have a radius being at least 20× greater than the nominal FRP thickness.
- The corner effect ratio (k_c) was accounted for the effects of the nonuniform confining pressure around rectangular sections. It was used to distribute equally the confining pressure at the corners of rectangular sections to the entire circumference of the sections.
- The actual rupture strain of FRP at the corners of the sections depends on the ratio of the corner radius and the length of the shorter side in addition to the confinement stiffness ratio as presented in Eq. (5). Additional equations were proposed that enable calculation of the actual rupture strain of FRP.
- The limit of the FRP amount to obtain sufficient confinement was proposed. This limit is based on the ratio of the corner radius, length of the shorter side, and confinement stiffness ratio.

Finally, this paper used the membrane hypothesis to formulate the confining behaviors of FRP confined rectangular columns. This approach directly analyzes the behavior of confined square sections without conversion from equivalent circular sections to create a model for rectangular sections. The proposed model results in a good correlation with experimental results.

Acknowledgments

The first writer acknowledges the Vietnamese Government and the University of Wollongong for support of his full Ph.D. scholarship.

Notation

The following symbols are used in this paper:

A = factor defined in Eq. (7);
b = short side of column sections;
D = diameter of circular sections;
E_f = elastic modulus of FRP;
f'_{cc} = confined concrete strength;
f'_{co} = unconfined concrete strength;
f_f = tensile strength of FRP;
f_{fe} = actual tensile stress of FRP;
f_l = nominal confining pressure of a column;
$f_{l,e}$ = effective confining pressure of a column;
h = long side of column sections;
k_c = corner-effect ratio;
k_s = shape factor;
k_ε = FRP strain efficiency factor;
N = total number of test data;
n = number of FRP layers;
p = hydrostatic pressure applied in a shell structure;
R_s = confinement stiffness ratio;
r = corner radius of a section;
T = tension force in a shell structure;
t = nominal thickness of FRP;
ε_{cc} = ultimate axial strain of confined concrete;
ε_{co} = axial strain of the unconfined concrete at the maximum stress; and
ε_{fe} = actual strain of FRP at rupture.

References

Al-Salloum, Y. A. (2007). "Influence of edge sharpness on the strength of square concrete columns confined with FRP composite laminates." *Compos. Part B Eng.*, 38(5), 640–650.

Bakis, C. E., et al. (2002). "Fiber-reinforced polymer composites for construction–State-of-the-art review." *J. Compos. Constr.*, 10.1061/(ASCE)1090-0268(2002)6:2(73), 73–87.

Calladine, C. R. (1983). *Theory of shell structures*, Cambridge University Press, Cambridge, UK.

Chaallal, O., Hassan, M., and Shahawy, M. (2003a). "Confinement model for axially loaded short rectangular columns strengthened with fiber-reinforced polymer wrapping." *ACI Struct. J.*, 100(2), 215–221.

Chaallal, O., Shahawy, M., and Hassan, M. (2003b). "Performance of axially loaded short rectangular columns strengthened with carbon fiber-reinforced polymer wrapping." *J. Compos. Constr.*, 10.1061/(ASCE)1090-0268(2003)7:3(200), 200–208.

Csuka, B., and Kollár, L. P. (2012). "Analysis of FRP confined columns under eccentric loading." *Compos. Struct.*, 94(3), 1106–1116.

Cui, C., and Sheikh, S. A. (2010). "Analytical model for circular normal- and high-strength concrete columns confined with FRP." *J. Compos. Constr.*, 10.1061/(ASCE)CC.1943-5614.0000115, 562–572.

Hadi, M. N. S., Pham, T. M., and Lei, X. (2013). "New method of strengthening reinforced concrete square columns by circularizing and wrapping with fiber-reinforced polymer or steel straps." *J. Compos. Constr.*, 10.1061/(ASCE)CC.1943-5614.0000335, 229–238.

Harajli, M. H., Hantouche, E., and Soudki, K. (2006). "Stress-strain model for fiber-reinforced polymer jacketed concrete columns." *ACI Struct. J.*, 103(5), 672–682.

Ilki, A., and Kumbasar, N. (2003). "Compressive behaviour of carbon fibre composite jacketed concrete with circular and non-circular cross-sections." *J. Earthq. Eng.*, 7(3), 381–406.

Lam, L., and Teng, J. G. (2003a). "Design-oriented stress-strain model for FRP-confined concrete." *Constr. Build. Mater.*, 17(6–7), 471–489.

Lam, L., and Teng, J. G. (2003b). "Design-oriented stress-strain model for FRP-confined concrete in rectangular columns." *J. Reinf. Plast. Compos.*, 22(13), 1149–1186.

Lee, C.-S., Hegemier, G. A., and Phillippi, D. J. (2010). "Analytical model for fiber-reinforced polymer-jacketed square concrete columns in axial compression." *ACI. Struct. J.*, 107(2), 208–217.

Masia, M. J., Gale, T. N., and Shrive, N. G. (2004). "Size effects in axially loaded square-section concrete prisms strengthened using carbon fibre reinforced polymer wrapping." *Can. J. Civ. Eng.*, 31(1), 1–13.

Pham, T. M., and Hadi, M. N. S. (2013). "Strain estimation of CFRP confined concrete columns using energy approach." *J. Compos. Constr.*, 10.1061/(ASCE)CC.1943-5614.0000397, 04013001.

Richart, F. E., Brandtzaeg, A., and Brown, R. L. (1928). "A study of the failure of concrete under combined compressive stress." *Bulletin 1985*, Univ. of Illinois Engineering Experimental Station, Champaign, IL.

Rochette, P., and Labossiére, P. (2000). "Axial testing of rectangular column models confined with composites." *J. Compos. Constr.*, 10.1061/(ASCE)1090-0268(2000)4:3(129), 129–136.

Rousakis, T. C., Karabinis, A. I., and Kiousis, P. D. (2007). "FRP-confined concrete members: Axial compression experiments and plasticity modelling." *Eng. Struct.*, 29(7), 1343–1353.

Shehata, I. A. E. M., Carneiro, L. A. V., and Shehata, L. C. D. (2002). "Strength of short concrete columns confined with CFRP sheets." *Mater. Struct.*, 35(1), 50–58.

Smith, S. T., Kim, S. J., and Zhang, H. W. (2010). "Behavior and effectiveness of FRP wrap in the confinement of large concrete cylinders." *J. Compos. Constr.*, 10.1061/(ASCE)CC.1943-5614.0000119, 573–582.

Spoelstra, M. R., and Monti, G. (1999). "FRP-confined concrete model." *J. Compos. Constr.*, 10.1061/(ASCE)1090-0268(1999)3:3(143), 143–150.

Tao, Z., Yu, Q., and Zhong, Y. Z. (2008). "Compressive behaviour of CFRP-confined rectangular concrete columns." *Mag. Concrete Res.*, 60(10), 735–745.

Tasdemir, M. A., et al. (1998). "Evaluation of strains at peak stresses in concrete: A three-phase composite model approach." *Cement Concrete Compos.*, 20(4), 301–318.

Teng, J. G., Jiang, T., Lam, L., and Luo, Y. Z. (2009). "Refinement of a design-oriented stress-strain model for FRP-confined concrete." *J. Compos. Constr.*, 10.1061/(ASCE)CC.1943-5614.0000012, 269–278.

Toutanji, H., Han, M., Gilbert, J., and Matthys, S. (2010). "Behavior of large-scale rectangular columns confined with FRP composites." *J. Compos. Constr.*, 10.1061/(ASCE)CC.1943-5614.0000051, 62–71.

Wang, L. M., and Wu, Y. F. (2008). "Effect of corner radius on the performance of CFRP-confined square concrete columns: Test." *Eng. Struct.*, 30(2), 493–505.

Wang, Z. Y., Wang, D. Y., Smith, S. T., and Lu, D. G. (2012). "CFRP-confined square RC columns. I: Experimental investigation." *J. Compos. Constr.*, 10.1061/(ASCE)CC.1943-5614.0000245, 150–160.

Wu, Y. F., and Wang, L. M. (2009). "Unified strength model for square and circular concrete columns confined by external jacket." *J. Struct. Eng.*, 10.1061/(ASCE)0733-9445(2009)135:3(253), 253–261.

Wu, Y. F., and Wei, Y. Y. (2010). "Effect of cross-sectional aspect ratio on the strength of CFRP-confined rectangular concrete columns." *Eng. Struct.*, 32(1), 32–45.

Wu, Y. F., and Zhou, Y. W. (2010). "Unified strength model based on Hoek-Brown failure criterion for circular and square concrete columns confined by FRP." *J. Compos. Constr.*, 10.1061/(ASCE)CC.1943-5614.0000062, 175–184.

Yazici, V., and Hadi, M. N. S. (2012). "Normalized confinement stiffness approach for modeling FRP-confined concrete." *J. Compos. Constr.*, 10.1061/(ASCE)CC.1943-5614.0000283, 520–528.

Youssef, M. N., Feng, M. Q., and Mosallam, A. S. (2007). "Stress–strain model for concrete confined by FRP composites." *Compos. B Eng.*, 38(5), 614–628.

3.2 Compressive Strain

Summary

A new model is presented for calculating the axial strain of carbon fibre reinforced polymer (CFRP) confined concrete columns. An energy balance approach is introduced to establish a relationship of the energy absorption between a confined concrete column and CFRP. The proposed model was verified using a large database collected from 167 CFRP-confined plain concrete specimens. This database contains 98 circular specimens with diameters ranging between 100 mm and 152 mm and 69 square specimens having a side length ranging between 100 mm and 152 mm. The database covers unconfined concrete strengths from 20 MPa to 50 MPa. The proposed model shows very good correlation with the experimental results. In addition, the proposed model also provides comparative prediction of strain of CFRP-confined concrete columns in two extreme cases: insufficient confinement and heavy confinement, which are not usually well predicted by other models.

Citation

This paper was published in Journal of Composites for Construction with the following citation:

Pham, T.M., and Hadi, M.N.S. (2013). "Strain Estimation of CFRP-confined Concrete Columns Using Energy Approach." *Journal of Composites for Construction*, 17(6), 04013001-1-04013001-11.

Strain Estimation of CFRP-Confined Concrete Columns Using Energy Approach

Thong M. Pham, S.M.ASCE[1]; and Muhammad N. S. Hadi, M.ASCE[2]

Abstract: A new model is presented for calculating the axial strain of carbon fiber-reinforced polymer (CFRP)-confined concrete columns. An energy-balance approach is introduced to establish a relationship of the energy absorption between a confined concrete column and CFRP. The proposed model was verified using a large database collected from 167 CFRP-confined plain concrete specimens. This database contains 98 circular specimens with diameters ranging between 100 and 152 mm, and 69 square specimens having a side length ranging between 100 and 152 mm. The database covers unconfined concrete strengths from 20 to 50 MPa. The proposed model shows very good correlation with the experimental results. In addition, the proposed model also provides a comparative prediction of the strain of CFRP-confined concrete columns in two extreme cases, i.e., (1) insufficient confinement, and (2) heavy confinement, which are not usually well predicted by other models. **DOI: 10.1061/(ASCE)CC.1943-5614.0000397.**

Author keywords: Carbon-fiber-reinforced polymer; Energy methods; Energy dissipation; Stress-strain relations.

Introduction

The use of carbon-fiber-reinforced polymers (CFRPs) in structural engineering has increased in recent years. However, estimating the capacity of FRP-confined concrete members is not very well-correlated with their actual behavior; as such, more attention must be paid to models for FRP-confined concrete. A complete model includes formulas to calculate the ultimate strength and ultimate strain of confined concrete and stress-strain relationships. Most of these studies have focused on the strength and stress-strain relationships of confined concrete. Not many models deal with strain prediction. Bisby et al. (2005) carried out an overview, and they conclude that existing models show a poor correlation with experimental results of confined concrete strain. Bisby et al. (2005) revealed that the mean absolute error of strain estimations ranges from 35 to 250%, whereas the error of strength estimation is less than 20%. The literature of FRP-confined concrete is excellent for calculating the confined concrete strength but not for calculating the corresponding strain.

Richart et al. (1929) reported that the axial strain at the compressive strength of confined concrete can be linearly related to the maximum confining pressure. Early studies, based on this assumption, that proposed formulas for strain estimation include Karbhari and Gao (1997), Miyauchi et al. (1999), Toutanji (1999), and Ilki et al. (2008). Another commonly used approach is based on volume strain and dilation behavior (Lam and Teng 2003a, b) or regression analysis of experiments (Shehata et al. 2002). All of the previously noted studies used the mechanism behavior of confined concrete to obtain strain estimations. In addition, Mander et al. (1988) proposed an energy-balanced method to calculate the strain of steel confined concrete. This method assumes that the additional strain energy of a confined concrete column is equal to the energy used to fracture the hoops. A study by Saadatmanesh et al. (1994) adopted this method to calculate the strain of FRP-confined concrete. The writers' paper develops relationships between the additional energy absorption of a confined concrete column and the energy absorbed by the confinement material. A new methodology is introduced to calculate the confined concrete strain in circular and square sections.

Analytical Investigation

Strain Energy and Energy Absorption

Strain energy is the energy stored in a structural elastic member as a result of the work performed on the member by an external load. It is defined as the energy absorbed by the structural member during the loading process. For an axially loaded column, the work done by the applied load is equal to the area under the load-displacement curve [Fig. 1(a) and Eq. (1)]. In a similar manner, the energy absorbed by the external FRP in an FRP-confined concrete column can be estimated

$$U = W = \int_0^l P dl \tag{1}$$

where U = strain energy; W = work done by the applied load; P = applied load; l = displacement; and dl is an increment of the displacement.

The energy stored in the column core is transferred to compress concrete, deform the FRP, create cracks in concrete, and vertically compress the FRP. Some energy is also lost in unknown consumptions. Because of the limited understanding of the behavior inside

[1]Ph.D. Candidate, School of Civil, Mining, and Environmental Engineering, Univ. of Wollongong, Wollongong, NSW 2522, Australia; formerly, Lecturer, Faculty of Civil Engineering, HCMC Univ. of Technology, Ho Chi Minh City 70000, Vietnam. E-mail: mtp027@uowmail.edu.au

[2]Associate Professor, School of Civil, Mining, and Environmental Engineering, Univ. of Wollongong, Wollongong, NSW 2522, Australia (corresponding author). E-mail: mhadi@uow.edu.au

Note. This manuscript was submitted on November 25, 2012; approved on May 14, 2013; published online on May 16, 2013. Discussion period open until February 9, 2014; separate discussions must be submitted for individual papers. This paper is part of the ***Journal of Composites for Construction***, © ASCE, ISSN 1090-0268/04013001(11)/$25.00.

FRP-confined concrete, it would be inappropriate to directly use the balanced-energy approach proposed by Mander et al. (1988) for steel confined concrete. In this paper, it is assumed that there is a possible linear relationship between the energy absorption of the column and the external FRP, which is discussed in a subsequent section.

To further investigate the energy transfer, early studies focused on FRP tubes made from high-strength and high-stiffness fibers. Unlike ductile metals, fibers and resins are brittle and they fail by fracture after an initial elastic deformation. The fracture strain of a typical carbon fiber is around 1.5–2.0% such that they may absorb less energy than conventional metals. However, they actually perform much better when a comparison is made in terms of the specific energy absorption, which is the energy per unit mass (Lu and Yu 2003). The specific energy absorption of fiber is affected by fiber strength, elastic properties, the diameter-to-thickness ratio of FRP, fiber orientation, and sectional geometries (Wolff et al. 1994). These studies confirm that directly using the balanced-energy method (proposed for steel confined concrete) for FRP-confined concrete is inappropriate.

Energy in Structural Members

The widely accepted model [Fig. 1(b)] is recommended by ACI 440-2R.08 (ACI 2008) for the stress-strain relationship of FRP-confined concrete columns. It was adopted in the writers' paper to calculate the energy absorption of a FRP-confined concrete column

$$W_{cc} = A_{cc} \int_0^{\varepsilon_{cc}} f_c d\varepsilon_c \tag{2}$$

where W_{cc} = strain energy of confined concrete; A_{cc} = gross-sectional area of confined concrete; f_c = stress of confined concrete; ε_c = strain of confined concrete; ε_{cc} = strain at peak stress of confined concrete; and $d\varepsilon_c$ is an increment of the axial strain.

The stress-strain curve [Fig. 1(b)] has been slightly modified to obtain a simple integration. An expression [Eq. (3)] was extracted from Eq. (2) to calculate the energy absorption of the concrete core, in which the volumetric strain energy equals the area under the experimental stress-strain curves. When the strain of confined concrete is less than the peak strain of the corresponding unconfined concrete, the effect of FRP is negligible. Thus, the writers assumed that the additional energy in the column core equals the area under the experimental stress-strain curves starting from the value of the unconfined concrete strain [Fig. 1(b) and Eq. (3)]

$$U_{cc} = \int_{\varepsilon_{co}}^{\varepsilon_{cc}} f_c d\varepsilon_c = \frac{(\varepsilon_{cc} - \varepsilon_{co})(f'_{co} + f'_{cc})}{2} \tag{3}$$

where U_{cc} = volumetric strain energy of confined concrete; f'_{cc} = confined concrete strength; f'_{co} = unconfined concrete strength; and ε_{co} = its corresponding strain.

Similarly, the energy absorbed by FRP can be calculated

$$W_f = \rho_f A_{cc}(0.5 f_f \varepsilon_f) \tag{4}$$

where W_f = strain energy of FRP; f_f and ε_f = rupture strength and rupture strain, respectively, of FRP obtained from flat-coupon tests; and ρ_f = volumetric ratio of FRP as shown in Eqs. (5) and (6).

The volumetric ratio (ρ_f) of FRP of circular and square sections can be calculated.

For circular sections

$$\rho_f = \frac{4t}{d} \tag{5}$$

and for square sections

$$\rho_f = \frac{t[4b - r(8 - 2\pi)]}{b^2 - r^2(4 - \pi)} = \Psi t \tag{6}$$

where t = thickness of FRP; d = diameter of the section; and r = radius of the round corner of the section.

The rupture strain of FRP on the confined concrete is much less than that obtained from flat-coupon tests (Xiao and Wu 2000; Pessiki et al. 2001; Carey and Harries 2005). Therefore, the volumetric strain energy of FRP on a column can be estimated as follows:

$$U_f = \rho_f(0.5 f_{fe} \varepsilon_{fe}) \tag{7}$$

where U_f = volumetric strain energy of FRP; and f_{fe} and ε_{fe} = actual rupture strength and rupture strain, respectively, of FRP on the columns.

The energy absorbed by the column was calculated using Eq. (3) and the energy absorbed by FRP was estimated using Eq. (7). Next, a regression analysis based on a database was used to obtain a linear relationship between them. Based on that linear relationship, a model to calculate the strain of confined concrete at peak stress was derived.

Experimental Database

Test Database

Several experimental tests have been conducted on FRP-confined concrete by researchers over the past few decades. The writers collated a test database of 329 FRP confined plain concrete specimens reported by Demers and Neale (1994), Watanabe et al. (1997), Matthys et al. (1999), Rochette and Labossière (2000), Xiao and Wu (2000), Suter and Pinzelli (2001), Parvin and Wang (2001), Pessiki et al. (2001), Shehata et al. (2002), De Lorenzis et al. (2002), Karabinis and Rousakis (2002), Lam and Teng (2003b), Chaallal et al. (2003), Ilki and Kumbasar (2003), Masia et al. (2004), Berthet et al. (2005), Lam et al. (2006), Saenz and Pantelides (2006), Jiang and Teng (2007), Valdmanis et al. (2007), Al-Salloum (2007), Rousakis et al. (2007), Wang and Wu (2008), Tao et al. (2008), Wu and Wei (2010), Rousakis and Karabinis (2012), and Hadi et al. (2013). The primary focus of this paper is on CFRP; as such, test results of materials other than CFRP were excluded from this database. Moreover, test results of circular sections not reporting the actual rupture strain (ε_{fe}) of FRP were excluded.

A few studies concluded that square columns confined with FRP provide a little (Mirmiran et al. 1998) or no (Wu and Zhou 2010) strength improvement. Thus, this paper deals only with round-corner square specimens; as such, specimens with sharp corners were excluded from the database. Because the procedure of calculating the strain of FRP-confined concrete is based on the ascending type of specimen (Fig. 1), the test results of square specimens that have a descending type were excluded from the database. After excluding all of the previously noted test results, the database contained the test results of 167 FRP confined plain concrete specimens, as follows: (1) 98 circular specimens, and (2) 69 square specimens. The circular specimens included in the database have diameters d ranging from 100 to 152 mm and have

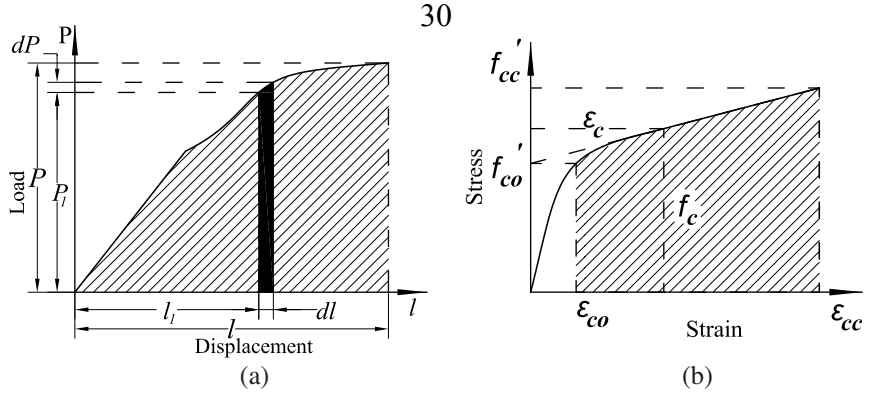

Fig. 1. (a) Load-displacement diagram; (b) typical stress-strain curve of FRP-confined concrete

unconfined concrete strengths f'_{cc} between 30 and 50 MPa. The square specimens have a side length ranging between 100 and 152 mm, and unconfined concrete strength ranging between 20 and 50 MPa.

The confinement ratio was calculated by dividing the confining pressure (f_l) by the unconfined concrete strength (f'_{cc}), which varied between 2 and 99% for circular specimens, and between 1 and 60% for square specimens. Tables 1 and 2 show the databases for circular and square specimens, respectively.

Assumptions

The actual rupture strain of CFRP is usually reported for circular sections but not for square sections. When the actual rupture strain of CFRP was not included in the test results, it was assumed to be 0.55 of the rupture strain from flat-coupon tests, as recommended by ACI 440.2R-08 (ACI 2008). In addition, when the axial strain at the peak stress of unconfined concrete (ε_{co}) was not specified, ε_{co} was assumed to be equal to 0.002 or values estimated by using the equation of Tasdemir et al. (1998). The performance of the proposed model was compared by using two different methods for estimating the values of ε_{co}. In the first method, ε_{co} was calculated using the equation proposed by Tasdemir et al. (1998). In the second method, ε_{co} was assumed to be 0.002. Results of using the first method proved to be better than the second method. Therefore, the equation proposed by Tasdemir et al. (1998) was used

$$\varepsilon_{co} = (-0.067f'^2_{co} + 29.9f'_{co} + 1{,}053)10^{-6} \tag{8}$$

Proposed Strain Model

A linear relationship was assumed between the energy absorbed by a column core and CFRP for both circular sections and square sections. The energy absorption was calculated using Eqs. (3) and (7), whereas a regression analysis was carried out to obtain an equation for the energy absorbed in the form shown in Eq. (9). Based on this regression analysis, a new formula is proposed to calculate the strain at the peak stress of CFRP-confined concrete

$$U_{cc} - kU_f \tag{9}$$

where k is the proportion factor, which is a function of fiber stiffness and sectional geometries.

Strain Estimation for Circular Sections

The energy absorption of 98 circular specimens was estimated using Eqs. (3) and (7), and Fig. 2 presents the results. Next, a regression analysis was undertaken to attain

$$U_{cc} = 7.6U_f \tag{10}$$

Substituting Eqs. (3) and (7) into Eq. (10) results in Eq. (11)

$$\varepsilon_{cc} = \varepsilon_{co} + \frac{4ktf_{fe}\varepsilon_{fe}}{d(f'_{co} + f'_{cc})} \tag{11}$$

where the proportion factor $k = 7.6$. Eq. (11) can be used to calculate the strain of CFRP-confined concrete columns in circular sections. Using this calculated strain, any model can be utilized to calculate the confined concrete strength. The Lam and Teng model (2003a) was adopted to express another form of Eq. (11)

$$\varepsilon_{cc} = \varepsilon_{co} + \frac{2ktf_{fe}\varepsilon_{fe}}{df'_{co} + 3.3f_{fe}t} \tag{12}$$

Strain Estimation for Square Sections

For circular sections, the methodology proposed in this paper was used to establish a relationship between the energy absorption of the entire column section and FRP. The energy absorption of the FRP was calculated with respect to the perimeter of the section. This calculation did not provide a comparable correlation between the two energies in Eq. (9). Thus, the energy absorption of the column core at the effective area [Fig. 3(a)] was considered for the square specimens, which accounts for stress concentration at the corners. Details of the previously noted modifications are analyzed in the subsequent sections.

The energy absorption is sensitive to the geometry of the column (Wolff et al. 1994). Thus, equations simulating the relationship between the absorption energies of a column and CFRP distinguish square from circular specimens. In addition, the confining pressure of a square column confined with CFRP is not uniform. Karabinis et al. (2008) and Csuka and Kollár (2012) proved that the confining pressure primarily concentrates on round corners of the column, whereas this confining pressure is negligible at other zones [Fig. 3(b)]. Therefore, the energy absorption used to rupture CFRP is assumed to be only available at the round corners. In such a case, a corner energy ratio k_c, which is the ratio of the total length of four round corners [Fig. 3(c)] to the circumference of the section, is introduced to account for the reduction of energy absorbed by CFRP

$$k_c = \frac{\pi r}{2b - r(4 - \pi)} \tag{13}$$

where b = side length of a square section; and r = round radius at the corners of the section.

Table 1. Database of Circular Specimens

Number	Source of data	d (mm)	h (mm)	f'_{co} (MPa)	ε_{co} (%)	t (mm)	f_f (MPa)	E_f (GPa)	ε_{cc} (%)	ε_{fe} (%)	f_{cc} (MPa)
1	Watanable et al. (1997)	100	200	30.2	0.23	0.17	2,716	225	1.51	0.94	46.6
2	Ibid	100	200	30.2	0.23	0.50	2,873	225	3.11	0.82	87.2
3	Ibid	100	200	30.2	0.23	0.14	1,579	629	0.57	0.23	41.7
4	Ibid	100	200	30.2	0.23	0.28	1,824	630	0.88	0.22	56.0
5	Ibid	100	200	30.2	0.23	0.42	1,285	577	1.30	0.22	63.3
6	Matthys et al. (1999)	150	300	34.9	0.21	0.12	2,600	200	0.85	1.15	44.3
7	Ibid	150	300	34.9	0.21	0.12	2,600	200	0.72	1.08	42.2
8	Ibid	150	300	34.9	0.21	0.24	1,100	420	0.40	0.19	41.3
9	Ibid	150	300	34.9	0.21	0.24	1,100	420	0.36	0.18	40.7
10	Rochette and Labossière (2000)	100	200	42	—	0.60	1,265	83	1.65	0.89	73.5
11	Ibid	100	200	42	—	0.60	1,265	83	1.57	0.95	73.5
12	Ibid	100	200	42	—	0.60	1,265	83	1.35	0.80	67.6
13	Xiao and Wu (2000)	152	305	33.7	—	0.38	1,577	105	1.20	0.84	47.9
14	Ibid	152	305	33.7	—	0.38	1,577	105	1.40	1.15	49.7
15	Ibid	152	305	33.7	—	0.38	1,577	105	1.24	0.87	49.4
16	Ibid	152	305	33.7	—	0.76	1,577	105	1.65	0.91	64.6
17	Ibid	152	305	33.7	—	0.76	1,577	105	2.25	1.00	75.2
18	Ibid	152	305	33.7	—	0.76	1,577	105	2.16	1.00	71.8
19	Ibid	152	305	33.7	—	1.14	1,577	105	2.45	0.82	82.9
20	Ibid	152	305	33.7	—	1.14	1,577	105	3.03	0.90	95.4
21	Ibid	152	305	43.8	—	0.38	1,577	105	0.98	0.81	54.8
22	Ibid	152	305	43.8	—	0.38	1,577	105	0.47	0.76	52.1
23	Ibid	152	305	43.8	—	0.38	1,577	105	0.37	0.28	48.7
24	Ibid	152	305	43.8	—	0.76	1,577	105	1.57	0.92	84.0
25	Ibid	152	305	43.8	—	0.76	1,577	105	1.37	1.00	79.2
26	Ibid	152	305	43.8	—	0.76	1,577	105	1.66	1.01	85.0
27	Ibid	152	305	43.8	—	1.14	1,577	105	1.74	0.79	96.5
28	Ibid	152	305	43.8	—	1.14	1,577	105	1.68	0.71	92.6
29	Ibid	152	305	43.8	—	1.14	1,577	105	1.75	0.84	94.0
30	Ibid	152	305	55.2	—	0.38	1,577	105	0.69	0.70	57.9
31	Ibid	152	305	55.2	—	0.38	1,577	105	0.48	0.62	62.9
32	Ibid	152	305	55.2	—	0.38	1,577	105	0.49	0.19	58.1
33	Ibid	152	305	55.2	—	0.76	1,577	105	1.21	0.74	74.6
34	Ibid	152	305	55.2	—	0.76	1,577	105	0.81	0.83	77.6
35	Ibid	152	305	55.2	—	1.14	1,577	105	1.43	0.76	106.5
36	Ibid	152	305	55.2	—	1.14	1,577	105	1.45	0.85	108.0
37	Ibid	152	305	55.2	—	1.14	1,577	105	1.18	0.70	103.3
38	De Lorenzis et al. (2002)	120	240	43	—	0.30	1,028	91	1.16	0.70	58.5
39	Ibid	120	240	43	—	0.30	1,028	91	0.95	0.80	65.6
40	Ibid	150	300	38	—	0.45	1,028	91	0.95	0.80	62.0
41	Ibid	150	300	38	—	0.45	1,028	91	1.35	0.80	67.3
42	Jiang and Teng (2007)	152	305	38	0.22	0.68	3,772	241	2.55	0.98	110.1
43	Ibid	152	305	38	0.22	0.68	3,772	241	2.61	0.97	107.4
44	Ibid	152	305	38	0.22	1.02	3,772	241	2.79	0.89	129.0
45	Ibid	152	305	38	0.22	1.02	3,772	241	3.08	0.93	135.7
46	Ibid	152	305	38	0.22	1.36	3,772	241	3.70	0.87	161.3
47	Ibid	152	305	38	0.22	1.36	3,772	241	3.54	0.88	158.5
48	Ibid	152	305	37.7	0.28	0.11	4,332	260	0.90	0.94	48.5
49	Ibid	152	305	37.7	0.28	0.11	4,332	260	0.91	1.09	50.3
50	Ibid	152	305	42.2	0.26	0.11	4,332	260	0.69	0.73	48.1
51	Ibid	152	305	42.2	0.26	0.11	4,332	260	0.89	0.97	51.1
52	Ibid	152	305	42.2	0.26	0.22	4,332	260	1.30	1.18	65.7
53	Ibid	152	305	42.2	0.26	0.22	4,332	260	1.03	0.94	62.9
54	Ibid	152	305	47.6	0.28	0.33	4,332	251	1.30	0.90	82.7
55	Ibid	152	305	47.6	0.28	0.33	4,332	251	1.94	1.13	85.5
56	Ibid	152	305	47.6	0.28	0.33	4,332	251	1.82	1.06	85.5
57	Lam et al. (2006)	152	304	41.1	0.26	0.17	3,795	251	0.90	0.81	52.6
58	Ibid	152.5	305	41.1	0.26	0.17	3,795	251	1.21	1.08	57.0
59	Ibid	152.5	305	41.1	0.26	0.17	3,795	251	1.11	1.07	55.4
60	Ibid	152.5	305	38.9	0.25	0.33	3,795	251	1.91	1.06	76.8
61	Ibid	152.5	305	38.9	0.25	0.33	3,795	251	2.08	1.13	79.1
62	Saenz and Pantelides (2006)	152	304	41.8	—	0.60	1,220	87	1.18	0.92	83.7
63	Ibid	152	304	47.5	—	0.60	1,220	87	0.88	0.93	81.5
64	Ibid	152	304	40.3	—	1.20	1,220	87	2.04	0.92	108.1
65	Ibid	152	304	41.7	—	1.20	1,220	87	1.76	1.08	109.5
66	Valdmanis et al. (2007)	150	300	40	0.17	0.17	1,906	201	0.63	0.89	66.0

Table 1. (*Continued.*)

Number	Source of data	d (mm)	h (mm)	f'_{co} (MPa)	ε_{co} (%)	t (mm)	f_f (MPa)	E_f (GPa)	ε_{cc} (%)	ε_{fe} (%)	f_{cc} (MPa)
67	Ibid	150	300	40	0.17	0.34	2,389	231	1.07	0.84	87.2
68	Ibid	150	300	40	0.17	0.51	2,661	236	1.36	0.69	96.0
69	Ibid	150	300	44.3	0.17	0.17	1,906	201	0.58	0.74	73.3
70	Ibid	150	300	44.3	0.17	0.34	2,389	231	0.54	0.43	82.6
71	Ibid	150	300	44.3	0.17	0.51	2,661	236	0.94	0.78	115.1
72	Berthet et al. (2005)	160	320	25	0.23	0.17	3,200	230	1.63	0.96	42.8
73	Ibid	160	320	25	0.23	0.17	3,200	230	0.93	0.96	37.8
74	Ibid	160	320	25	0.23	0.17	3,200	230	1.67	0.96	45.8
75	Ibid	160	320	25	0.23	0.33	3,200	230	1.73	0.90	56.7
76	Ibid	160	320	25	0.23	0.33	3,200	230	1.58	0.91	55.2
77	Ibid	160	320	25	0.23	0.33	3,200	230	1.68	0.91	56.1
78	Ibid	160	320	40.1	0.2	0.11	3,200	230	0.55	1.02	49.8
79	Ibid	160	320	40.1	0.2	0.11	3,200	230	0.66	0.95	50.8
80	Ibid	160	320	40.1	0.2	0.11	3,200	230	0.61	1.20	48.8
81	Ibid	160	320	40.1	0.2	0.17	3,200	230	0.66	0.88	53.7
82	Ibid	160	320	40.1	0.2	0.17	3,200	230	0.62	0.85	54.7
83	Ibid	160	320	40.1	0.2	0.17	3,200	230	0.64	1.04	51.8
84	Ibid	160	320	40.1	0.2	0.22	3,200	230	0.60	0.79	59.7
85	Ibid	160	320	40.1	0.2	0.22	3,200	230	0.69	0.83	60.7
86	Ibid	160	320	40.1	0.2	0.22	3,200	230	0.73	0.81	60.2
87	Ibid	160	320	40.1	0.2	0.44	3,200	230	1.44	0.92	91.6
88	Ibid	160	320	40.1	0.20	0.44	3,200	230	1.36	0.97	89.6
89	Ibid	160	320	40.1	0.20	0.44	3,200	230	1.17	0.89	86.6
90	Ibid	160	320	40.1	0.20	0.99	3,200	230	2.46	0.99	142.4
91	Ibid	160	320	40.1	0.20	0.99	3,200	230	2.39	1.00	140.4
92	Ibid	160	320	40.1	0.20	1.32	3,200	230	2.70	1.00	166.3
93	Ibid	160	320	52	0.23	0.33	3,200	230	0.83	0.93	82.6
94	Ibid	160	320	52	0.23	0.33	3,200	230	0.70	0.87	82.8
95	Ibid	160	320	52	0.23	0.33	3,200	230	0.77	0.89	82.3
96	Ibid	160	320	52	0.23	0.66	3,200	230	1.14	0.67	108.1
97	Ibid	160	320	52	0.23	0.66	3,200	230	1.12	0.87	112
98	Ibid	160	320	52	0.23	0.66	3,200	230	1.12	0.882	107.9

For square sections, the energy absorbed by CFRP (Fig. 4) was modified by adding the corner energy ratio k_c

$$U_f = \sqrt{k_c}\rho_f(0.5 f_{fe}\varepsilon_{fe}) \tag{14}$$

Early studies on steel confined concrete have reported the well-known assumption that the concrete in a square section is confined by the transverse reinforcement through arching actions (Mander et al. 1988; Cusson and Paultre 1995). Consequently, only the concrete contained by four second-degree parabolas [Fig. 3(a)] is well-confined, whereas the confinement effect at other zones is negligible. As further evidence, a few experimental (Mirmiran et al. 1998; Rochette and Labossiére 2000) and analytical (Karabinis et al. 2008) studies also confirmed that only part of the section is fully confined in terms of FRP-confined concrete columns. The writers assumed that the energy absorption of the effective area is proportional to the total energy absorbed of the entire section [Eq. (3)]. In this paper, the energy absorption of square specimens is assumed as the energy absorbed by the effective area only. This energy can be calculated by combining Eq. (3) and the shape factor k_s, as introduced by ACI 440.2R-08 (ACI 2008)

$$U_{cc} = k_s \frac{(\varepsilon_{cc} - \varepsilon_{co})(f'_{cc} + f'_{co})}{2} \tag{15}$$

$$k_s = 1 - \frac{2(b-2r)^2}{3[b^2 - r^2(4-\pi)]} \tag{16}$$

The same methodology used in establishing the expression for circular sections was utilized for square columns. Fig. 4 and Eq. (17) show the relationship of the energy absorption in this case

$$U_{cc} = 8.3 U_f \tag{17}$$

Substituting Eqs. (14) and (15) into Eq. (17) results in Eq. (18)

$$\varepsilon_{cc} = \varepsilon_{co} + \frac{tk\sqrt{k_c}\Psi f_{fe}\varepsilon_{fe}}{k_s(f'_{cc} + f'_{co})} \tag{18}$$

where the proportion factor $k = 8.3$. Eq. (18) can be used to calculate the strain of CFRP-confined concrete columns in square sections. The Lam and Teng (2003b) model was adopted to express another form of Eq. (18)

$$\varepsilon_{cc} = \varepsilon_{co} + \frac{tk\sqrt{k_c}\Psi f_{fe}\varepsilon_{fe}}{k_s(2f'_{co} + 3.3k_s f_l)} \tag{19}$$

where f_l = equivalent confining pressure of a square section, which can be estimated (Lam and Teng 2003b) as

$$f_l = \frac{\sqrt{2}tf_{fe}}{b} \tag{20}$$

Table 2. Database of Square Specimens

Number	Source of data	b (mm)	h (mm)	r (mm)	f'_{co} (MPa)	t (mm)	f_f (MPa)	E_f (GPa)	ε_{cc} (%)	ε_{fe} (%)	f'_{cc} (MPa)
1	Rochette and Labossière (2000)	152	500	25	42	0.90	1,265	83	0.94	0.56	50.9
2	Ibid	152	500	25	42	0.90	1,265	83	0.89	0.63	52.0
3	Ibid	152	500	38	42	0.90	1,265	83	1.08	0.71	55.4
4	Ibid	152	500	25	44	1.20	1,265	83	1.35	0.59	56.4
5	Ibid	152	500	25	36	1.20	1,265	83	2.04	0.70	50.6
6	Ibid	152	500	25	36	1.50	1,265	83	2.12	0.65	52.9
7	Ibid	152	500	38	36	1.20	1,265	83	1.92	0.89	58.1
8	Ibid	152	500	38	36	1.50	1,265	83	2.39	0.86	62.8
9	Lam and Teng (2003b)	150	600	25	34	0.17	1,577	105	0.96	1.05	37.6
10	Ibid	150	600	15	34	0.33	1,577	105	0.87	0.97	39.7
11	Ibid	150	600	25	34	0.33	1,577	105	0.85	1.08	41.8
12	Ibid	150	600	15	24	0.50	1,577	105	1.80	0.87	32.0
13	Ibid	150	600	25	24	0.50	1,577	105	1.52	1.16	37.1
14	Pessiki et al. (2001)	152	610	38	26	1.00	580	38	1.50	0.83	34.4
15	Ibid	152	610	38	26	2.00	580	38	1.90	0.90	43.7
16	Chaallal et al. (2003)	133	305	25	21	0.12	3,650	231	0.40	0.40	23.6
17	Ibid	133	305	25	21	0.24	3,650	231	0.40	0.50	27.8
18	Ibid	133	305	25	21	0.36	3,650	231	0.60	0.52	31.8
19	Ibid	133	305	25	21	0.48	3,650	231	0.70	0.53	35.8
20	Ibid	133	305	25	41	0.12	3,650	231	0.30	0.08	42.0
21	Ibid	133	305	25	41	0.24	3,650	231	0.30	0.11	43.0
22	Ibid	133	305	25	41	0.36	3,650	231	0.40	0.15	44.6
23	Ibid	133	305	25	41	0.48	3,650	231	0.40	0.20	47.1
24	Ibid	150	300	15	33	0.33	4,364	219	1.22	—	46.9
25	Ibid	150	300	15	32	0.33	4,364	219	1.22	—	46.2
26	Ibid	150	300	15	31	0.33	4,364	219	1.22	—	44.7
27	Ibid	150	300	30	33	0.17	4,364	219	1.34	—	41.9
28	Ibid	150	300	30	31	0.17	4,364	219	1.34	—	40.4
29	Ibid	150	300	30	33	0.17	4,364	219	1.34	—	42.4
30	Ibid	150	300	30	33	0.33	4,364	219	1.44	—	51.1
31	Ibid	150	300	30	31	0.33	4,364	219	1.44	—	49.6
32	Ibid	150	300	30	33	0.33	4,364	219	1.44	—	51.6
33	Ibid	150	300	45	30	0.17	4,364	219	1.39	—	41.0
34	Ibid	150	300	45	33	0.17	4,364	219	1.39	—	43.5
35	Ibid	150	300	45	29	0.17	4,364	219	1.39	—	40.2
36	Ibid	150	300	45	30	0.33	4,364	219	1.57	—	51.9
37	Ibid	150	300	45	33	0.33	4,364	219	1.57	—	54.4
38	Ibid	150	300	45	29	0.33	4,364	219	1.57	—	51.1
39	Ibid	150	300	60	31	0.17	4,364	219	1.65	—	42.8
40	Ibid	150	300	60	31	0.17	4,364	219	1.65	—	43.0
41	Ibid	150	300	60	34	0.17	4,364	219	1.65	—	45.4
42	Ibid	150	300	60	31	0.33	4,364	219	1.76	—	54.8
43	Ibid	150	300	60	31	0.33	4,364	219	1.76	—	55.0
44	Ibid	150	300	60	34	0.33	4,364	219	1.76	—	57.4
45	Ibid	150	300	30	54	0.33	3,788	226	1.37	—	69.6
46	Ibid	150	300	30	53	0.33	3,788	226	1.37	—	69.2
47	Ibid	150	300	30	49	0.33	3,788	226	1.37	—	65.5
48	Ibid	150	300	45	53	0.17	3,788	226	1.51	—	62.7
49	Ibid	150	300	45	52	0.17	3,788	226	1.51	—	61.0
50	Ibid	150	300	45	53	0.17	3,788	226	1.51	—	62.8
51	Ibid	150	300	45	53	0.33	3,788	226	1.65	—	72.1
52	Ibid	150	300	45	52	0.33	3,788	226	1.65	—	70.4
53	Ibid	150	300	45	53	0.33	3,788	226	1.65	—	72.2
54	Ibid	150	300	60	54	0.17	3,788	226	1.28	—	64.3
55	Ibid	150	300	60	52	0.17	3,788	226	1.28	—	62.4
56	Ibid	150	300	60	52	0.17	3,788	226	1.28	—	62.7
57	Ibid	150	300	60	54	0.33	3,788	226	1.37	—	74.6
58	Ibid	150	300	60	52	0.33	3,788	226	1.37	—	72.7
59	Ibid	150	300	60	52	0.33	3,788	226	1.37	—	73.0
60	Tao et al. (2008)	150	450	20	22	0.17	4,470	239	2.53	—	30.3
61	Ibid	150	450	20	22	0.34	4,470	239	3.95	—	38.5
62	Ibid	150	450	20	20	0.34	4,470	239	3.34	—	36.0
63	Ibid	150	450	35	22	0.34	4,470	239	3.66	—	42.8
64	Ibid	150	450	35	20	0.34	4,470	239	3.48	—	40.3
65	Ibid	150	450	50	22	0.34	4,470	239	3.87	—	45.9
66	Ibid	150	450	50	20	0.34	4,470	239	3.43	—	43.4

Table 2. (*Continued.*)

Number	Source of data	b (mm)	h (mm)	r (mm)	f'_{co} (MPa)	t (mm)	f_f (MPa)	E_f (GPa)	ε_{cc} (%)	ε_{fe} (%)	f'_{cc} (MPa)
67	Ibid	150	450	20	50	0.34	4,200	241	1.66	—	65.0
68	Ibid	150	450	35	50	0.34	4,200	241	2.08	—	69.1
69	Ibid	150	450	50	50	0.34	4,200	241	1.65	—	71.9

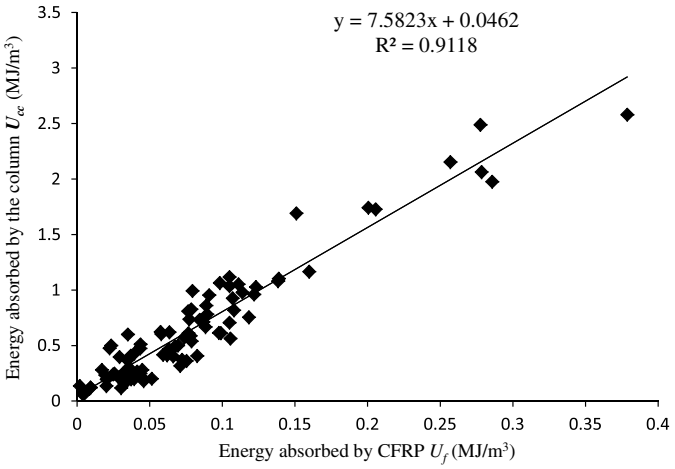

Fig. 2. Energy relationship of circular sections

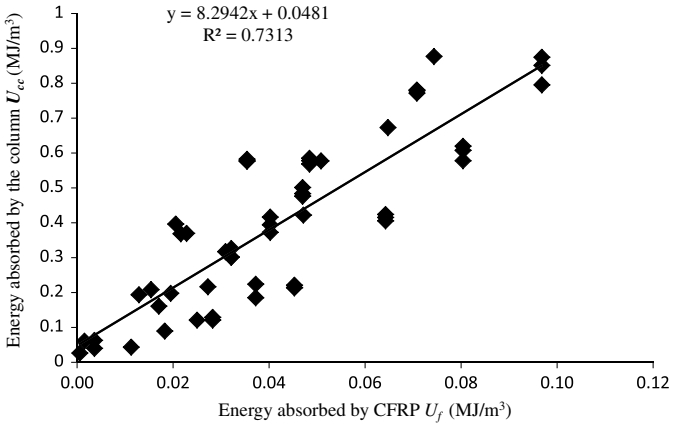

Fig. 4. Energy relationship of square sections

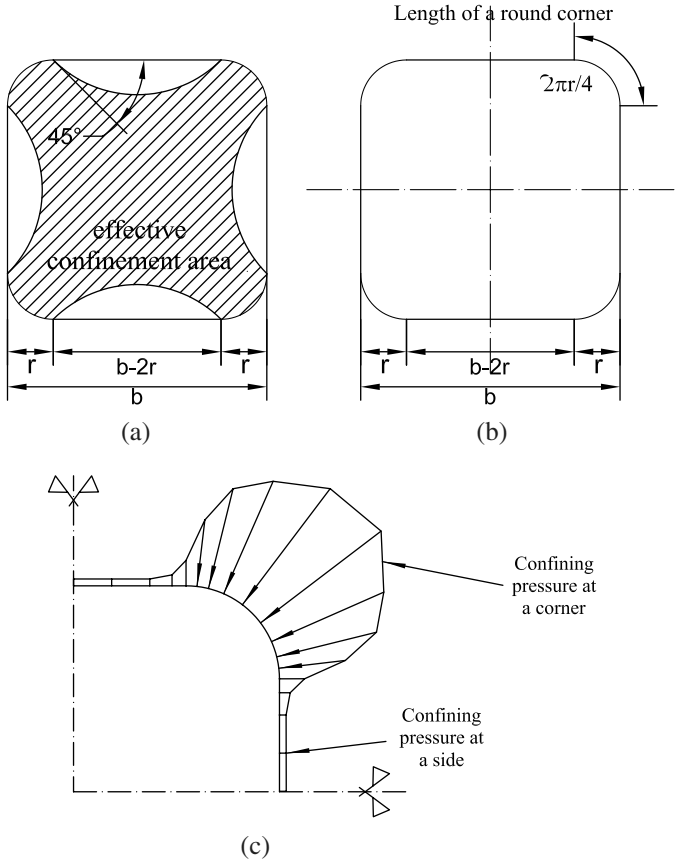

Fig. 3. (a) Effective confinement area; (b) confining pressure of square sections; (c) round corners of square sections

Verification of the Proposed Model

Statistical Methods of Verification

In the writers' paper, the model performance was tested by using two statistical indicators, as follows: (1) mean square error (MSE), and (2) average absolute error (AAE), as determined by Eqs. (21) and (22):

$$\text{MSE} = \frac{\sum_1^n \left(\frac{\text{pre}_i - \text{exp}_i}{\text{exp}_i}\right)^2}{N} \tag{21}$$

$$\text{AAE} = \frac{\sum_1^n \left|\frac{\text{pre}_i - \text{exp}_i}{\text{exp}_i}\right|}{N} \tag{22}$$

where pre = model predictions; exp = experimental results; and N = total number of test data. In general, the mean square error shows the errors to be more significant compared with the average absolute error.

Circular FRP-Confined Concrete Columns

A total of 98 data points were plotted (Fig. 5) to assess the performance of existing models and the proposed model. Seven existing models were considered in this verification [Karbhari and Gao 1997; Toutanji 1999; De Lorenzis and Tepfers 2003; ACI 440.2R-08 (ACI 2008); Teng et al. 2009; Rousakis et al. 2012; Yazici and Hadi 2012]. Because of the limited space in the writers' paper, only four models that have comparable performance are shown (Fig. 5). Fig. 6 presents all seven models to illustrate a comparison of the models' performance.

Based on the two statistical indicators, the models of ACI 440.2R-08 (ACI 2008) and Rousakis et al. (2012) provide the best

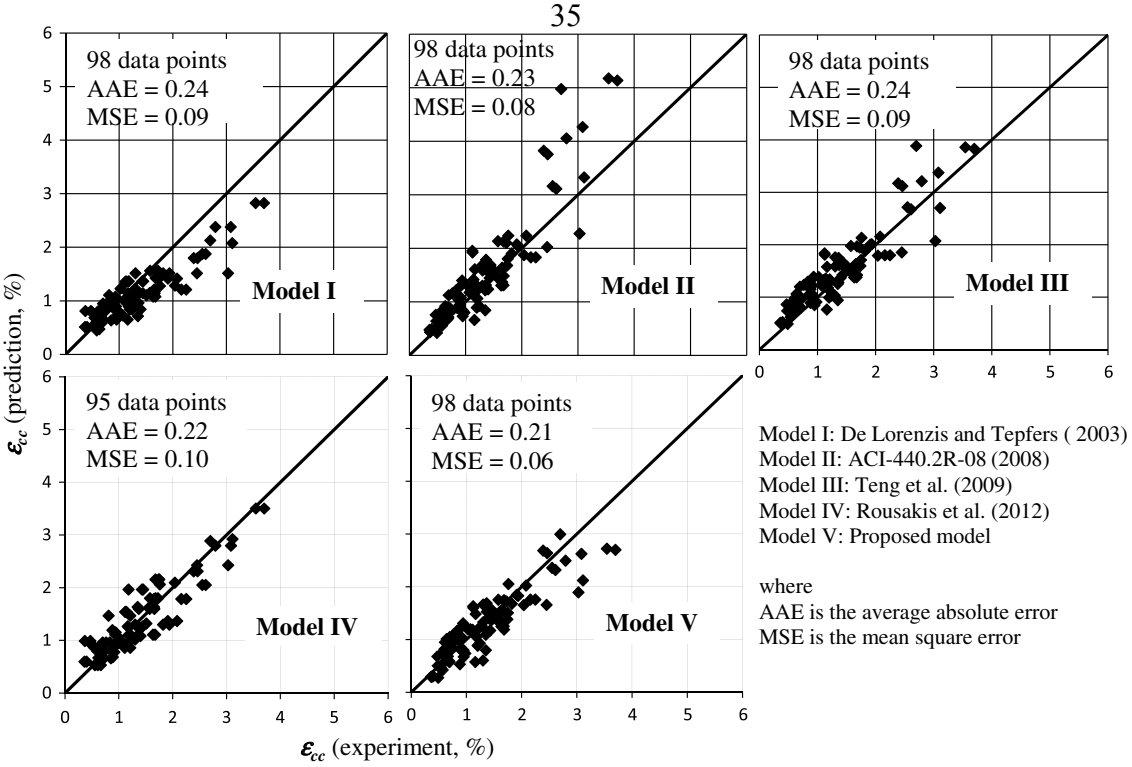

Fig. 5. Performance of models on circular specimens

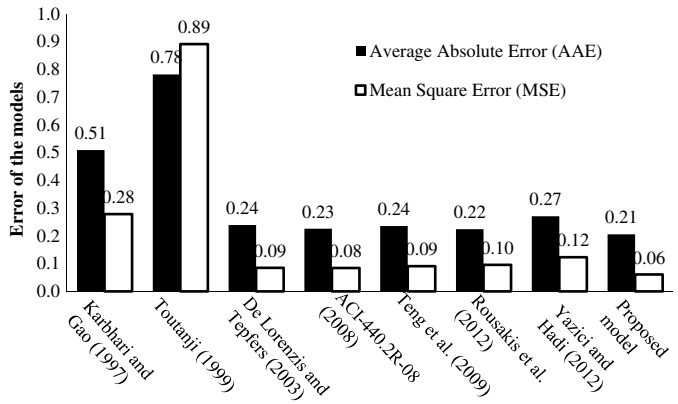

Fig. 6. Accuracy comparisons for strain prediction of circular specimens among the models

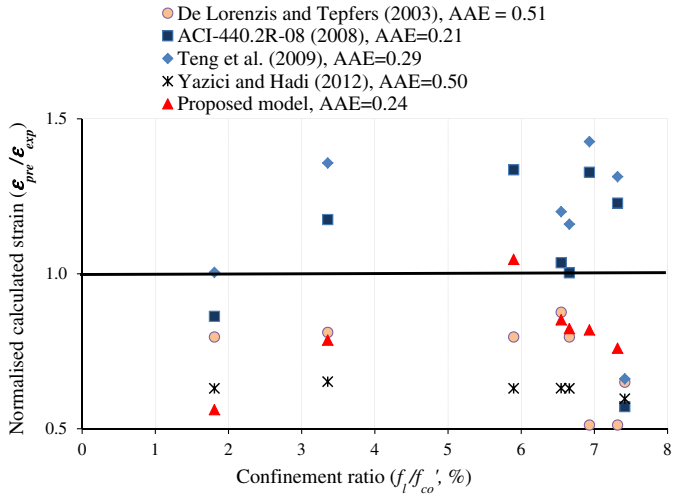

Fig. 7. Performance of models on circular specimens (insufficient confinement)

strain prediction, followed by the models of Lam and Teng (2003a) and De Lorenzis and Tepfers (2003). The model of Rousakis et al. (2012) shows good agreement with experimental results, with the exception of high-modulus (HM) CFRP such that three specimens using HM CFRP were excluded from the verification of this model. The proposed model in this paper shows slightly better estimates than the model of ACI 440.2R-08 (ACI 2008) and Rousakis et al. (2012).

The model of ACI 440.2R-08 (ACI 2008) suggests that the minimum confinement ratio f_l/f'_{co} of 0.08 should be used. This minimum limit was recommended based on increasing the strength of CFRP-confined concrete. In particular, in earthquake-prone regions the ductility of a column may need to be increased, leading to a case of insufficient strength confinement, whereas the ductility enhancement still could be expected (Mirmiran et al. 1998; Wang and Wu 2008). Therefore, eight specimens (insufficient confinement) having a confinement ratio of less than 0.08 were extracted from the full database to verify the models in this case (Fig. 7). Based on the strain-estimation equations of the subsequent models, if the confinement pressure is equal to zero, the strain of confined concrete calculated by the models of ACI 440.2R-08 (ACI 2008) would be 1.5× the unconfined concrete strain. Consequently, when the confinement pressure f_l reaches zero the strain prediction from the model of ACI 440.2R-08 (ACI 2008) will overestimate the actual strain. When that model was verified by the database, it exhibited good predictions for insufficient confined specimens. The prediction of the proposed model still shows a quite good correlation with the test data, whereas other models show scatter of the test data (Fig. 7).

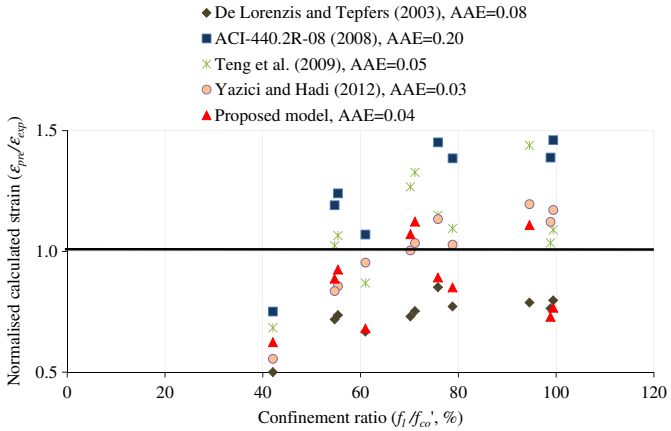

Fig. 8. Performance of models on circular specimens (heavy confinement)

In addition, the models of ACI 440.2R-08 (ACI 2008) and Teng et al. (2009) generally tend to overestimate the strain of confined concrete when the confinement ratio (f_l/f'_{co}) is large. The differences between the experimental and predicted values become considerably larger when the confinement ratio was larger than 40% (Fig. 5), remarked as heavy confinement. Thus, eleven heavy confined specimens were extracted from the database to compare these models (Fig. 8). The models of ACI 440.2R-08 (ACI 2008), Teng et al. (2009), and De Lorenzis and Tepfers (2003) show that the precision of these models are not good, whereas the model of Yazici and Hadi (2012) exhibits good predictions in this case. For further verification, Fig. 8 shows a very good correlation between the predicted and actual strain of heavily confined circular sections. The average absolute error of the proposed model is 5× less than the model of ACI 440.2R-08 (ACI 2008).

In summary, the proposed model predicts very close results for the strain of CFRP-confined concrete. In addition, the proposed model also shows good agreement with the test data in the range of insufficient and heavy confinement as defined previously.

Square FRP-Confined Concrete Columns

The same procedure was carried out to verify the proposed model for square sections. A total of 69 data points (Fig. 9) were plotted to assess the performance of existing models and the proposed model. Four existing models were considered in this verification [Shehata et al. 2002; Lam and Teng 2003b; ACI 440.2R-08 (ACI 2008); Ilki et al. 2008].

Comparing the existing models for square sections, the models of Lam and Teng (2003a), ACI 440.2R-08 (ACI 2008), and Ilki et al. (2008) show quite good predictions for the strain of CFRP-confined concrete. Among these existing models, the results from the model of Ilki et al. (2008) overestimate the actual values, whereas the other models present a good general trend. However, the proposed model gives a better precision than the other models in estimating the strain of CFRP-confined concrete columns (Figs. 9 and 10).

For insufficient confined specimens (places close to the origin of the coordinates), the models of Lam and Teng (2003b), ACI 440.2R-08 (ACI 2008), and the proposed model show good predictions. The models of Ilki et al. (2008) and Shehata et al. (2002) do not exhibit close correlation in this case. In addition, all five models underestimate the strain of confined concrete when the confinement ratio is high [six data points have a measured strain greater than 3 (Fig. 9)].

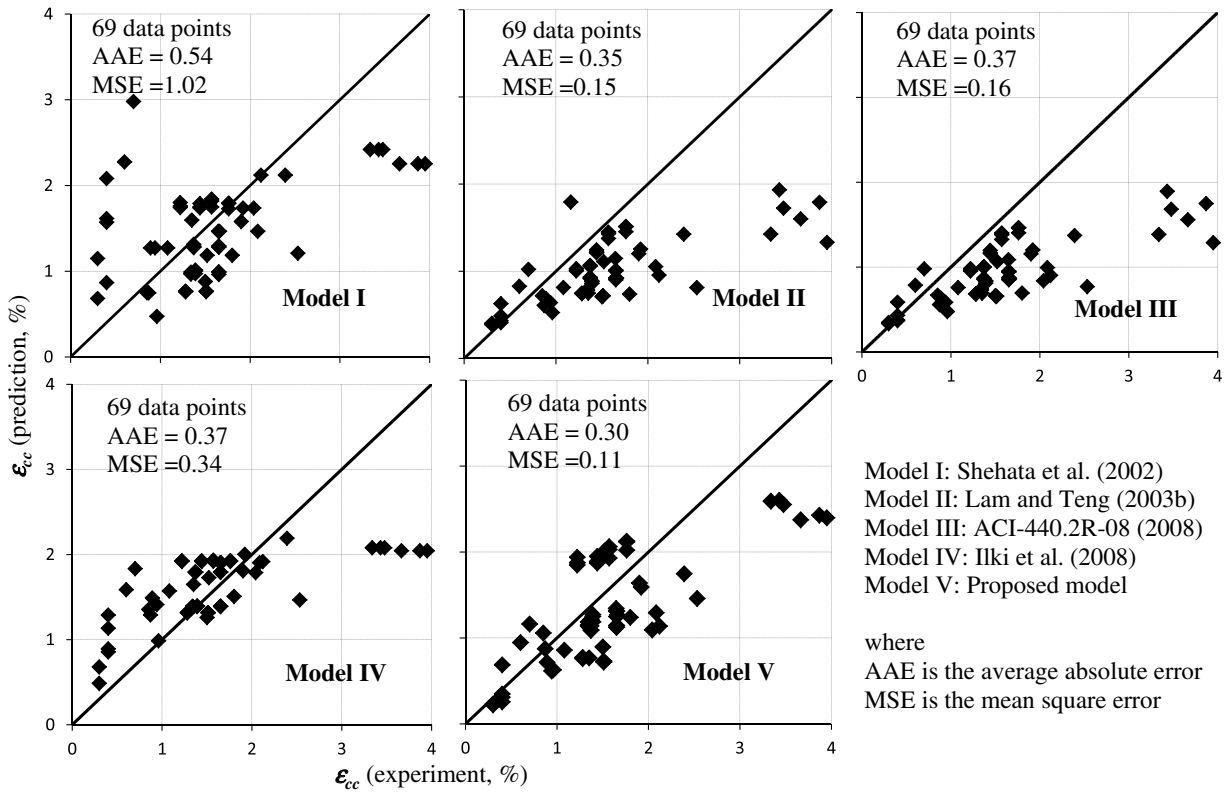

Fig. 9. Performance of models on square specimens

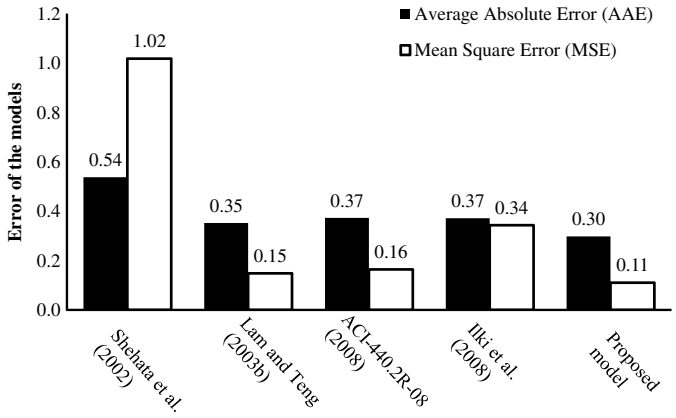

Fig. 10. Accuracy comparisons for strain prediction of square specimens among the models

Conclusions

From the theoretical analyses presented in this paper, the following conclusions are drawn:

- The proposed model provides very good predictions compared with the experimental results, and it also shows a good agreement with the test data in the range of insufficient and heavy confinement, which are usually not predicted well by other models;
- Only a proportion of the energy absorbed by the entire column is transferred to rupture the FRP; and
- The formula to calculate the strain of square sections is still not as good as that of circular sections; thus, further study needs to be carried out in this case.

Finally, a new model is proposed in this paper to calculate the strain of confined concrete based on the energy-absorption method. The performance of the proposed model shows very good correlations with experimental results. However, the precision of the proposed model should improve when it is calibrated with a larger reliable database in the future. This methodology can be developed to cover reinforced concrete columns confined with FRP.

Acknowledgments

The first writer acknowledges the Vietnamese Government and the University of Wollongong for the support of his full Ph.D. scholarship. The writers thank Ph.D. scholar Mr. Ida Bagus Rai Widiarsa for his database. Furthermore, the constructive comments of the editor and reviewers are gratefully appreciated.

Notation

The following symbols are used in this paper:

A_{cc} = gross-sectional area of confined concrete;
b = side length of a square section;
d = diameter of the section;
dl = increment of the displacement;
$d\varepsilon_c$ = increment of the axial strain;
f_c = stress of concrete;
f_f = rupture strength of FRP obtained from flat-coupon tests;
f_{fe} = actual rupture strength of FRP on the columns;
f_l = confining pressure of the confined concrete specimen;
f'_{cc} = confined concrete strength;
f'_{co} = unconfined concrete strength;
k = proportion factor showing the relationship between the energy absorption of the column core and external FRP;
k_c = corner-energy ratio;
l = displacement;
P = applied load;
r = radius of the round corner of the section;
t = thickness of FRP;
U = strain energy;
U_{cc} = volumetric strain energy of confined concrete;
U_f = volumetric strain energy of FRP;
W = work done by the applied load;
W_{cc} = strain energy of confined concrete;
W_f = strain energy of FRP;
ε_c = axial strain of concrete;
ε_{cc} = axial strain at the peak stress of confined concrete;
ε_{co} = axial strain at the peak stress of unconfined concrete;
ε_f = rupture strain of FRP obtained from flat-coupon tests;
ε_{fe} = rupture strain of FRP on the columns; and
ρ_f = volumetric ratio of FRP.

References

Al-Salloum, Y. A. (2007). "Influence of edge sharpness on the strength of square concrete columns confined with FRP composite laminates." *Compos. Part B Eng.*, 38(5), 640–650.

American Concrete Institute (ACI). (2008). "Guide for the design and construction of externally bonded FRP systems for strengthening concrete structures." *ACI 440.2R-08*, Farmington Hills, MI.

Berthet, J. F., Ferrier, E., and Hamelin, P. (2005). "Compressive behavior of concrete externally confined by composite jackets. Part A: Experimental study." *Construct. Build. Mater.*, 19(3), 223–232.

Bisby, L. A., Dent, A. J. S., and Green, M. F. (2005). "Comparison of confinement models for fiber-reinforced polymer-wrapped concrete." *ACI Struct. J.*, 102(1), 62–72.

Carey, S. A., and Harries, K. A. (2005). "Axial behavior and modeling of confined small-, medium-, and large-scale circular sections with carbon fiber-reinforced polymer jackets." *ACI Struct. J.*, 102(4), 596–604.

Chaallal, O., Shahawy, M., and Hassan, M. (2003). "Performance of axially loaded short rectangular columns strengthened with carbon fiber-reinforced polymer wrapping." *J. Compos. Construct.*, 10.1061/(ASCE)1090-0268(2003)7:3(200), 200–208.

Csuka, B., and Kollár, L. P. (2012). "Analysis of FRP confined columns under eccentric loading." *Compos. Struct.*, 94(3), 1106–1116.

Cusson, D., and Paultre, P. (1995). "Stress-strain model for confined high-strength concrete." *J. Struct. Eng.*, 10.1061/(ASCE)0733-9445(1995)121:3(468), 468–477.

De Lorenzis, L., Micelli, F., and La Tegola, A. (2002). "Influence of specimen size and resin type on the behavior of FRP-confined concrete cylinders." *Proc., 1st Int. Conf., Advanced Polymer Composites for Structural Applications in Construction*, R. A. Shenoi, S. S. J. Moy, and L. C. Hollaway, eds., Thomas Telford Publishing, London, 231–239.

De Lorenzis, L., and Tepfers, R. (2003). "Comparative study of models on confinement of concrete cylinders with fiber-reinforced polymer composites." *J. Compos. Construct.*, 7(3), 10.1061/(ASCE)1090-0268(2003)7:3(219), 219–237.

Demers, M., and Neale, K. W. (1994). "Strengthening of concrete columns with unidirectional composite sheets." *Developments in short and medium span bridge engineering*, A. A. Mufti, B. Bakht, and L. G. Jaeger, eds., Canadian Society for Civil Engineering, Montreal, 895–905.

Hadi, M. N. S., Pham, T. M., and Lei, X. (2013). "New method of strengthening reinforced concrete square columns by circularizing and wrapping with fiber-reinforced polymer or steel straps." *J. Compos. Construct.*, 10.1061/(ASCE)CC.1943-5614.0000335, 229–238.

Ilki, A., and Kumbasar, N. (2003). "Compressive behaviour of carbon fibre composite jacketed concrete with circular and non-circular cross-sections." *J. Earthquake Eng.*, 7(3), 381–406.

Ilki, A., Peker, O., Karamuk, E., Demir, C., and Kumbasar, N. (2008). "FRP retrofit of low and medium strength circular and rectangular reinforced concrete columns." *J. Mater. Civ. Eng.*, 10.1061/(ASCE)0899-1561(2008)20:2(169), 169–188.

Jiang, T., and Teng, J. G. (2007). "Analysis-oriented stress-strain models for FRP-confined concrete." *Eng. Struct.*, 29(11), 2968–2986.

Karabinis, A., Rousakis, T., and Manolitsi, G. (2008). "3D finite-element analysis of substandard RC columns strengthened by fiber-reinforced polymer sheets." *J. Compos. Construct.*, 10.1061/(ASCE)1090-0268(2008)12:5(531), 531–540.

Karabinis, A. I., and Rousakis, T. C. (2002). "Concrete confined by FRP material: A plasticity approach." *Eng. Struct.*, 24(7), 923–932.

Karbhari, V. M., and Gao, Y. (1997). "Composite jacketed concrete under uniaxial compression verification of simple design equations." *J. Mater. Civ. Eng.*, 10.1061/(ASCE)0899-1561(1997)9:4(185), 185–193.

Lam, L., and Teng, J. G. (2003a). "Design-oriented stress-strain model for FRP-confined concrete." *Constr. Build. Mater.*, 17(6–7), 471–489.

Lam, L., and Teng, J. G. (2003b). "Design-oriented stress-strain model for FRP-confined concrete in rectangular columns." *J. Reinforc. Plast. Compos.*, 22(13), 1149–1186.

Lam, L., Teng, J. G., Cheung, C. H., and Xiao, Y. (2006). "FRP-confined concrete under axial cyclic compression." *Cement Concr. Compos.*, 28(10), 949–958.

Lu, G., and Yu, T. X. (2003). *Energy absorption of structures and materials*, Woodhead Publishing, Boca Raton, FL.

Mander, J. B., Park, R., and Priestley, M. J. N. (1988). "Theoretical stress-strain model for confined concrete." *J. Struct. Eng.*, 10.1061/(ASCE)0733-9445(1988)114:8(1804), 1804–1826.

Masia, M. J., Gale, T. N., and Shrive, N. G. (2004). "Size effects in axially loaded square-section concrete prisms strengthened using carbon fibre reinforced polymer wrapping." *Can. J. Civ. Eng.*, 31(1), 1–13.

Matthys, S., Taerwe, L., and Audenaert, K. (1999). "Tests on axially loaded concrete columns confined by fiber reinforced polymer sheet wrapping." *Proc., 4th Int. Symp. on Fiber Reinforced Polymer Reinforcement for Reinforced Concrete Structures*, C. W. Dolan, S. H. Rizkalla, and S. H. Nanni, eds., 188, American Concrete Institute, Farmington Hills, MI, 217–229.

Mirmiran, A., Shahawy, M., Samaan, M., Echary, H. E., Mastrapa, J. C., and Pico, O. (1998). "Effect of column parameters on FRP-confined concrete." *J. Compos. Construct.*, 10.1061/(ASCE)1090-0268(1998)2:4(175), 175–185.

Miyauchi, K., Inoue, I., Kuroda, T., and Kobayashi, A. (1999). "Strengthening effects of concrete column with carbon fiber sheet." *Trans. Japan Concr. Inst.*, 21(1), 143–150.

Parvin, A., and Wang, W. (2001). "Behavior of FRP jacketed concrete columns under eccentric loading." *J. Compos. Construct.*, 10.1061/(ASCE)1090-0268(2001)5:3(146), 146–152.

Pessiki, S., Harries, K. A., Kestner, J. T., Sause, R., and Ricles, J. M. (2001). "Axial behavior of reinforced concrete columns confined with FRP jackets." *J. Compos. Construct.*, 10.1061/(ASCE)1090-0268(2001)5:4(237), 237–245.

Richart, F. E., Brandtzaeg, A., and Brown, R. L. (1929). "The failure of plain and spirally reinforced concrete in compression." *Bulletin 1990*, Univ. of Illinois Engineering Experimental Station, Champaign, IL.

Rochette, P., and Labossiére, P. (2000). "Axial testing of rectangular column models confined with composites." *J. Compos. Construct.*, 10.1061/(ASCE)1090-0268(2000)4:3(129), 129–136.

Rousakis, T. C., and Karabinis, A. I. (2012). "Adequately FRP confined reinforced concrete columns under axial compressive monotonic or cyclic loading." *Mater. Struct.*, 45(7), 957–975.

Rousakis, T. C., Karabinis, A. I., and Kiousis, P. D. (2007). "FRP-confined concrete members: Axial compression experiments and plasticity modelling." *Eng. Struct.*, 29(7), 1343–1353.

Rousakis, T. C., Rakitzis, T., and Karabinis, A. I. (2012). "Empirical modelling of failure strains of uniformly FRP confined concrete columns." *Proc., Int. Conf. on FRP Composites in Civil Engineering*, Int. Institute for FRP in Construction, Queen's Univ., Kingston, ON, 1–8.

Saadatmanesh, H., Ehsani, M. R., and Li, M. W. (1994). "Strength and ductility of concrete columns externally reinforced with fiber-composite straps." *ACI Struct. J.* 91(4), 434–447.

Saenz, N., and Pantelides, C. (2006). "Short and medium term durability evaluation of FRP-confined circular concrete." *J. Compos. Construct.*, 10.1061/(ASCE)1090-0268(2006)10:3(244), 244–253.

Shehata, I. A. E. M., Carneiro, L. A. V., and Shehata, L. C. D. (2002). "Strength of short concrete columns confined with CFRP sheets." *Mater. Struct.*, 35(1), 50–58.

Suter, R., and Pinzelli, R. (2001). "Confinement of concrete columns with FRP sheets." *Proc., Int. Symp. on Fiber-Reinforced Polymer Reinforcement for Concrete Structures*, C. Burgoyne, ed., Thomas Telford Publishing, London, 793–802.

Tao, Z., Yu, Q., and Zhong, Y. Z. (2008). "Compressive behaviour of CFRP-confined rectangular concrete columns." *Mag. Concr. Res.*, 60(10), 735–745.

Tasdemir, M. A., Tasdemir, C., Akyüz, S., Jefferson, A. D., Lydon, F. D., and Barr, B. I. G. (1998). "Evaluation of strains at peak stresses in concrete: A three-phase composite model approach." *Cement Concr. Compos.*, 20(4), 301–318.

Teng, J. G., Jiang, T., Lam, L., and Luo, Y. Z. (2009). "Refinement of a design-oriented stress-strain model for FRP-confined concrete." *J. Compos. Construct.*, 10.1061/(ASCE)CC.1943-5614.0000012, 269–278.

Toutanji, H. A. (1999). "Stress-strain characteristics of concrete columns externally confined with advanced fiber composite sheets." *ACI Mater. J.*, 96(3), 397–404.

Valdmanis, V., De Lorenzis, L., Rousakis, T., and Tepfers, R. (2007). "Behaviour and capacity of CFRP-confined concrete cylinders subjected to monotonic and cyclic axial compressive load." *Struct. Concr.*, 8(4), 187–190.

Wang, L. M., and Wu, Y. F. (2008). "Effect of corner radius on the performance of CFRP-confined square concrete columns: Test." *Eng. Struct.*, 30(2), 493–505.

Watanabe, K., et al. (1997). "Confinement effect of FRP sheet on strength and ductility of concrete cylinders under uniaxial compression." *Proc., Int. Symp., Non-Metallic (FRP) Reinforcement for Concrete Structures*, Vol. 1, Japan Concrete Institute, Sapporo, Japan, 233–240.

Wolff, C., Bastid, P., and Bunsell, A. R. (1994). "Relation of energy absorption of composite structures to material strength." *Compos. Eng.*, 4(2), 195–218.

Wu, Y. F., and Wei, Y. Y. (2010). "Effect of cross-sectional aspect ratio on the strength of CFRP-confined rectangular concrete columns." *Eng. Struct.*, 32(1), 32–45.

Wu, Y. F., and Zhou, Y. W. (2010). "Unified strength model based on Hoek-Brown failure criterion for circular and square concrete columns confined by FRP." *J. Compos. Construct.*, 10.1061/(ASCE)CC.1943-5614.0000062, 175–184.

Xiao, Y., and Wu, H. (2000). "Compressive behavior of concrete confined by carbon fiber composite jackets." *J. Mater. Civ. Eng.*, 10.1061/(ASCE)0899-1561(2000)12:2(139), 139–146.

Yazici, V., and Hadi, M. N. S. (2012). "Normalized confinement stiffness approach for modeling FRP-confined concrete." *J. Compos. Construct.*, 10.1061/(ASCE)CC.1943-5614.0000283, 520–528.

4 PREDICTING STRESS/STRAIN OF FRP-CONFINED SQUARE CONCRETE COLUMNS BY ARTIFICIAL NEURAL NETWORKS

Summary

This study proposes the use of artificial neural networks (ANNs) to calculate the compressive strength and strain of fiber reinforced polymer (FRP) confined square/rectangular columns. Modelling results have shown that the two proposed ANN models fit the testing data very well. Specifically, the average absolute errors of the two proposed models are less than 5%. The ANNs were trained, validated, and tested on two databases. The first database contains the experimental compressive strength results of 104 FRP-confined rectangular concrete columns. The second database consists of the experimental compressive strain of 69 FRP-confined square concrete columns. Furthermore, this study proposes a new potential approach to generate a user-friendly equation from a trained ANN model. The proposed equations estimate the compressive strength/strain with small error. As such the equations could be easily used in engineering designs instead of the “invisible” processes inside the ANN.

Citation

This paper was accepted for publication in Journal of Composites for Construction with the following citation:

Pham, T.M., and Hadi, M.N.S. (2014). "Predicting Stress and Strain of FRP-confined Rectangular/Square Columns Using Artificial Neural Networks." *Journal of Composites for Construction*, DOI 10.1061/(ASCE)CC.1943-5614.0000477.

Predicting Stress and Strain of FRP-Confined Square/Rectangular Columns Using Artificial Neural Networks

Thong M. Pham, S.M.ASCE[1]; and Muhammad N. S. Hadi, M.ASCE[2]

Abstract: This study proposes the use of artificial neural networks (ANNs) to calculate the compressive strength and strain of fiber reinforced polymer (FRP)–confined square/rectangular columns. Modeling results have shown that the two proposed ANN models fit the testing data very well. Specifically, the average absolute errors of the two proposed models are less than 5%. The ANNs were trained, validated, and tested on two databases. The first database contains the experimental compressive strength results of 104 FRP confined rectangular concrete columns. The second database consists of the experimental compressive strain of 69 FRP confined square concrete columns. Furthermore, this study proposes a new potential approach to generate a user-friendly equation from a trained ANN model. The proposed equations estimate the compressive strength/strain with small error. As such, the equations could be easily used in engineering design instead of the *invisible* processes inside the ANN. **DOI: 10.1061/(ASCE)CC.1943-5614.0000477.** © *2014 American Society of Civil Engineers.*

Author keywords: Fiber reinforced polymer; Confinement; Concrete columns; Neural networks; Compressive strength; Computer model.

Introduction

The use of FRP confined concrete columns has been proven in enhancing the strength and the ductility of columns. Over the last two decades, a large number of experimental and analytical studies have been conducted to understand and simulate the compressive behavior of FRP confined concrete. Experimental studies have confirmed the advantages of FRP confined concrete columns in increasing the compressive strength, strain, and ductility of columns (Hadi and Li 2004; Hadi 2006a, b, 2007a, b; Rousakis et al. 2007; Hadi 2009; Wu and Wei 2010; Hadi and Widiarsa 2012; Hadi et al. 2013; Pham et al. 2013). Meanwhile, many stress-strain models were developed to simulate the results from experimental studies. Most of the existing models were based on the mechanism of confinement together with calibration of test results to predict the compressive stress and strain of FRP confined concrete columns (Lam and Teng 2003a; Ilki et al. 2008; Wu and Wang 2009; Wu and Wei 2010; Rousakis et al. 2012; Yazici and Hadi 2012; Pham and Hadi 2013, 2014). Models developed by this approach provide a good understanding of stress-strain curve of the confined concrete, but their errors in estimating the compressive strength and strain are still considerable. Bisby et al. (2005) had carried out an overview on confinement models for FRP confined concrete and indicated that the average absolute error of strain estimation ranges from 35–250%, whereas the error of strength estimation is approximately 14–27%. In addition, Ozbakkaloglu et al. (2013) had reviewed 88 existing FRP confinement models for circular columns. That study showed that the average absolute errors of the above models in estimating stress and strain are greater than 10 and 23%, respectively. Thus, it is necessary for the research community to improve the accuracy of estimating both the compressive stress and strain of FRP confined concrete. This study introduces the use of artificial neural networks (ANNs) to predict the compressive strength and strain of FRP confined square/rectangular concrete columns because of the input parameters including geometry of the section and mechanical properties of the materials.

ANN can be applied to problems where patterns of information represented in one form need to be mapped into patterns of information in another form. As a result, various ANN applications can be categorized as classification or pattern recognition or prediction and modeling. ANN is commonly used in many industrial disciplines, for example, banking, finance, forecasting, process engineering, structural control and monitoring, robotics, and transportation. In civil engineering, ANN has been applied to many areas, including damage detection (Wu et al. 1992; Elkordy et al. 1993), identification and control (Masri et al. 1992; Chen et al. 1995), optimization (Hadi 2003; Kim et al. 2006), structural analysis and design (Hajela and Berke 1991; Adeli and Park 1995), and shear resistance of beams strengthened with FRP (Perera et al. 2010a, b).

In addition, ANN has also been used to predict the compressive strength of FRP confined circular concrete columns (Naderpour et al. 2010; Jalal and Ramezanianpour 2012). This study uses ANN to predict both the compressive strength and strain of FRP confined square/rectangular concrete columns. Furthermore, a new potential approach is introduced to generate predictive user-friendly equations for the compressive strength and strain.

Experimental Databases

The test databases used in this study is adopted from the studies by Pham and Hadi (2013, 2014). Details of the databases could be found elsewhere in these studies, but for convenience the main properties of specimens are summarized. It is noted that when the axial strain of unconfined concrete at the peak stress (εco)

[1]Ph.D. Candidate, School of Civil, Mining and Environmental Engineering, Univ. of Wollongong, Wollongong, NSW 2522, Australia; formerly, Lecturer, Faculty of Civil Engineering, Ho Chi Minh Univ. of Technology, Ho Chi Minh City, Vietnam.

[2]Associate Professor, School of Civil, Mining and Environmental Engineering, Univ. of Wollongong, NSW 2522, Australia (corresponding author). E-mail: mhadi@uow.edu.au

Note. This manuscript was submitted on November 14, 2013; approved on February 3, 2014; published online on March 13, 2014. Discussion period open until August 13, 2014; separate discussions must be submitted for individual papers. This paper is part of the ***Journal of Composites for Construction***, © ASCE, ISSN 1090-0268/04014019(9)/$25.00.

is not specified, it can be estimated using the equation proposed by Tasdemir et al. (1998) as follows:

$$\varepsilon_{co} = (-0.067 f_{co}'^2 + 29.9 f_{co}' + 1,053)10^{-6} \quad (1)$$

In the literature, test results of the compressive strain of FRP confined concrete is relatively less than that of the compressive strength. If a database is used to verify both the strain and strength models, the size of this database will be limited by the number of specimens having results of the strain. Thus, to maximize the database size, this study uses two different databases for the two proposed models. In addition, studies about FRP confined rectangular specimens focused on confined strength but not strain. Thus data about confined strain of rectangular specimens reported are extremely limited. When the number of rectangular specimens is much fewer than that of square columns, it is not reliable to predict the compressive strain of the rectangular specimens by using a mixed database. Therefore, this paper deals with strain of square specimens only.

All specimens collated in the databases were chosen based on similar testing schemes, ratio of the height and the side length, failure modes, and similar stress-strain curves. The ratio of the height and the side length is 2. The aspect ratio of the rectangular specimens ranged between 1 and 2.7. Test results of the specimens which have a descending type in the stress-strain curves were excluded from the databases. In addition, a few studies concluded that square columns confined with FRP provide a little (Mirmiran et al. 1998) or no strength improvement (Wu and Zhou 2010). Thus, this study deals only with specimens with round corner, as such specimens with sharp corners were excluded from the databases. After excluding all the above, the databases contained the test results of 104 FRP confined rectangular concrete columns and 69 FRP confined square concrete columns for the strength and strain models, respectively.

Artificial Neural Network Modeling

Compressive Strength of FRP Confined Rectangular Columns

The ANN strength model was developed by the ANN toolbox of *MATLAB* R2012b (*MATLAB*) to estimate the compressive strength of FRP confined rectangular specimens. The data used to train, validate and test the proposed model were obtained from the paper by Pham and Hadi (2014). The database contained 104 FRP confined rectangular concrete columns having unconfined concrete strength between 18.3 and 55.2 MPa. The database was randomly divided into training (70%), validation (15%), and test (15%) by the function *Dividerand*.

Following the data division and preprocessing, the optimum model architecture (the number of hidden layers and the corresponding number of hidden nodes) needs to be investigated. Hornik et al. (1989) provided a proof that multilayer feed forward networks with as few as one hidden layer of neurons are indeed capable of universal approximation in a very precise and satisfactory sense. Thus, one hidden layer was used in this study. The optimal number of hidden nodes was obtained by a trial and error approach in which the network was trained with a set of random initial weights and a fixed learning rate of 0.01.

Because the number of input, hidden, and output neurons is determined, it is possible to estimate an appropriate number of samples in the training data set. Upadhyaya and Eryurek (1992) proposed an equation to calculate the necessary number of training samples as follows:

$$\frac{w}{o} \le n \le \frac{w}{o}\log_2^{w/o} \quad (2)$$

where w is the number of weights, o is the number of the output parameters, and n is the number of the training samples. Substituting the number of weights and the number of the output parameters into Eq. (2), the following condition is achieved:

$$54 \le n = 73 \le 310 \quad (3)$$

Once the network has been designed and the input/output have been normalized, the network would be trained. The *MATLAB* neural network toolbox supports a variety of learning algorithms, including gradient descent methods, conjugate gradient methods, the Levenberg-Marquardt (LM) algorithm, and the resilient back-propagation algorithm (Rprop). The LM algorithm was used in this study. In the *MATLAB* neural network toolbox, the LM method (denoted by function *Trainlm*) requires more memory than other methods. However, the LM method is highly recommended because it is often the fastest back-propagation algorithm in the toolbox. In addition, it does not cause any memory problem with the small training dataset though the learning process was performed on a conventional computer.

In brief, the network parameters are: network type is feed-forward back propagation, number of input layer neurons is eight, number of hidden layer neurons is six, one neuron of output layer is used, type of back propagation is Levenberg-Marquardt, training function is Trainlm, adaption learning function is *Learngdm*, performance function is MSE, transfer functions in both hidden and output layers are *Tansig*. The network architecture of the proposed ANN strength model is illustrated in Fig. 1.

In the development of an artificial neural network to predict the compressive strength of FRP confined rectangular concrete specimens (f'_{cc} in MPa), the selection of the appropriate input parameters is a very important process. The compressive strength of confined concrete should be dependent on the geometric dimensions and the material properties of concrete and FRP. The geometric dimensions are defined as the short side length (b in mm), the long side length (h in mm), and the corner radius (r in mm). Meanwhile, the material properties considered are: the axial compressive strength (f'_{co} in MPa) and strain (εco in %) of concrete, the nominal thickness of FRP (tf in mm), the elastic modulus of FRP (Ef in GPa), and the tensile strength of FRP (ff in MPa).

Compressive Strain of FRP Confined Square Columns

The ANN strain model was developed to estimate the compressive strain of FRP confined square specimens. The data used in this

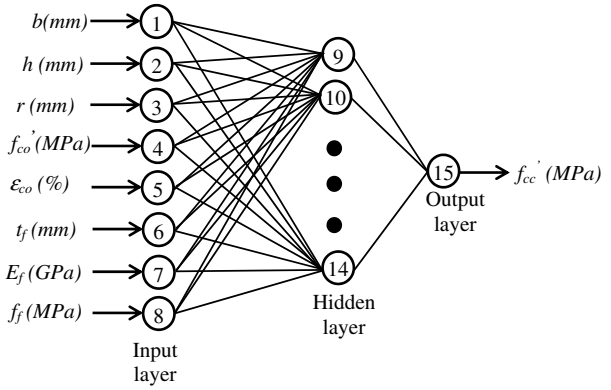

Fig. 1. Architecture of the proposed ANN strength model

model were adopted from the study by Pham and Hadi (2013). The database contained 69 FRP confined square concrete columns having unconfined concrete strength between 19.5 and 53.9 MPa.

The algorithm and design of the ANN strain model are the same as the proposed ANN strength model with details as follows: network type is feed-forward back propagation, number of input layer neurons is seven, number of hidden layer neurons is six, one neuron of output layer, type of back propagation is Levenberg-Marquardt, training function is Trainlm, adaption learning function is Learngdm, performance function is MSE, transfer functions in both hidden and output layers are Tansig. The architecture of the proposed model is similar to Fig. 1 with exclusion of variable h.

Once the network was designed, the necessary number of training samples could be estimated by using Eq. (2) as follows:

$$48 \leq n = 48 \leq 268 \tag{4}$$

Performance of the Proposed Models

The performance of the proposed ANN strength model was verified by the database of 104 rectangular specimens. Fig. 2 shows the predictions of the ANN strength model as compared with the experimental values. Many existing models for FRP confined concrete were adopted to compare with the proposed model. However, because of space limitations of the paper, five existing models were studied in this verification (Lam and Teng 2003b; Wu and Wang 2009; Toutanji et al. 2010; Wu and Wei 2010; Pham and Hadi 2014). These models were chosen herein because they have had high citations and yielded good agreement with the database. The comparison between the predictions and the test results in Fig. 2 shows improvement of the selected models in predicting the strength of FRP confined rectangular columns over the last decade. The proposed ANN strength model has the highest general correlation factor ($R^2 = 96\%$) for a linear trend between the prediction and the test results while the other models have a correlation factor between approximately 78 and 88%.

To examine the accuracy of the proposed strength model, three statistical indicators were used: the mean square error (MSE), the average absolute error (AAE), and the standard deviation (SD). Among the presented models, the proposed ANN strength model depicts a significant improvement in calculation errors as shown in Fig. 3. A low SD of the proposed ANN strength model indicates that the data points tend to be very close to the mean values.

Meanwhile, the performance of the proposed ANN strain model is verified by the database which had 69 square specimens. Fig. 4 shows the compressive strain of the specimens predicted by the ANN strain model versus the experimental values. To make a comparison with other models, five existing models were considered in this verification [Shehata et al. 2002; Lam and Teng 2003b; ACI 440.2R-08 (ACI 2008); Ilki et al. 2008; Pham and Hadi 2013]. The proposed ANN strain model outperforms the selected models in estimating the compressive strain of confined square columns as shown in Fig. 4. The highest general correlation factor ($R^2 = 98\%$) was achieved by the proposed model while the correlation factor of the other models was less than 60%. For further evaluation, the values of MSE, AAE, and SD were calculated and presented. Fig. 5 shows that the proposed model significantly reduces the error in estimating the compressive strain of FRP

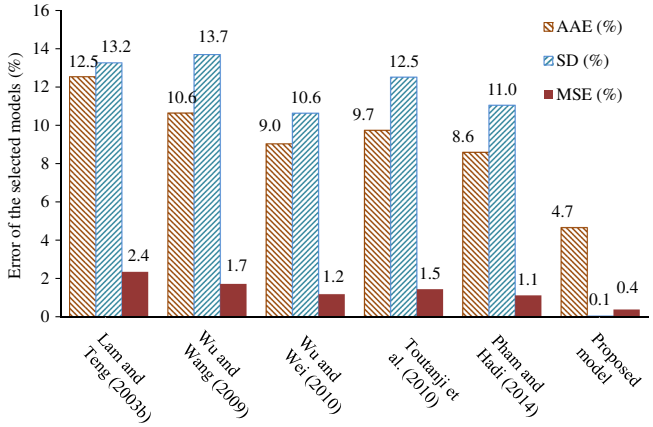

Fig. 3. Accuracy of the selected strength models

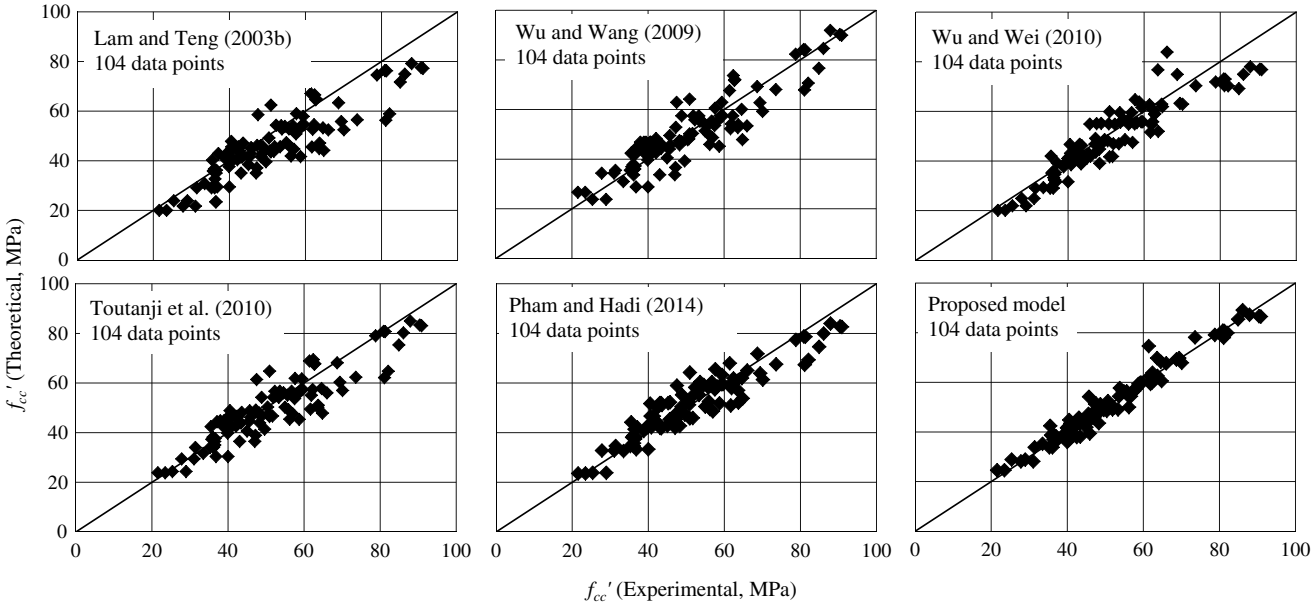

Fig. 2. Comparison of the selected strength models

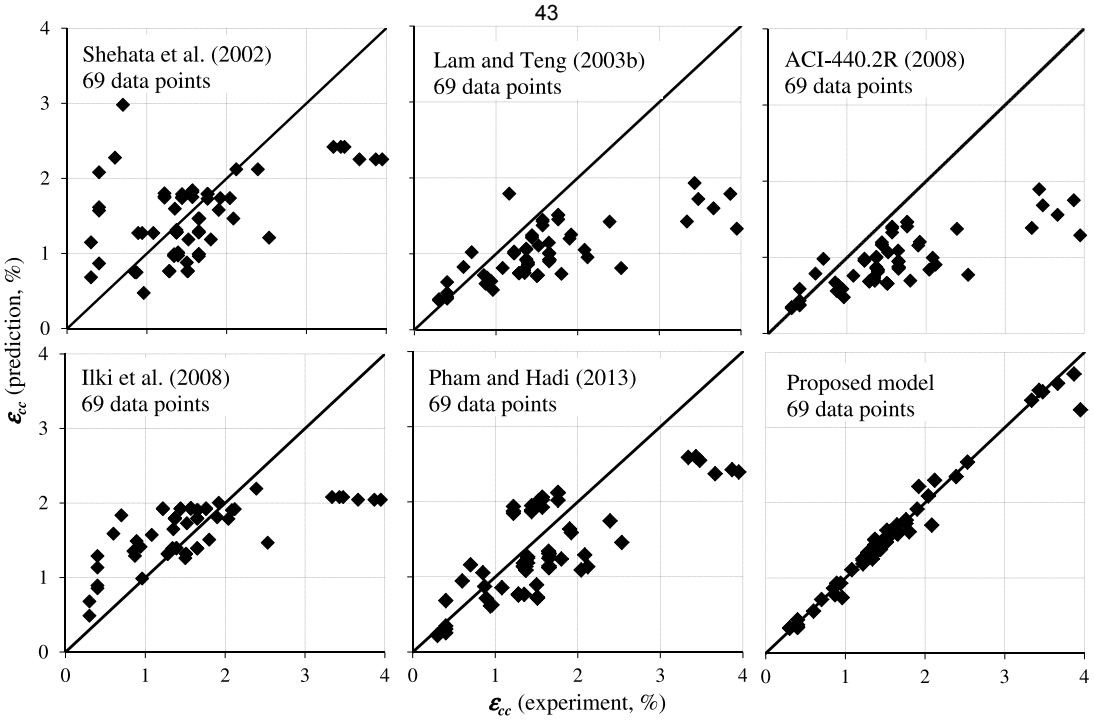

Fig. 4. Comparison of the selected strain models

confined square specimens by approximately five times as compared with the other models. The average absolute error (AAE) of the existing models is approximately 30%, whereas the AAE of the proposed model is approximately 5%.

Proposal of User-Friendly Equations

In the previous section, the Tansig transfer function was used in the ANN as it provides better results than *Pureline* transfer function. Although the simulated results from the proposed ANNs have a good agreement with the experimental data, it is inconvenient for engineers to use the networks in engineering design. It is logical and possible that a functional-form equation could be explicitly derived from the trained networks by combining the weight matrix and the bias matrix. Nevertheless, the final equations will become very complicated because the proposed ANN models contain complex transfer functions, which are Tansig as shown in Eq. (5) below.

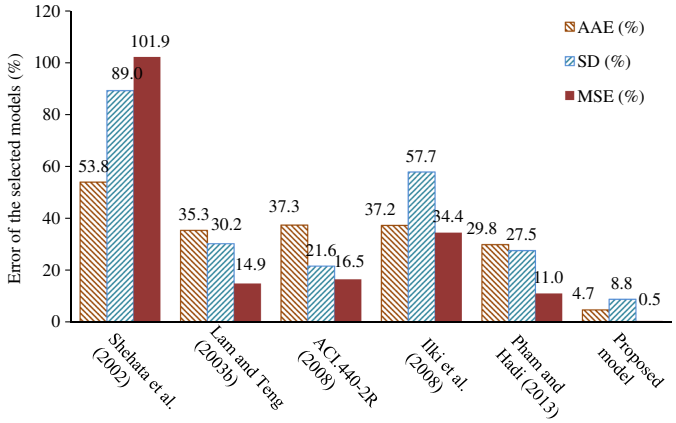

Fig. 5. Accuracy of the selected strain models

Therefore, to generate user-friendly equations to calculate stress and strain of FRP confined concrete, the Tansig transfer function used in the previous section was replaced by the Pureline transfer function [Eq. (6)]. A method that uses ANNs to generate user-friendly equations for calculating the compressive strength or strain of FRP confined square/rectangular columns is proposed. As a result, the proposed equation could replace the ANN to yield the same results. Once an ANN is trained and yields good results, a user-friendly equation could be derived following the procedure described below.

$$\tan sig(x) = \frac{2}{1+e^{-2x}} - 1 \tag{5}$$

$$\text{purelin}(x) = x \tag{6}$$

Mathematical Derivations

The architecture of the proposed models is modified to create a simpler relationship between the inputs and the output as shown in Fig 6. The following equations illustrate the notation in Fig. 6.

$$\mathbf{X} = [bhrf'_{co}\varepsilon_{co}t_f E_f f_f]^T = [x_1 x_2 x_3 x_4 x_5 x_6 x_7 x_8]^T \tag{7}$$

where X is the input matrix, which contains eight input parameters, and superscript T denotes a transpose matrix. Functions that illustrate the relationships of neurons inside the network are presented as follows:

$$\mathbf{u} = \mathbf{IWX} + \mathbf{b}_1 = \sum_{j=1}^{6}\sum_{i=1}^{8} IW_{j,i}x_i + b_{1j} \tag{8}$$

$$\mathbf{u}_1 = \text{purelin}(\mathbf{u}) = \mathbf{u} \tag{9}$$

$$\mathbf{u_2} = \mathbf{LW u_1} + \mathbf{b}_2 = \sum_{i=1}^{6} LW_i u_{1i} + b_{2i} \tag{10}$$

$$\mathbf{y} = \text{purelin}(\mathbf{u_2}) = \mathbf{u_2} \tag{11}$$

where u, u_1, and u_2 are the intermediary matrices; Purelin is the transfer function; y is the output parameter which is the compressive strength of FRP confined square/rectangular columns (f'_{cc} in MPa); IW is the input weight matrix; b_1 is the bias matrix of Layer 1; LW is the layer weight matrix; and b_2 is the bias matrix of Layer 2.

From Eqs. (7)–(11) and Fig. 6, the output could be calculated from the input parameters by the following equation:

$$\mathbf{y} = \mathbf{LW} \times \mathbf{IW} \times \mathbf{X} + \mathbf{LW} \times \mathbf{b_1} + \mathbf{b_2} \tag{12}$$

Based on Eq. (12), it is obvious that a user-friendly equation could be derived from a trained network. To simplify the above equation, another expression could be derived as follows:

$$\mathbf{y} = \mathbf{W} \times \mathbf{X} + \mathbf{a} \tag{13}$$

where W is a proportional matrix and a is a scalar, which are calculated as follows:

$$\mathbf{W} = \mathbf{LW} \times \mathbf{IW} \tag{14}$$

$$\mathbf{a} = \mathbf{LW} \times \mathbf{b}_1 + \mathbf{b}_2 \tag{15}$$

where the matrix W is denoted as follows:

$$\mathbf{W} = [w_1 \quad w_2 \quad w_3 \quad w_4 \quad w_5 \quad w_6 \quad w_7 \quad w_8] \tag{16}$$

Proposed Equation for Compressive Strength

A modified ANN strength model was proposed to estimate the compressive strength of FRP confined rectangular concrete columns. The modified ANN strength model was trained on the database of 104 FRP confined rectangular concrete columns. All procedures introduced in the previous sections were applied for this model with exception of the transfer function. As described in Fig. 6, the Purelin transfer function was used instead of the Tansig transfer function. After training, the input weight matrix (IW), the layer weight matrix (LW), and the bias matrices (b_1 and b_2) were obtained. From Eqs. (14) and (15), the proportional matrix (W) and the scalar (a) were determined as follows:

$$\mathbf{W} = \mathbf{LW} \times \mathbf{IW}$$

$$\mathbf{W} = [-0.21 \quad -0.36 \quad 0.39 \quad 5.68 \quad -5.36 \quad 1.33 \quad 0.40 \quad 0.64] \tag{17}$$

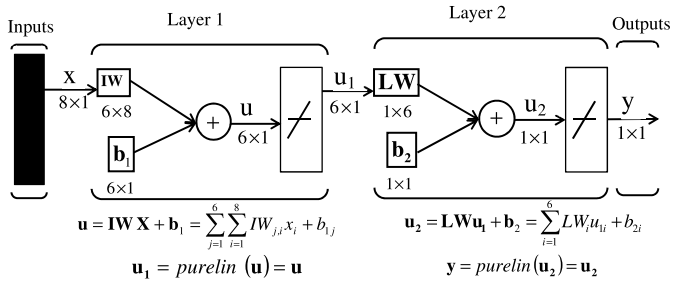

Fig. 6. Architecture of the proposed ANN strength equation

$$\mathbf{a} = \mathbf{LW} \times \mathbf{b}_1 + \mathbf{b}_2 = 0.24 \tag{18}$$

It is to be noted that the inputs and the output in Eq. (13) are normalized. The relationship between the actual inputs and the actual output is presented in the equations below:

$$y = \frac{y_{\max} + y_{\min}}{2} + \frac{y_{\max} - y_{iin}}{2}\left\{\sum_{i=1}^{8} w_i \left[\frac{2(x_i - x_{i\min})}{x_{i\max} - x_{i\min}} - 1\right] + \mathbf{a}\right\} \tag{19}$$

$$y = \sum_{i=1}^{8} \frac{(y_{\max} - y_{\min})w_i}{x_{i\max} - x_{i\min}} x_i + \left(\frac{y_{\max} + y_{\min}}{2} + \frac{y_{\max} - y_{\min}}{2}\mathbf{a}\right) - \sum_{i=1}^{8}\left[\frac{(y_{\max} - y_{\min})w_i x_{i\min}}{x_{i\max} - x_{i\min}} + \frac{y_{\max} + y_{\min}}{2} w_i\right] \tag{20}$$

Based on the equations above, the output could be calculated from the inputs as follows:

$$y = \sum_{i=1}^{8} k_i x_i + c \tag{21}$$

where ki are proportional factors, and c is a constant.

$$k_i = \sum_{i=1}^{8} \frac{(y_{\max} - y_{\min})w_i}{x_{i\max} - x_{i\min}} \tag{22}$$

$$c = \frac{(y_{\max} + y_{\min})}{2} + \frac{(y_{\max} - y_{\min})}{2}\mathbf{a} - \sum_{i=1}^{8}\left[\frac{(y_{\max} - y_{\min})w_i x_{i\min}}{x_{i\max} - x_{i\min}} + \frac{(y_{\max} - y_{\min})}{2} w_i\right] \tag{23}$$

Based on the trained ANN and Eqs. (22) and (23), the constant c is 414.61, while the proportional factor ki is obtained as follows:

$$\mathbf{k} = [-0.1 \quad -0.12 \quad 0.6 \quad 11.07 \quad -4170.85 \quad 67.21 \quad 0.15 \quad 0.01] \tag{24}$$

In brief, the user-friendly equation was successfully derived from the trained ANN. The compressive strength of FRP confined rectangular concrete column now is calculated by using Eqs. (21) and (24).

Proposed Equation for the Compressive Strain

A modified ANN strain model was proposed to estimate the compressive strain of FRP confined square concrete columns. The proposed ANN strain model was verified by the database which contained 69 FRP confined square concrete columns having unconfined concrete strength between 19.5 and 53.9 MPa. All procedures introduced in the sections above were applied for this model with the exception of the transfer function, which was the Purelin function. The total number of input parameters herein is seven with exclusion of one variable as shown in Fig. 6. The architecture of the proposed ANN strain model and the size of the weight matrices and biases are also similar to Fig. 6 but with seven inputs. Following the same procedure of the proposed strength model, the proportional matrix (W) and the scalar (a) are determined as follows:

$$\mathbf{W} = \mathbf{LW} \times \mathbf{IW}$$

$$\mathbf{W} = [\,1.49 \quad 0.05 \quad -5.99 \quad 5.08 \quad 0.66 \quad 4.32 \quad -3.30\,] \tag{25}$$

$$\mathbf{a} = \mathbf{LW} \times \mathbf{b}_1 + \mathbf{b}_2 = -1.76 \tag{26}$$

The compressive strain now could be calculated by using Eq. (21) in which the proportional factor ki and the constant c are as follows:

$$\mathbf{k} = [\,0.284 \quad 0.004 \quad -0.618 \quad 209.593 \quad 1.24 \quad 0.076 \quad -0.003\,] \tag{27}$$

$$c = -66.012 \tag{28}$$

In brief, the user-friendly equation was successfully derived from the trained ANN. The compressive strain of FRP confined square concrete columns now is calculated by using Eqs. (21), (27) and (28).

Performance of the Proposed User-Friendly Equations

The performance of the proposed strength equation [Eqs. (21) and (24)] is shown in Fig. 7. This figure shows that the proposed user-friendly equation for strength estimation provides the compressive strength that fits the experimental results well. In addition, the proposed model's performance was compared with other existing models as shown in Fig. 7. The five existing models mentioned in the section above were studied in this comparison. The performance of these models is comparable in calculating the compressive strength of FRP confined rectangular columns.

In addition, Fig. 8 shows the performance of the proposed strain equation [Eqs. (21), (27) and (28)]. This figure illustrates the compressive strain of the specimens estimated by the proposed strain equation versus the experimental results. In addition, the proposed strain equation's performance was compared with other existing models as shown in Fig. 8. The five models mentioned in the above sections were adopted. The proposed ANN strain equation outperforms the selected models in estimating the compressive strain of confined concrete as shown in Fig. 8. The highest general correlation factor ($R^2 = 90\%$) was achieved by the proposed model, although the corresponding number of other models is less than 60%. This general correlation factor (R^2) is less than that in the above sections when the Tansig transfer function was replaced by the Purelin transfer function. Although using the Purelin transfer function reduces the accuracy of the proposed models, it provides a much simpler derivation of the proposed equations. For further evaluation, the values of AAE were calculated and are presented in Fig. 8. It demonstrates that the proposed equation significantly reduces the error in estimating the compressive strain of FRP confined square specimens by approximately three times as compared with the other models. The average absolute error of the selected models is approximately 30%, whereas the corresponding number of the proposed model is approximately 12%.

Analysis and Discussion

Effect of Corner Radius on the Compressive Strength and Strain

Based on the proportional matrix (W) as presented in Eq. (12), the contribution of the input parameters to the output could be examined. The magnitude of the elements in the proportional matrix of the proposed ANN strength equation is comparable, which was presented in Eq. (16). Thus all eight input parameters significantly contribute to the compressive strength of the columns. On the other hand, the element w_2 of the proportional matrix in the proposed ANN strain equation is extremely small as compared with the others [Eq. (25)]. Hence, the contribution of the input r to the compressive strain of the columns could be negligible.

The proposed ANN strain equation was modified by using six input parameters, in which the input r was removed. The input parameters are: the side length, the unconfined concrete strength and its corresponding strain, the tensile strength of FRP, the nominal thickness of FRP, and the elastic modulus of FRP. The performance of the modified strain equation is shown in Fig. 9 which shows that the AAE of the predictions increased slightly from

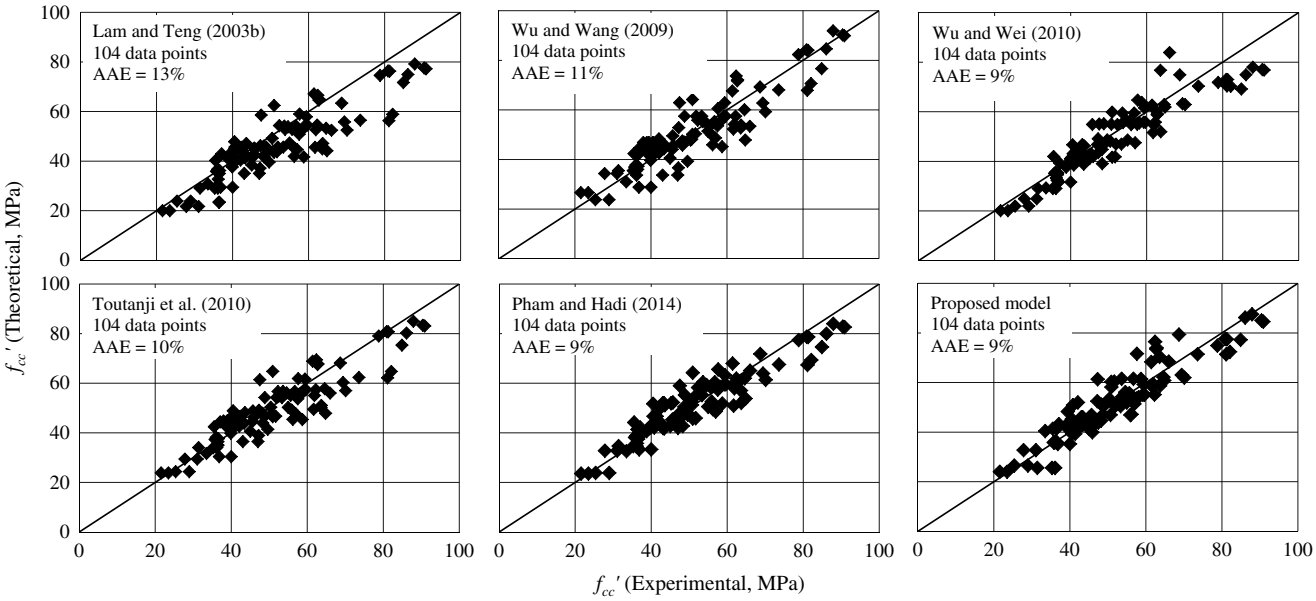

Fig. 7. Accuracy of the selected strength models

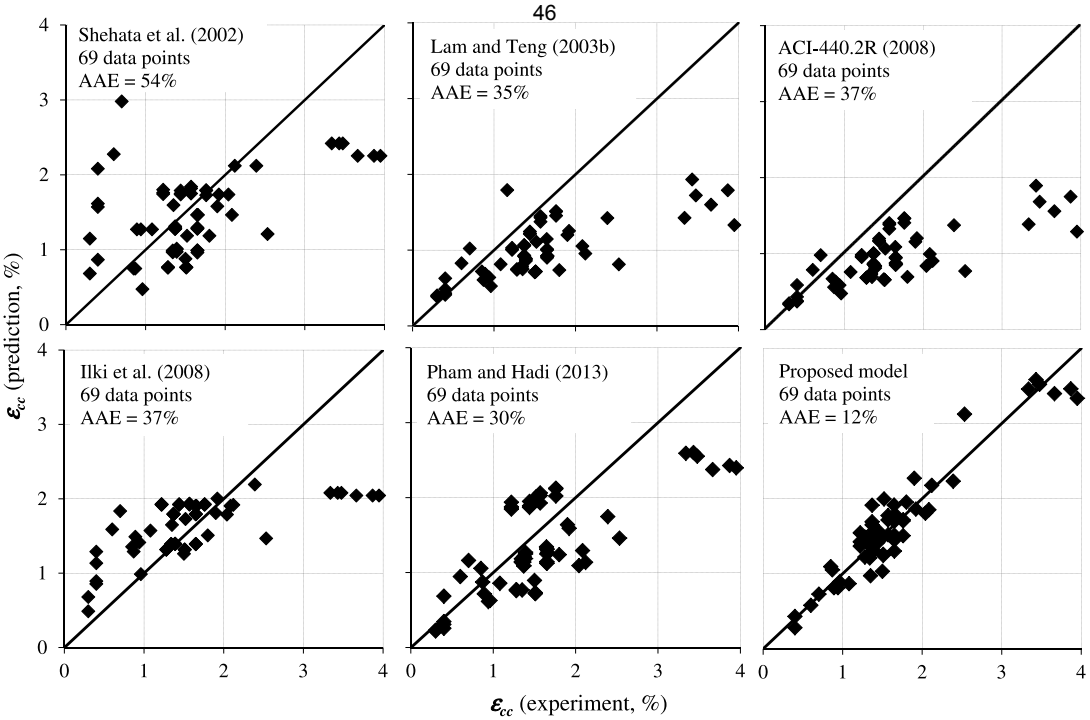

Fig. 8. Accuracy of the selected strain models

12–13%. Therefore, it is concluded that the contribution of the corner radius to the compressive strain of the columns is negligible. The proportional factor ki and the constant c are as follows:

$$\mathbf{k} = [0.26 \quad 0.038 \quad -51.314 \quad 1.329 \quad 0.059 \quad -0.002] \tag{29}$$

$$c = -32.119 \tag{30}$$

Scope and Applicability of the Proposed ANN Models

From the performance of the proposed models, it can be seen that artificial neural networks are a powerful regression tool. The proposed ANN models significantly increase the accuracy of predicting the compressive stress and strain of FRP confined concrete. The distribution of the training data within the problem domain can have a significant effect on the learning and generation performance of a network (Flood and Kartam 1994). The function *Deviderand* recommended by *MATLAB* was used to evenly distribute the training data. Artificial neural networks are not usually able to extrapolate, so the straining data should go at most to the edges of the problem domain in all dimensions. In other words, future test data should fall between the maximum and the minimum of the training data in all dimensions. Table 1 presents the maximum and the minimum values of each input parameter. It is recommended that the proposed ANN models are applicable for the range shown in Table 1 only. To extend the applicability of the proposed ANN models, a larger database containing a large number of specimens reported should be used to retrain and test the models. When the artificial neural network has been properly trained, verified, and tested with a comprehensive experimental database, it can be used with a high degree of confidence.

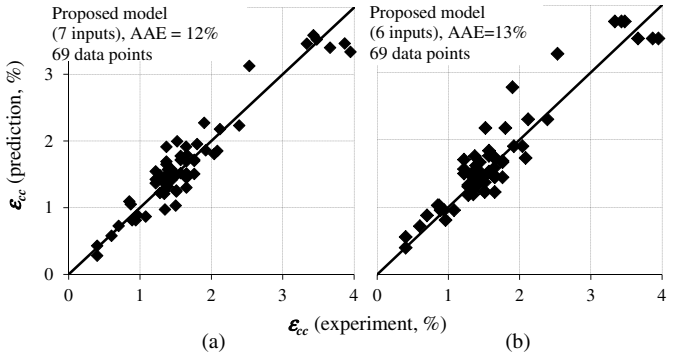

Fig. 9. Performance of the proposed strain model with or without the input r

Simulating an ANN by MS Excel

The finding in this study indicates that a trained ANN could be used to generate a user-friendly equation if the following conditions are satisfied. Firstly, the problem is well simulated by the ANN, which yields a small error and high value of general correlation

Table 1. Statistics of the Input Parameters for the Proposed Models

Input/output parameters	Strength model		Strain model	
	Maximum	Minimum	Maximum	Minimum
b (mm)	250	100	152	133
h (mm)	305	100	—	—
r (mm)	60	15	60	15
f'_{co} (MPa)	53.9	18.3	53.9	19.5
ε_{co} (%)	0.25	0.16	0.25	0.16
t_f (mm)	1.5	0.13	2	0.12
E_f (GPa)	257	75.1	241	38.1
f_f (MPa)	4,519	935	4,470	580
f_{cc} (MPa)	90.9	21.5	—	—
ε_{cc} (%)	—	—	3.9	0.4

factor (R^2). Secondly, the Purelin transfer function must be used in that algorithm. A very complicated problem is then simulated by using a user-friendly equation as followed in the proposed procedure.

However, if using the Purelin transfer function instead of other transfer functions increases significantly errors of the model, the proposed ANN models that have the Tansig transfer function should be used. So, a user-friendly equation cannot be generated in such a case. The following procedure could be used to simulate the trained ANN by using MS Excel

Step 1: Normalize the inputs to fall in the interval [−1, 1].

Step 2: Calculate the proportional matrix W and the scalar a by using Eqs. (14) and (15), respectively.

Step 3: Calculate the normalized output y' by using Eq. (13).

Step 4: Return the output to the actual values.

By following the four steps above, a MS Excel file was built to confirm that the predicted results from the MS Excel file are identical with those results yielded from the ANN.

Conclusions

Two ANN strength and strain models are proposed to calculate the compressive strength and strain of FRP confined square/rectangular columns. The prediction of the proposed ANN models fits well the experimental results. They yield results with marginal errors, approximately half of the errors of the other existing models. This study also develops new models coming up with a user-friendly equation rather than the complex computational models. The findings in this paper are summarized as follows:

1. The two proposed ANN models accurately estimate the compressive strength and strain of FRP confined square/rectangular columns with very small errors (AAE < 5%), which outperform the existing models.
2. The proposed ANN strength equation provides a simpler predictive equation as compared with the existing strength models with comparable errors.
3. The proposed ANN strain equation also delivers a simple-form equation with very small errors. The proposed model's error is approximately 12%, which is one third in comparison with the existing strain models.
4. For FRP confined rectangular columns, the corner radius significantly affects the compressive strength but marginally affects the compressive strain.

The ANN has been successfully applied for calculating the compressive strength and strain of FRP confined concrete columns. It is a promising approach to provide better accuracy in estimating the compressive strength and strain of FRP confined concrete than the existing conventional methods.

Acknowledgments

The first author would like to acknowledge the Vietnamese Government and the University of Wollongong for the support of his full Ph.D. scholarship. Both authors also thank Dr. Duc Thanh Nguyen, Research Associate—University of Wollongong, for his advice about ANN.

References

ACI 440.2R-08. (2008). "Guide for the design and construction of externally bonded FRP systems for strengthening concrete structures." *440.2R-08*, Farmington Hills, MI.

Adeli, H., and Park, H. S. (1995). "Counterpropagation neural networks in structural engineering." *J. Struct. Eng.*, 10.1061/(ASCE)0733-9445(1995)121:8(1205), 1205–1212.

Bisby, L. A., Dent, A. J. S., and Green, M. F. (2005). "Comparison of confinement models for fiber-reinforced polymer-wrapped concrete." *ACI Struct. J.*, 102(1), 62–72.

Chen, H. M., Tsai, K. H., Qi, G. Z., Yang, J. C. S., and Amini, F. (1995). "Neural-network for structural control." *J. Comput. Civ. Eng.*, 10.1061/(ASCE)0887-3801(1995)9:2(168), 168–176.

Elkordy, M. F., Chang, K. C., and Lee, G. C. (1993). "Neural networks trained by analytically simulated damage states." *J. Comput. Civ. Eng.*, 10.1061/(ASCE)0887-3801(1993)7:2(130), 130–145.

Flood, I., and Kartam, N. (1994). "Neural networks in civil engineering. I: Principles and understanding." *J. Comput. Civ. Eng.*, 10.1061/(ASCE)0887-3801(1994)8:2(131), 131–148.

Hadi, M. N. S. (2003). "Neural networks applications in concrete structures." *Comput. Struct.*, 81(6), 373–381.

Hadi, M. N. S. (2006a). "Behaviour of FRP wrapped normal strength concrete columns under eccentric loading." *Compos. Struct.*, 72(4), 503–511.

Hadi, M. N. S. (2006b). "Comparative study of eccentrically loaded FRP wrapped columns." *Compos. Struct.*, 74(2), 127–135.

Hadi, M. N. S. (2007a). "Behaviour of FRP strengthened concrete columns under eccentric compression loading." *Compos. Struct.*, 77(1), 92–96.

Hadi, M. N. S. (2007b). "The behaviour of FRP wrapped HSC columns under different eccentric loads." *Compos. Struct.*, 78(4), 560–566.

Hadi, M. N. S. (2009). "Behaviour of eccentric loading of FRP confined fibre steel reinforced concrete columns." *Constr. Build. Mater.*, 23(2), 1102–1108.

Hadi, M. N. S., and Li, J. (2004). "External reinforcement of high strength concrete columns." *Compos. Struct.*, 65(3–4), 279–287.

Hadi, M. N. S., Pham, T. M., and Lei, X. (2013). "New method of strengthening reinforced concrete square columns by circularizing and wrapping with fiber-reinforced polymer or steel straps." *J. Compos. Constr.*, 10.1061/(ASCE)CC.1943-5614.0000335, 229–238.

Hadi, M. N. S., and Widiarsa, I. B. R. (2012). "Axial and flexural performance of square RC columns wrapped with CFRP under eccentric loading." *J. Compos. Constr.*, 10.1061/(ASCE)CC.1943-5614.0000301, 640–649.

Hajela, P., and Berke, L. (1991). "Neurobiological computational models in structural analysis and design." *Comput. Struct.*, 41(4), 657–667.

Hornik, K., Stinchcombe, M., and White, H. (1989). "Multilayer feedforward networks are universal approximators." *Neural Networks*, 2(5), 359–366.

Ilki, A., Peker, O., Karamuk, E., Demir, C., and Kumbasar, N. (2008). "FRP retrofit of low and medium strength circular and rectangular reinforced concrete columns." *J. Mater. Civ. Eng.*, 10.1061/(ASCE)0899-1561(2008)20:2(169), 169–188.

Jalal, M., and Ramezanianpour, A. A. (2012). "Strength enhancement modeling of concrete cylinders confined with CFRP composites using artificial neural networks." *Compos. Part B Eng.*, 43(8), 2990–3000.

Kim, Y. Y., et al. (2006). "Dynamic analysis and structural optimization of a fiber optic sensor using neural networks." *J. Mech. Sci. Technol.*, 20(2), 251–261.

Lam, L., and Teng, J. G. (2003a). "Design-oriented stress-strain model for FRP-confined concrete." *Constr. Build. Mater.*, 17(6–7), 471–489.

Lam, L., and Teng, J. G. (2003b). "Design-oriented stress-strain model for FRP-confined concrete in rectangular columns." *J. Reinf. Plast. Compos.*, 22(13), 1149–1186.

Masri, S. F., Chassiakos, A. G., and Caughey, T. K. (1992). "Structure-unknown non-linear dynamic systems: Identification through neural networks." *Smart Mater. Struct.*, 1(1), 45.

MATLAB R2012b. [Computer software]. The Math Works, Natick, MA.

Mirmiran, A., Shahawy, M., Samaan, M., Echary, H. E., Mastrapa, J. C., and Pico, O. (1998). "Effect of column parameters on FRP-confined concrete." *J. Compos. Constr.*, 10.1061/(ASCE)1090-0268(1998)2:4(175), 175–185.

Naderpour, H., Kheyroddin, A., and Amiri, G. G. (2010). "Prediction of FRP-confined compressive strength of concrete using artificial neural networks." *Compos. Struct.*, 92(12), 2817–2829.

Ozbakkaloglu, T., Lim, J. C., and Vincent, T. (2013). "FRP-confined concrete in circular sections: Review and assessment of stress–strain models." *Eng. Struct.*, 49, 1068–1088.

Perera, R., Arteaga, A., and Diego, A. D. (2010a). "Artificial intelligence techniques for prediction of the capacity of RC beams strengthened in shear with external FRP reinforcement." *Compos. Struct.*, 92(5), 1169–1175.

Perera, R., Barchín, M., Arteaga, A., and Diego, A. D. (2010b). "Prediction of the ultimate strength of reinforced concrete beams FRP-strengthened in shear using neural networks." *Compos. Part B Eng.*, 41(4), 287–298.

Pham, T. M., Doan, L. V., and Hadi, M. N. S. (2013). "Strengthening square reinforced concrete columns by circularisation and FRP confinement." *Constr. Build. Mater.*, 49, 490–499.

Pham, T. M., and Hadi, M. N. S. (2013). "Strain estimation of CFRP confined concrete columns using energy approach." *J. Compos. Constr.*, 10.1061/(ASCE)CC.1943-5614.0000397, 04013001-1–04013001-11.

Pham, T. M., and Hadi, M. N. S. (2014). "Stress prediction model for FRP confined rectangular concrete columns with rounded corners." *J. Compos. Constr.*, 10.1061/(ASCE)CC.1943-5614.0000407, 04013019-1–04013019-10.

Rousakis, T., Rakitzis, T., and Karabinis, A. (2012). "Design-oriented strength model for FRP-confined concrete members." *J. Compos. Constr.*, 10.1061/(ASCE)CC.1943-5614.0000295, 615–625.

Rousakis, T. C., Karabinis, A. I., and Kiousis, P. D. (2007). "FRP-confined concrete members: Axial compression experiments and plasticity modelling." *Eng. Struct.*, 29(7), 1343–1353.

Shehata, I. A. E. M., Carneiro, L. A. V., and Shehata, L. C. D. (2002). "Strength of short concrete columns confined with CFRP sheets." *Mater. Struct.*, 35(1), 50–58.

Tasdemir, M. A., Tasdemir, C., Akyüz, S., Jefferson, A. D., Lydon, F. D., and Barr, B. I. G. (1998). "Evaluation of strains at peak stresses in concrete: A three-phase composite model approach." *Cem. Concr. Compos.*, 20(4), 301–318.

Toutanji, H., Han, M., Gilbert, J., and Matthys, S. (2010). "Behavior of large-scale rectangular columns confined with FRP composites." *J. Compos. Constr.*, 10.1061/(ASCE)CC.1943-5614.0000051, 62–71.

Upadhyaya, B. R., and Eryurek, E. (1992). "Application of neural networks for sensor validation and plant monitoring." *Nuclear Technol.*, 97(2), 170–176.

Wu, X., Ghaboussi, J., and Garrett, J. H. (1992). "Use of neural networks in detection of structural damage." *Comput. Struct.*, 42(4), 649–659.

Wu, Y. F., and Wang, L. M. (2009). "Unified strength model for square and circular concrete columns confined by external jacket." *J. Struct. Eng.*, 10.1061/(ASCE)0733-9445(2009)135:3(253), 253–261.

Wu, Y. F., and Wei, Y. Y. (2010). "Effect of cross-sectional aspect ratio on the strength of CFRP-confined rectangular concrete columns." *Eng. Struct.*, 32(1), 32–45.

Wu, Y. F., and Zhou, Y. W. (2010). "Unified strength model based on Hoek-Brown failure criterion for circular and square concrete columns confined by FRP." *J. Compos. Constr.*, 10.1061/(ASCE)CC.1943-5614.0000062, 175–184.

Yazici, V., and Hadi, M. N. S. (2012). "Normalized confinement stiffness approach for modeling FRP-confined concrete." *J. Compos. Constr.*, 10.1061/(ASCE)CC.1943-5614.0000283, 520–528.

5 MAXIMUM USABLE STRAIN OF FRP-CONFINED CONCRETE

Summary

This study investigates the progressive failure of FRP-confined concrete. Ten FRP-confined concrete specimens were divided into two groups with different jacket stiffness. One specimen in each group was tested until failure while the others were loaded to target strains and then unloaded in order to monitor the residual strength of the concrete cores. At 1% axial strain of FRP-confined concrete, the residual strength of the concrete cores were reduced more than 56% compared to the reference specimens. Experimental results have shown that the maximum usable strain of 1% is un-conservative for FRP-confined concrete. A model is proposed to estimate the residual strength of concrete cores. Predictions from the proposed model fit the experimental results well. In addition, a new procedure is proposed to determine the maximum usable strain of FRP-confined concrete based on the maximum usable strain of unconfined concrete.

Citation

This paper was submitted for publication in Engineering Structures with the following citation:

Pham, T.M., Hadi, M.N.S., and Tran, T.M. (2014). "Maximum Usable Strain of FRP-Confined Concrete." *Engineering Structures*, under review.

Maximum Usable Strain of FRP-Confined Concrete

Thong M. Pham[1], Muhammad N.S. Hadi[2] and Tung M. Tran[3]

[1] Ph.D. Candidate, School of Civil, Mining and Environmental Engineering, University of Wollongong, Wollongong, NSW 2522, Australia; Formerly, Lecturer, Faculty of Civil Engineering, HCMC University of Technology, Ho Chi Minh City, Vietnam. Email: mtp027@uowmail.edu.au

[2]Associate Professor, School of Civil, Mining and Environmental Engineering, University of Wollongong, NSW 2522, Australia (corresponding author). Email: mhadi@uow.edu.au

[3]Lecturer, Department of Civil Engineering, Ton Duc Thang University, Ho Chi Minh, Vietnam, currently a PhD Scholar at the School of Civil, Mining and Environmental Engineering, University of Wollongong, Wollongong NSW 2522, Australia. E-mail: tmt954@uowmail.edu.au

1. Introduction

Fiber Reinforced Polymer (FRP) has been commonly used to strengthen existing reinforced concrete (RC) columns in recent years [1-3]. In such cases, FRP is a confining material for concrete in which the confinement effect leads to increase the strength and ductility of columns. In early experimental studies of FRP retrofitted RC columns, the axial capacities of strengthened columns increased significantly as compared to reference columns. The database collected by Lee and Hegemier [4] showed that FRP-confined concrete cylinders have axial strain ranging from 0.6% to 4.2% while Teng et al. [5] showed that the axial strain of specimens varied from 0.8% to 3.7%. Pham and Hadi [6] collected a database of 167 FRP-confined concrete columns where the axial strain of the columns ranged between 0.5% and 4%. Ilki et al. [7] conducted experiments on FRP-confined circular and rectangular RC columns. Results from this study had shown that the axial strain of FRP-confined concrete ranged from 1.3% to 8.6%. The axial strain up to 9.66% was recorded from the experimental study carried out by Dai et al. [8] on RC columns confined with large rupture strain and the axial strain up to 10.4 % was reached in Ilki et al.'s study [9] on FRP confined low strength concrete members. From the literature, it can be seen that the axial strain of FRP-confined concrete varies in a broad range and no study has shown a maximum usable strain of confined

concrete [10-14]. Meanwhile, ACI-440.2R [15] and Concrete Society [16] provided maximum usable strain of 1% for FRP-confined concrete to prevent excessive cracking and the resulting loss of concrete integrity.

As mentioned above, experimental studies have shown that the axial strain of FRP-confined concrete varies in a wide range from 0.5% to 10.4%. However, these studies did not investigate the integrity of the concrete during testing. No study has investigated the precise nature of the progressive failure mechanisms occurring during experimental tests. In other words, a limit of 1% recommended by two guidelines [15, 16] seems small as compared to the experimental results. Therefore, determining the nature of the progressive failure mechanisms and the maximum usable strain of FRP-confined concrete is essentially necessary. This study conducted experimental tests to investigate the progressive failure mechanisms of FRP-confined concrete at many stages of testing.

2. Axial Strain of Concrete

A typical stress-strain relation of unconfined concrete is shown in Fig. 1. The stress-strain curve rises to a maximum stress, reached at a strain between 0.15% and 0.3%, followed by a descending branch [17]. The length of the descending branch of the curve is strongly affected by the test conditions. Usually, an axially loaded concrete cylinder fails at the maximum stress. In such cases, the stress-strain curve suddenly drops from the maximum stress. On the other hand, if a structural member is loaded in compression due to bending (or bending plus axial load), the descending branch might exist as shown in the solid line after the maximum stress in Fig. 1 [17]. This study deals with pure compression tests so that the failure of unconfined concrete is approximately determined at the maximum stress stage that has a corresponding strain between 0.15% and 0.3%.

In addition, stress-strain relations of FRP-confined concrete are also presented in Fig. 1. Based on the confinement ratio, the stress-strain relation of FRP-confined concrete may belong to an ascending branch or a descending branch. Specimens with low stiffness confinement yield a descending branch stress-strain curve as described by Concrete Society [16]. The axial stress of these specimens reaches the maximum stress before FRP rupture. Conversely, the axial stress of specimens that have stiff confinement reaches the maximum stress at the FRP rupture. Therefore, the ultimate axial strain of FRP-confined concrete is the measured axial strain of specimens as FRP ruptures due to hoop tension. There is a consensus that the core of FRP-confined concrete can resist the applied load until FRP ruptured without any investigation about the progressive failure mechanisms. No study about confined concrete has verified the integrity of the concrete core during testing. As a result, the failure indicator of FRP-confined concrete is controlled by the failure of the FRP jacket. This failure determination complies with the failure definition of concrete confined by helical steel reinforcement [18]. Mander et al. [18] defined that the maximum axial strain of confined concrete was reached when the first lateral reinforcement fractures. However, this study focuses on the failure of the concrete cores not the FRP.

3. Experimental Program

3.1. Design of Experiments

A total of thirteen standard concrete cylinders were cast and tested at the High Bay laboratory of the University of Wollongong. The dimensions of the specimens were 150 mm by 300 mm and the design compressive strength of concrete was 50 MPa. The specimens were classified into three groups, namely, the reference group (R), two layers group (C2) and three layers group (C3). Details of the specimens are presented in Table 1. The notation of the specimens consists of two parts: the first part is “R”, “C2”, and “C3” stating the name of the groups. The

second part indicates the target strains of the specimens at which the loading was stopped. For example, Specimen C2-1.9 indicates the specimen which was wrapped with two layers of FRP and loaded up to 1.9% axial strain.

After 28 days, each specimen was symmetrically bonded at midheight with two 60 mm strain gages in the vertical direction and two 60 mm strain gages in the horizontal direction. The specimens on group C2 and C3 were then fully wrapped with CFRP layers using wet lay-up method. The adhesive was a mixture of epoxy resin and hardener at 5:1 ratio and the amount of FRP layers in the specimens is described in Table 1. For each specimen, four CFRP rings of 75 mm width were applied in the hoop direction to ensure that the whole specimen (300 mm length) was wrapped with layers of CFRP. Before the first layer of CFRP was attached, the adhesive was spread onto the surface of the specimen and CFRP was attached onto the surface. After the first layer, the adhesive was spread onto the surface of the first layer of CFRP and the second layer was continuously bonded. The third layer of CFRP was applied in a similar manner, ensuring that an overlap of 100 mm was maintained.

In order to measure the lateral strain of the specimens, four strain gages were symmetrically bonded in the hoop direction of the jacket. Details of the positions of the strain gages are shown in Fig 2. During the testing, FRP jacket would cause confining pressure perpendicularly to the concrete surface and thus the strain gages on the concrete surface. This confining pressure could affect readings from these strain gages.

3.2. Instrumentation

The Denison 5000 kN testing machine was used for testing all the specimens. The columns were capped with high strength plaster at both ends to ensure full contact between the loading heads and the column. Calibration was then performed to ensure that the columns were placed at the center of the testing machine. The tests were conducted as displacement controlled with

a rate of 0.5 mm/min. All the strain gages were connected with a data logger and simultaneously saved in a control computer.

Furthermore, the longitudinal compressometer as shown in Fig. 3 was used to measure the axial strain of the specimens and then these readings were compared to those from the strain gages. A linear variable differential transformer (LVDT) was mounted on the upper ring and the tip of the LVDT rests on an anvil. The readability, the accuracy, and the repeatability of the LVDT comply with the Australian standard [19]. This LVDT was also connected to the data logger and the readings were saved in the control computer.

3.3. Testing Scheme

The axial stress and strain of the specimens were predicted using the study by Jiang and Teng [20]. Since the maximum strain of the specimens was determined, each specimen was tested to reach the single target axial strain as described in Table 1. The first specimen in that group was tested until the axial strain reached 0.6% that was the average value between 0.2% and 1%. The value of 0.2% was adopted from the widely accepted maximum axial strain of unconfined concrete while the value of 1% was proposed by ACI-440.2R [15] for the maximum usable strain of FRP-confined concrete. The other specimens were tested to a target axial strain that range equally from 1% to the maximum axial strain of the group. After the tested specimens were loaded to the target strains, these specimens were unloaded and unwrapped in order to investigate any cracks which may have developed during the testing. The concrete cores of these specimens were then tested again under compression load to examine their residual strengths.

4. Experimental Results

4.1. Preliminary tests

The actual compressive strength of unconfined concrete calculated from three reference Specimens (R-1, R-2, and R-3) was 52.08 MPa. The axial strain of unconfined concrete at the maximum load was 0.24%. CFRP used in this study was 75 mm in width with a unidirectional fiber density of 340 g/m^2. Five CFRP coupons were made according to ASTM D7565 [21] and tested to determine their mechanical properties. The coupons were made of three layers of FRP and had a nominal thickness of 1.45 mm. The average width of the coupons was 24.86 mm and the average maximum tensile force per unit width was 2037 N/mm. The strain at the maximum tensile force and the average elastic modulus were 0.0165 mm/mm and 123 kN/mm, respectively.

The axial strain of specimens was measured by both strain gages attached on the surface of concrete and LVDT mounted on the compressometer. Two readings were almost identical at early stages of the testing. However, the strain gages on the concrete failed at a strain about 0.6 -0.7%, which may have resulted from the high confining pressure of the jacket. As a result, the experimental axial strains reported in this study are the readings from the LVDT.

4.2. Stress-strain Relation

Specimens C2-1.9 and C3-2.4 were tested until fail. These specimens failed by FRP rupture, resulting in loud explosive sounds. The rupture strain of FRP is the average values from three strain gages outside the overlap zone. The other specimens were loaded to the target strains and then their jackets were peeled off to investigate the damage level of the column cores. Specimens with high axial strain (C2-1.2, C2-1.4, C3-1.4, and C3-1.7) had wide and long cracks on the cores as shown in Fig. 4. These cracks were formed vertically and they cut throughout the core from the top to the bottom. These specimens were damaged and could not be used as the section of the cores was significantly reduced. Cores of the remaining specimens were loaded again until failure to examine the residual compressive strength and

the results are shown in Table 2. The residual strength of these specimens was less than 20% as compared to the reference specimens. Meanwhile, specimens with lower axial strain (C2-0.6, C2-1.0, C3-0.6, and C3-1.0) had less serious cracks and the cores still kept the cylindrical shape as shown in Fig. 5. These cracks formed locally and they had small width and short length. The residual strength of these specimens ranged from 40% to 60% as compared to the reference specimens (Table 2).

4.3. Residual Strength of the Cores

It is obvious that FRP prevents the cores from expanding under the applied loads. At the same value of axial strain, the lateral strain of specimens in Group C3 is lower than that of specimens in Group C2. Thus the residual strength of specimens in Group C3 is expected to be higher than that of the corresponding specimens in Group C2. Fig. 6 shows the residual strengths of Group C2 and Group C3. These experimental results confirm that with a similar axial strain the core of specimens that were wrapped with a thicker jacket will have higher residual strength as compared to the one wrapped with a thinner jacket. Thus it can be seen that the damage level of the cores is due to both the axial strain and the lateral strain, which is controlled by the stiffness of the jacket.

From the experimental results presented in Figs. 7-8, it can be seen that the residual strengths of the cores had values very close to the ordinate of the intersection between the unload curve and the unconfined concrete curve. These values are summarized in Table 2. Thus it is assumed that the residual strength of the column cores is equal to the ordinate of the intersection between the unload curve and the unconfined concrete curve.

5. Theoretical Verification

5.1. Behavior of FRP-confined Concrete under Cyclic Load

Theoretical models about behavior of FRP-confined concrete under cyclic loads are studied and summarized to simulate the experimental results [22, 23]. The loading scheme of this study is illustrated in Fig. 9. FRP-confined concrete specimens were tested to Point *a*, that has the unloading strain (ε_{un}) and the unloading stress (σ_{un}), and then unloaded until Point *c*. Point *c* is determined by the reloading strain (ε_{re}) and the reloading stress (σ_{re}) that is equal to zero in this study. When Point *c* lies on the horizontal axis, the loading strain (ε_{re}) is equal to the plastic strain (ε_{pl}) (or permanent strain). During the unloading process, the unloading curve intersects the stress-strain curve of unconfined concrete at Point *b* that has the intersect strain (ε_{in}) and the intersect stress (σ_{in}).

The loading curve in Fig. 9 is the envelop curve in the study by Lam and Teng [22]. The model proposed by Lam and Teng [24] was adopted by Lam and Teng [22] to predict the envelop curve. However, this model did not yield good results as compared to the experimental results in this paper. Thus, the envelop curve (loading path) is estimated by the model proposed by Jiang and Teng [20], which is summarized in the section below. Meanwhile, the unloading path was calculated as follows [22]:

176 $$\sigma_c = a\varepsilon_c^{\eta} + b\varepsilon_c + c \tag{1}$$

177 $$a = \frac{\sigma_{un} - E_{un,0}\left(\varepsilon_{un} - \varepsilon_{pl}\right)}{\varepsilon_{un}^{\eta} - \varepsilon_{pl}^{\eta} - \eta\varepsilon_{pl}^{\eta-1}\left(\varepsilon_{un} - \varepsilon_{pl}\right)} \tag{2}$$

178 $$b = E_{un,0} - \eta\varepsilon_{pl}^{\eta-1}a \tag{3}$$

179 $$c = -a\varepsilon_{pl}^{\eta} - b\varepsilon_{pl} \tag{4}$$

180 $$\varepsilon_{pl} = \begin{cases} 0, & 0 < \varepsilon_{un} \le 0.001 \\ \left[1.4\left(0.87 - 0.004\, f_{co}^{'}\right) - 0.64\right]\left(\varepsilon_{un} - 0.001\right), & 0.001 < \varepsilon_{un} < 0.0035 \\ \left(0.87 - 0.004\, f_{co}^{'}\right)\varepsilon_{un} - 0.0016, & 0.0035 \le \varepsilon_{un} < \varepsilon_{cc} \end{cases} \tag{5}$$

181 where η is an exponent and $E_{un,0}$ is the slope of the unloading path at zero stress. The shape of
182 an unloading path is controlled by the two parameters: η and $E_{un,0}$ that are calculated as
183 follows [22]:

184 $$\eta = 350\varepsilon_{un} + 3 \tag{6}$$

185 $$E_{un,0} = min\left\{\frac{0.5\, f_{co}^{'}}{\varepsilon_{un}}; \frac{\sigma_{un}}{\varepsilon_{un} - \varepsilon_{pl}}\right\} \tag{7}$$

186 In addition, the stress-strain curve of unconfined concrete is predicted using the equations
187 proposed by Sargin et al. [25] as follows:

188 $$\frac{\sigma_c}{\sigma_{co}} = \frac{A\frac{\varepsilon_c}{\varepsilon_{co}} + (D-1)\left(\frac{\varepsilon_c}{\varepsilon_{co}}\right)^2}{1 + (A-2)\frac{\varepsilon_c}{\varepsilon_{co}} + D\left(\frac{\varepsilon_c}{\varepsilon_{co}}\right)^2} \tag{8}$$

189 $$A = \frac{E_0}{E_c} \tag{9}$$

190 $$E_c = \frac{f_{co}^{'}}{\varepsilon_{co}} \tag{10}$$

191 where E_0 is the Young's modulus of elasticity (E_0 = 4730$\sqrt{f_{co}^{'}}$, MPa), E_c is the secant
192 modulus of elasticity at the peak, and D = 1 is the parameter which primarily governs the

193 descending part of the stress-strain curve. The reloading path is predicted by the same
194 equations proposed Sargin et al. [25] with the exception of replacing the Young's modulus of
195 elasticity (E_0) by the reloading stiffness (E_{re}), which is discussed in the section below. It is
196 noted that the residual strength of the column core (Point *d*) is assumed to be equal to the
197 ordinate of Point *b* in Fig. 9.

198 ***5.2. Envelop Curve and Reloading Stiffness***

199 The model for FRP-confined concrete proposed by Jiang and Teng [20] was adopted to
200 predict the envelop curve of the stress-strain curve. In that model, the axial stress and the axial
201 strain of FRP-confined concrete at a given lateral strain are the same as those of the same
202 concrete actively confined with a constant confining pressure equal to that provided by the
203 FRP jacket. Fig. 10 illustrates the concept of this incremental approach. The stress-strain
204 curve of FRP-confined concrete is obtained as presented by Jiang and Teng [20]:

205 1) For a given axial strain, find the corresponding lateral strain according to the lateral-
206 to-axial strain relationship;

207 2) Based on force equilibrium and radial displacement compatibility between the
208 concrete core and the FRP jacket, calculate the corresponding lateral confining
209 pressure provided by the FRP jacket;

210 3) Use the axial strain and the confining pressure obtained from Steps (1) and (2) in
211 conjunction with an active-confinement base model to evaluate the corresponding
212 axial stress, leading to the identification of one point on the stress–strain curve of
213 FRP–confined concrete;

214 4) Repeat the above steps to generate the entire stress–strain curve.

The following equations were adopted in the procedure above [20]:

$$\sigma_l = \frac{2E_f t\varepsilon_l}{d} \tag{11}$$

$$\frac{\varepsilon_c}{\varepsilon_{co}} = 0.85\left(1+8\frac{\varepsilon_l}{f_{co}^{'}}\right)\left\{\left[1+0.75\left(\frac{-\varepsilon_l}{\varepsilon_{co}}\right)\right]^{0.7} - e^{-7\left(\frac{-\varepsilon_l}{\varepsilon_{co}}\right)}\right\} \tag{12}$$

$$f_{cc}^{'*} = f_{co}^{'} + 3.5f_l \tag{13}$$

$$\frac{\varepsilon_{cc}^{*}}{\varepsilon_{co}} = 1+17.5\frac{\varepsilon_l}{f_{co}^{'}} \tag{14}$$

$$\frac{\varepsilon_c}{f_{cc}^{'*}} = \frac{r\frac{\varepsilon_c}{\varepsilon_{cc}^{*}}}{r-1+\left(\frac{\varepsilon_c}{\varepsilon_{cc}^{*}}\right)^r} \tag{15}$$

$$r = \frac{E_0}{E_0 - \frac{f_{cc}^{'*}}{\varepsilon_{cc}^{*}}} \tag{16}$$

where ε_l is the lateral strain, E_f is the elastic modulus of FRP, t is the thickness of FRP, d is the diameter of specimens, $f_{cc}^{'*}$ is the peak stress of concrete under a specific constant confining pressure f_l, ε_{cc}^{*} is the axial strain at $f_{cc}^{'*}$, and r is the constant defined by Eq. 16.

The reloading stiffness E_{re} presented in the study by Lam and Teng [22] is shown in Fig. 11. The reloading stiffness is the slope of Line *cd* that is estimated as follows:

$$E_{re} = \frac{\sigma_{new}}{\varepsilon_{un} - \varepsilon_{pl}} \tag{17}$$

$$\phi = \frac{\sigma_{new}}{\sigma_{un}} \tag{18}$$

where ϕ is the stress deterioration ratio for the unloading/reloading cycle and σ_{new} is the new stress at the reference strain.

$$\phi = \begin{cases} 1, & 0 < \varepsilon_{un} \le 0.001 \\ 1 - 80(\varepsilon_{un} - 0.001), & 0.001 < \varepsilon_{un} < 0.002 \\ 0.92, & 0.002 \le \varepsilon_{un} < \varepsilon_{cc} \end{cases} \quad (19)$$

It is widely accepted that the confining effect of FRP is ignored as FRP-confined concrete is compressed at a stress level lower than the peak stress of unconfined concrete. Thus it is assumed that the Young's modulus of elasticity of the FRP-confined concrete and the column core is the same. In this study, the specimens were unloaded and the FRP jacket was peeled off before reloading to the peak stress of the column cores. The reloading stiffness of the column cores now is estimated based on the equations above, which are used for reloading FRP-confined concrete.

5.3. Comparison with Experimental Results

The procedure presented above is used to predict the residual strength of a column core. The experimental results and theoretical calculations of specimens in Group C3 are presented in Fig. 12. The theoretical calculations fit the experimental results well. Thus at a given axial strain of FRP-confined concrete, the residual strength of the column core can be estimated.

6. Maximum Usable Strain

The progressive failure mechanisms of FRP-confined concrete are not due to the FRP failing progressively but rather due to the concrete failing progressively [26]. In addition, Priestley et al. [27] recommended that the lateral strain of FRP-confined concrete columns should be limited to the value of 0.4% to prevent the degradation of aggregate interlock action, which is essential to the concrete shear resisting mechanism. Based on the experimental observations and the arguments above, this study recommends that the maximum usable strain of confined concrete should be controlled by the maximum usable strain of the concrete cores.

The maximum usable strain of FRP-confined concrete must maintain the bond between reinforcement and the concrete core and the aggregate interlock. The specimens of Group C3 could resist axial loads until the axial strain of 2.64% was reached. Specimen C3-0.6 was loaded to reach the axial strain at 0.66% and then reloaded. However, the residual strength of this specimen reduced significantly by 42%, which led to considerable decrease of the bonding between reinforcement and concrete as well as the aggregate interlock. This axial strain is much smaller than 1% as proposed by ACI 440.2R [15]. Therefore, the maximum usable strain of FRP-confined concrete should be controlled by the maximum usable strain of the concrete core.

However, the maximum usable strain of the concrete core in FRP-confined concrete has not been investigated. The maximum usable strain of unconfined concrete ($\varepsilon_{lim,\,u}$) proposed by ACI 318 [28] was adopted. ACI 318 [28] recommended that the maximum usable strain of unconfined concrete is 0.3%, which is equal to σ_{in} in Fig. 9. Given a stress-strain curve of unconfined concrete, Point *b* in Fig. 9 can be determined (*b* (0.3, 50)). Next, the maximum usable strain at Point *a* is also determined by iterative processes (*a* (0.32, 57)) for specimens of Group C3). Fig. 13 describes a flow chart to determine the maximum usable strain of FRP-confined concrete ($\varepsilon_{lim,\,u}$). Therefore, the maximum usable strain of FRP-confined concrete (ε_{lim}) given the properties of materials can be estimated if the maximum usable strain of unconfined concrete ($\varepsilon_{lim,\,u}$) is proposed. It is necessary to investigate the maximum usable strain of the concrete core in FRP-confined concrete.

7. Conclusions

This study investigated the progressive failure of FRP-confined concrete based on the failure of the concrete cores. The residual strengths of the concrete cores were determined

experimentally and theoretically at many axial strain levels. The findings presented in this paper are summarized as follows:

1. The residual strengths of the concrete cores were reduced more than 56% at the axial strain 1% of FRP-confined concrete.

2. A model was proposed to estimate the residual strength of the concrete cores of a FRP-confined concrete column at a certain axial strain.

3. The maximum usable strain of FRP-confined concrete is much smaller than the value of 1% proposed by ACI 440-2R [15].

Finally, the experimental results show that the maximum usable strain of FRP-confined concrete should be determined from that of unconfined concrete. The predictions of the proposed model fit the experimental results very well.

Acknowledgement

The first and third authors would like to acknowledge the Vietnamese Government and the University of Wollongong for the support of their full PhD scholarships. The authors thank Mr. Guan Lin, Ph.D. candidate at the Hong Kong Polytechnic University, for his useful comments.

References

[1] Pham TM , Doan LV, Hadi MNS. Strengthening square reinforced concrete columns by circularisation and FRP confinement. Constr Build Mater 2013;49(0):490-499.

[2] Hadi MNS , Pham TM, Lei X. New Method of Strengthening Reinforced Concrete Square Columns by Circularizing and Wrapping with Fiber-Reinforced Polymer or Steel Straps. J Compos Constr 2013;17(2):229-238.

[3] Hadi MNS, Widiarsa IBR. Axial and Flexural Performance of Square RC Columns Wrapped with CFRP under Eccentric Loading. J Compos Constr 2012;16(6):640-649.

[4] Lee CS, Hegemier GA. Model of FRP-Confined Concrete Cylinders in Axial Compression. J Compos Constr 2009;13(5):442-454.

[5] Teng JG , Jiang T , Lam L, Luo YZ. Refinement of a Design-Oriented Stress-Strain Model for FRP-Confined Concrete. J Compos Constr 2009;13(4):269-278.

[6] Pham TM, Hadi MNS. Strain Estimation of CFRP Confined Concrete Columns Using Energy Approach. J Compos Constr 2013;17(6):04013001-1-04013001-11.

[7] Ilki A , Peker O , Karamuk E , Demir C, Kumbasar N. FRP retrofit of low and medium strength circular and rectangular reinforced concrete columns. Journal of Materials in Civil Engineering 2008;20(2):169-188.

[8] Dai J-G , Bai Y-L, Teng JG. Behavior and modeling of concrete confined with FRP composites of large deformability. J Compos Constr 2011;15(6):963-973.

[9] Ilki A , Kumbasar N, Koc V. Low strength concrete members externally confined with FRP sheets. Struct. Eng. Mechan. 2004;18(2):167-194.

[10] Rousakis TC, Karabinis AI. Adequately FRP confined reinforced concrete columns under axial compressive monotonic or cyclic loading. Materials and Structures 2012;45(7):957-975.

[11] Toutanji H , Han M , Gilbert J, Matthys S. Behavior of Large-Scale Rectangular Columns Confined with FRP Composites. J Compos Constr 2010;14(1):62-71.

[12] Wang ZY , Wang DY , Smith ST, Lu DG. CFRP-Confined Square RC Columns. I: Experimental Investigation. J Compos Constr 2012;16(2):150-160.

[13] Rousakis TC. Elastic fiber ropes of ultrahigh-extension capacity in strengthening of concrete through confinement. Journal of Materials in Civil Engineering 2014;26(1):34-44.

[14] Rousakis TC, Tourtouras IS. RC columns of square section - Passive and active confinement with composite ropes. COMPOSITES PART B-ENGINEERING 2014;58(Journal Article):573-581.

[15] ACI 440.2R-08. Guide for the Design and Construction of Externally Bonded FRP Systems for Strengthening Concrete Structures. 440.2R-08 2008, Farmington Hills, MI.

[16] TR 55, *Design guidance for strengthening concrete structures using fibre composite materials*. 2012, Camberley: Concrete Society.

[17] MacGregor JG, *Reinforced concrete: mechanics and design*. 2005, Upper Saddle River, N.J: Prentice Hall.

[18] Mander JB , Park R, Priestley MJN. Theoretical Stress-Strain Model for Confined Concrete. J Struct Eng 1988;114(8):1804-1826.

[19] Australian Standard-1545. Methods for the Calibration and Grading of Extenometers. 1545-1976 1976, Homebush, NSW 2140.

[20] Jiang T, Teng JG. Analysis-oriented stress-strain models for FRP-confined concrete. Eng Struct 2007;29(11):2968-2986.

[21] ASTM. Standard test method for tensile properties of fiber reinforced polymer matrix composites used for strengthening of civil structures. D7565:2010 2010, West Conshohocken, PA.

341 [22] Lam L, Teng JG. Stress–strain model for FRP-confined concrete under cyclic axial
342 compression. Eng Struct 2009;31(2):308-321.

343 [23] Wang ZY , Wang DY , Smith ST, Lu DG. CFRP-Confined Square RC Columns. II:
344 Cyclic Axial Compression Stress-Strain Model. J Compos Constr 2012;16(2):161-170.

345 [24] Lam L, Teng JG. Design-oriented stress-strain model for FRP-confined concrete.
346 Constr Build Mater 2003;17(6-7):471-489.

347 [25] Sargin M , Ghosh SK, Handa VK. Effects of lateral reinforcement upon the strength
348 and deformation properties of concrete. Mag Concr Res 1971;23(Compendex):99-110.

349 [26] Bank LC. Progressive Failure and Ductility of FRP Composites for Construction:
350 Review. J Compos Constr 2013;17(3):406-419.

351 [27] Priestley MJN , Seible F, Calvi GM, *Seismic design and retrofit of bridges*. 1996, New
352 York: Wiley.

353 [28] ACI 318-11, *Building Code Requirements for Structural Concrete and Commentary*.
354 2011, Farmington Hills, Michigan, USA: American Concrete Institute (ACI).

List of Figures

List of Tables

373 Table 1. Test matrix

ID	Unconfined concrete strength (MPa)	Target axial strain (%)	Actual axial strain (%)	Predicted lateral strain (%)	Actual lateral strain (%)	Predicted strength (MPa)	Actual strength (MPa)	No. of FRP layers
C2-0.6	52	0.6	0.62	0.46	0.44	69	70	2
C2-1.0	52	1.0	1.12	0.77	0.68	80	83	2
C2-1.2	52	1.2	1.33	0.91	0.94	84	89	2
C2-1.4	52	1.4	1.56	1.04	0.92	88	88	2
C2-1.9	52	1.9	1.99	1.25	1.40	95	97	2
C3-0.6	52	0.6	0.66	0.37	0.34	73	77	3
C3-1.0	52	1.0	1.02	0.62	0.67	87	90	3
C3-1.4	52	1.4	1.35	0.83	0.70	98	96	3
C3-1.9	52	1.9	1.87	1.05	1.08	109	106	3
C3-2.4	52	2.4	2.64	1.25	1.31	120	124	3

374

375 Table 2. Residual strength of tested specimens

ID	Residual strength (MPa)	Compared to f_c' (%)	Ordinate of intersection* (MPa)
C2-0.6	28	54	33
C2-1.0	17	33	18
C2-1.2	-	-	13
C2-1.4	9	17	8
C3-0.6	30	58	32
C3-1.0	23	44	20
C3-1.4	9	17	12
C3-1.7	9	17	-

376 * The intersection was made between the unload curve of the corresponding specimen and the
377 unconfined concrete curve.

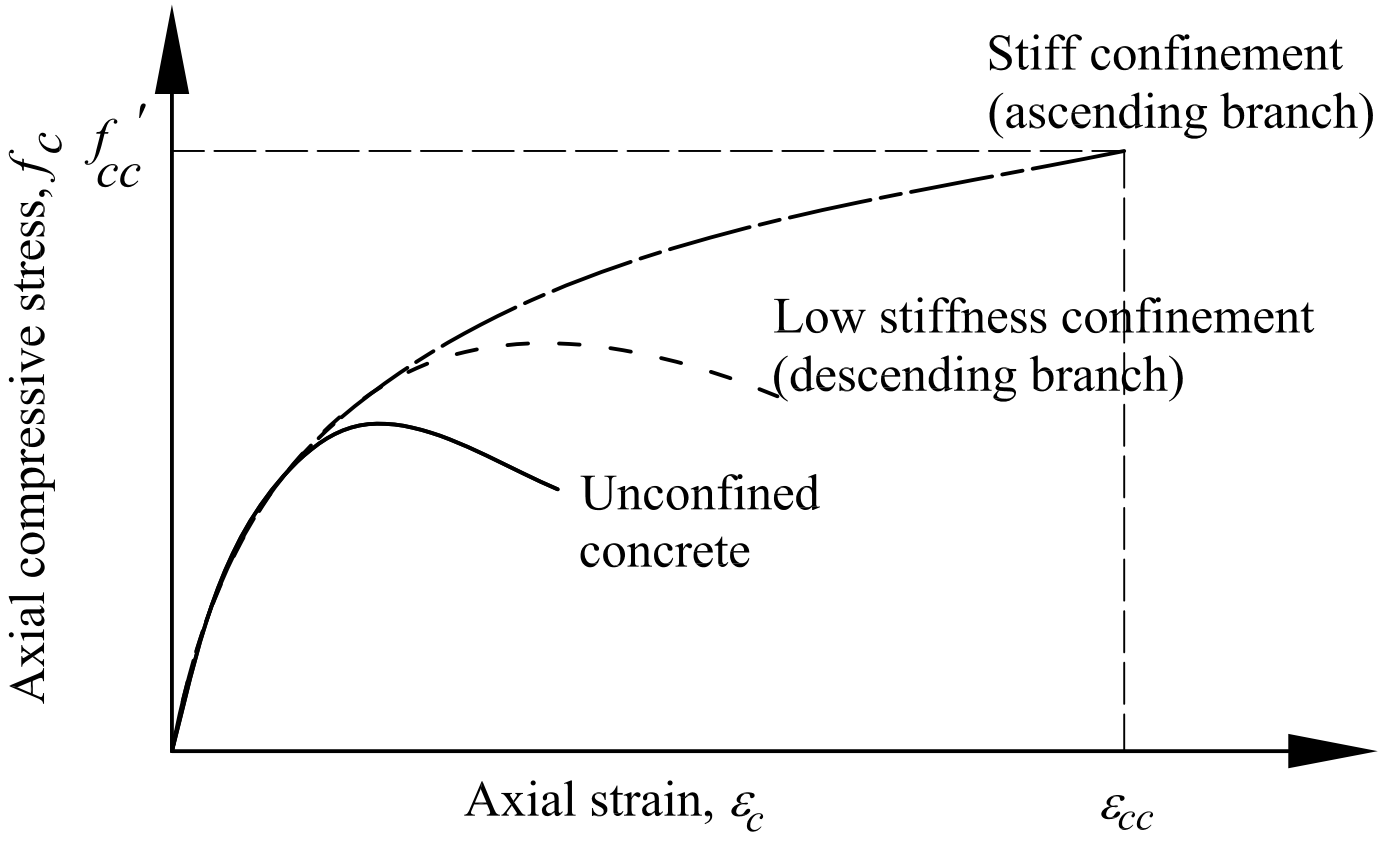
Stiff confinement
(ascending branch)
f_{cc}'
Axial compressive stress, f_c
Low stiffness confinement
(descending branch)
Unconfined
concrete
Axial strain, ε_c
ε_{cc}

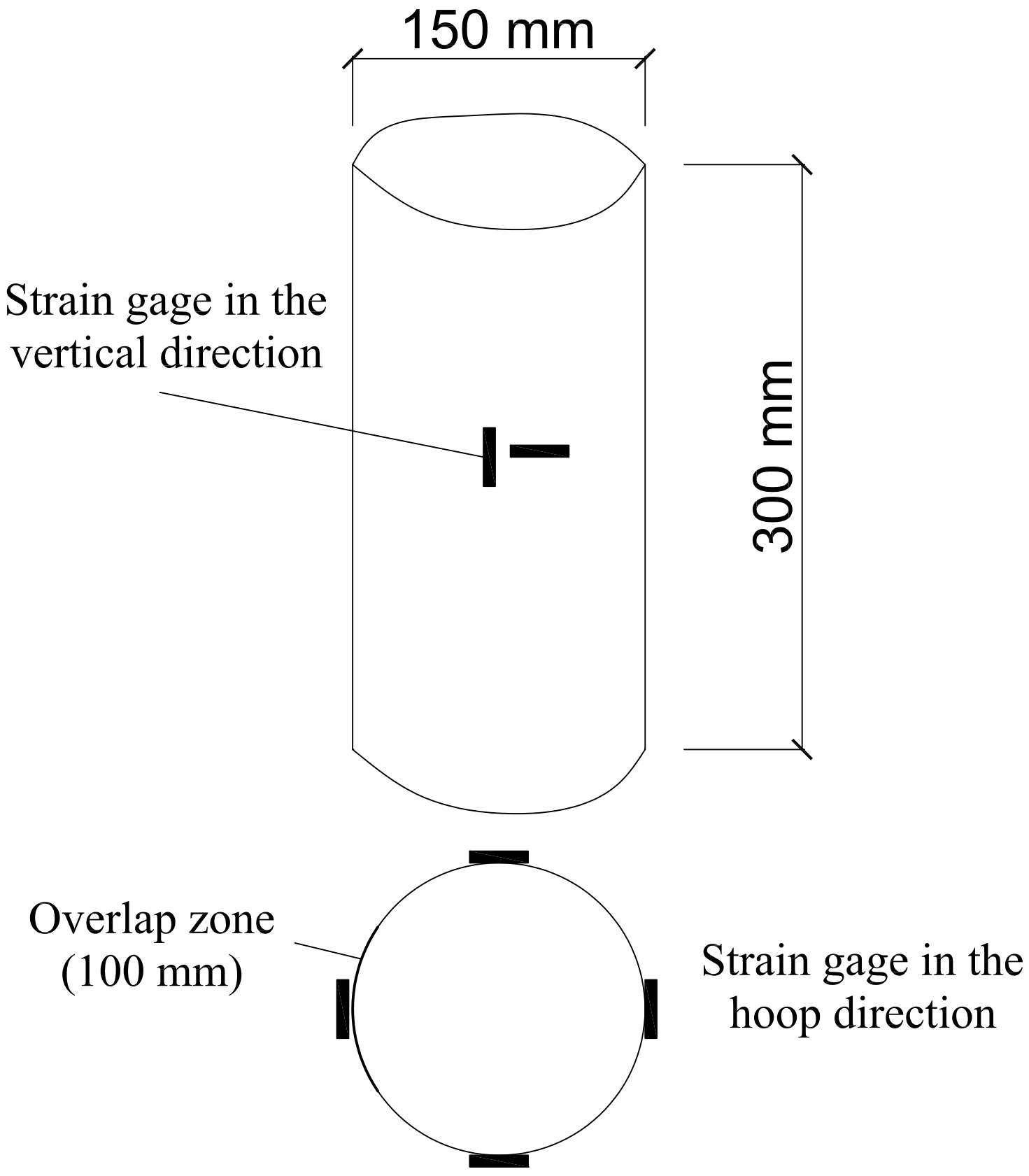
150 mm
Strain gage in the vertical direction
300 mm
Overlap zone (100 mm)
Strain gage in the hoop direction

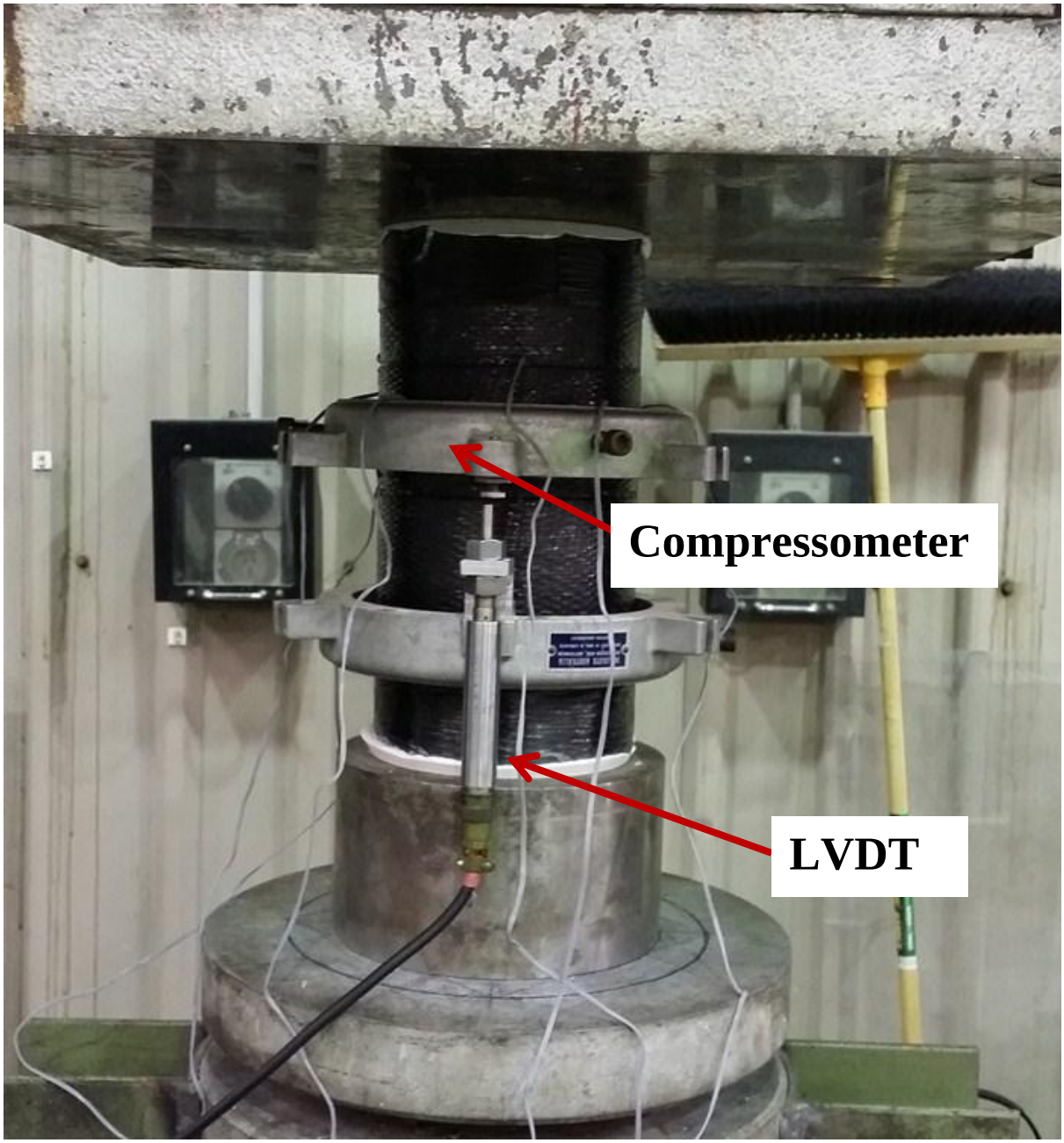
Compressometer
LVDT

C2-1.2

C2-1.4

C3-1.4

C3-1.7

C2-0.6

C2-1.0

C3-0.6

C3-1.0

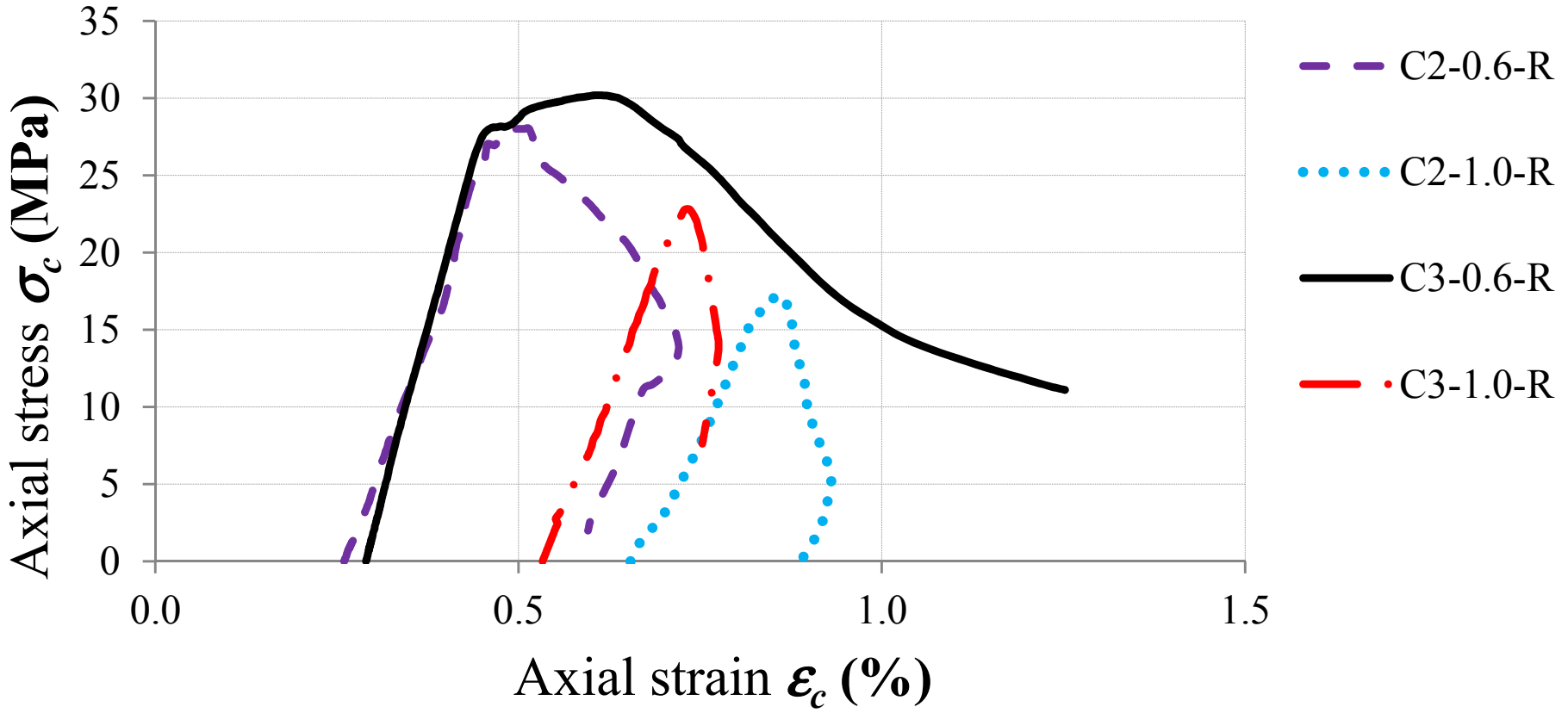
35
30
25
20
15
10
5
0
0.0
0.5
1.0
1.5
Axial stress σ_c (MPa)
Axial strain ε_c (%)
C2-0.6-R
C2-1.0-R
C3-0.6-R
C3-1.0-R

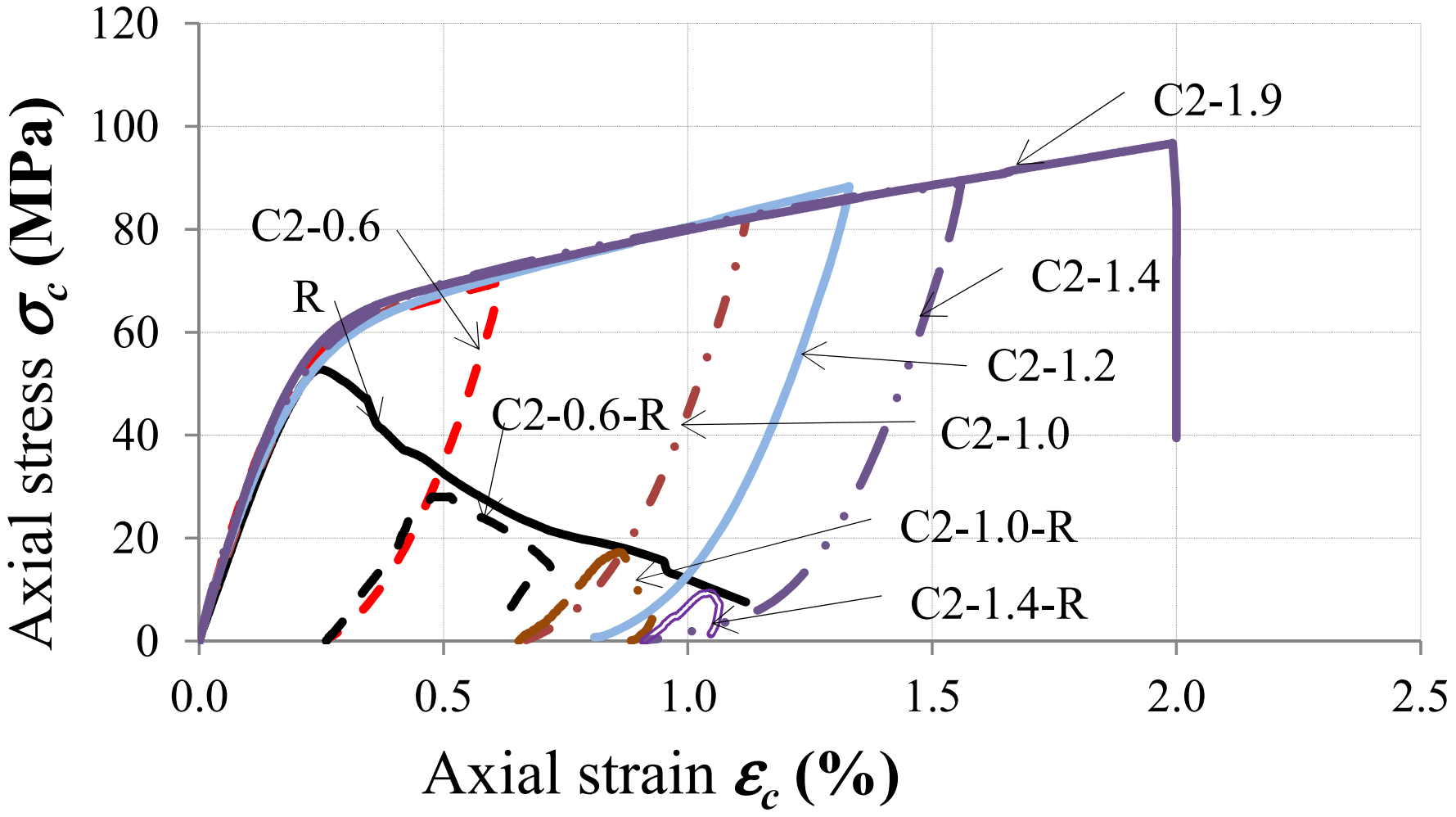
120
100
80
60
40
20
0
0.0
0.5
1.0
1.5
2.0
2.5
Axial stress σ_c (MPa)
Axial strain ε_c (%)
C2-1.9
C2-0.6
R
C2-1.4
C2-1.2
C2-0.6-R
C2-1.0
C2-1.0-R
C2-1.4-R

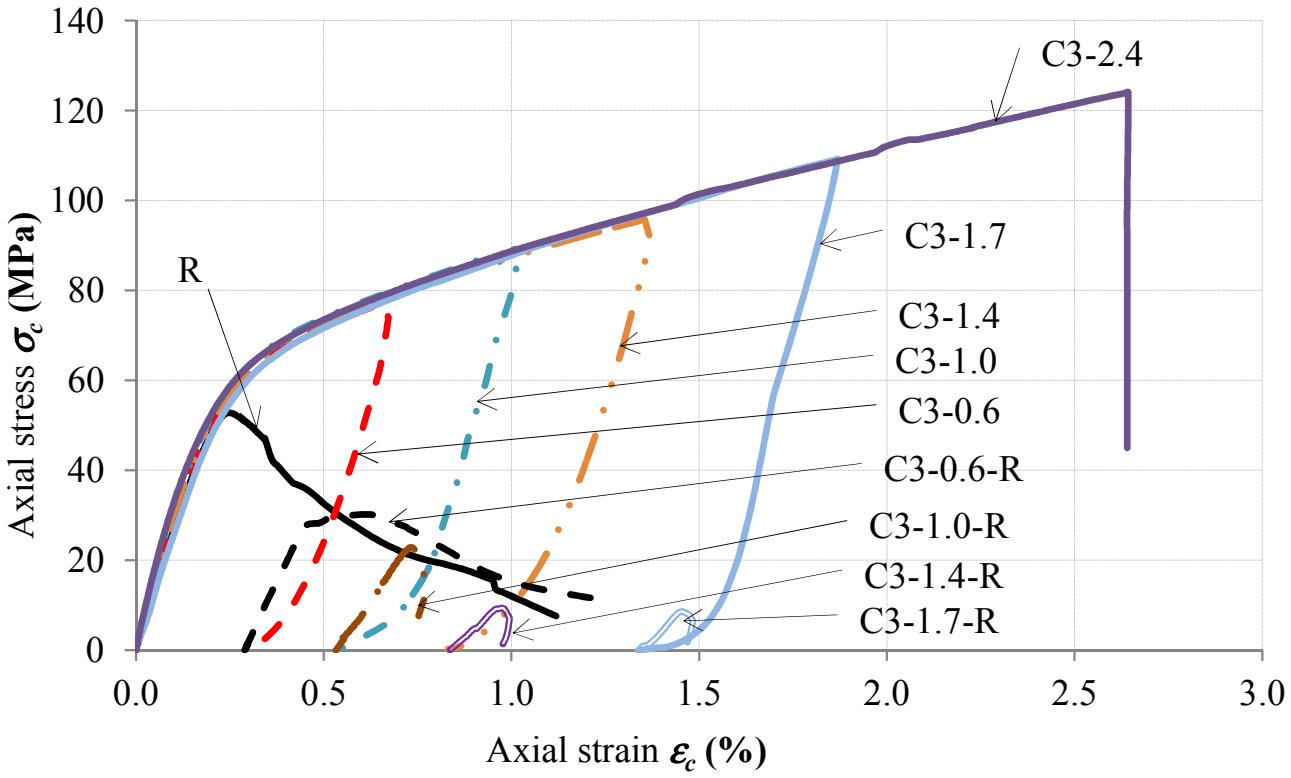
140
120
100
80
60
40
20
0
0.0
0.5
1.0
1.5
2.0
2.5
3.0
Axial stress σ_c (MPa)
Axial strain ε_c (%)
C3-2.4
C3-1.7
C3-1.4
C3-1.0
C3-0.6
C3-0.6-R
C3-1.0-R
C3-1.4-R
C3-1.7-R
R

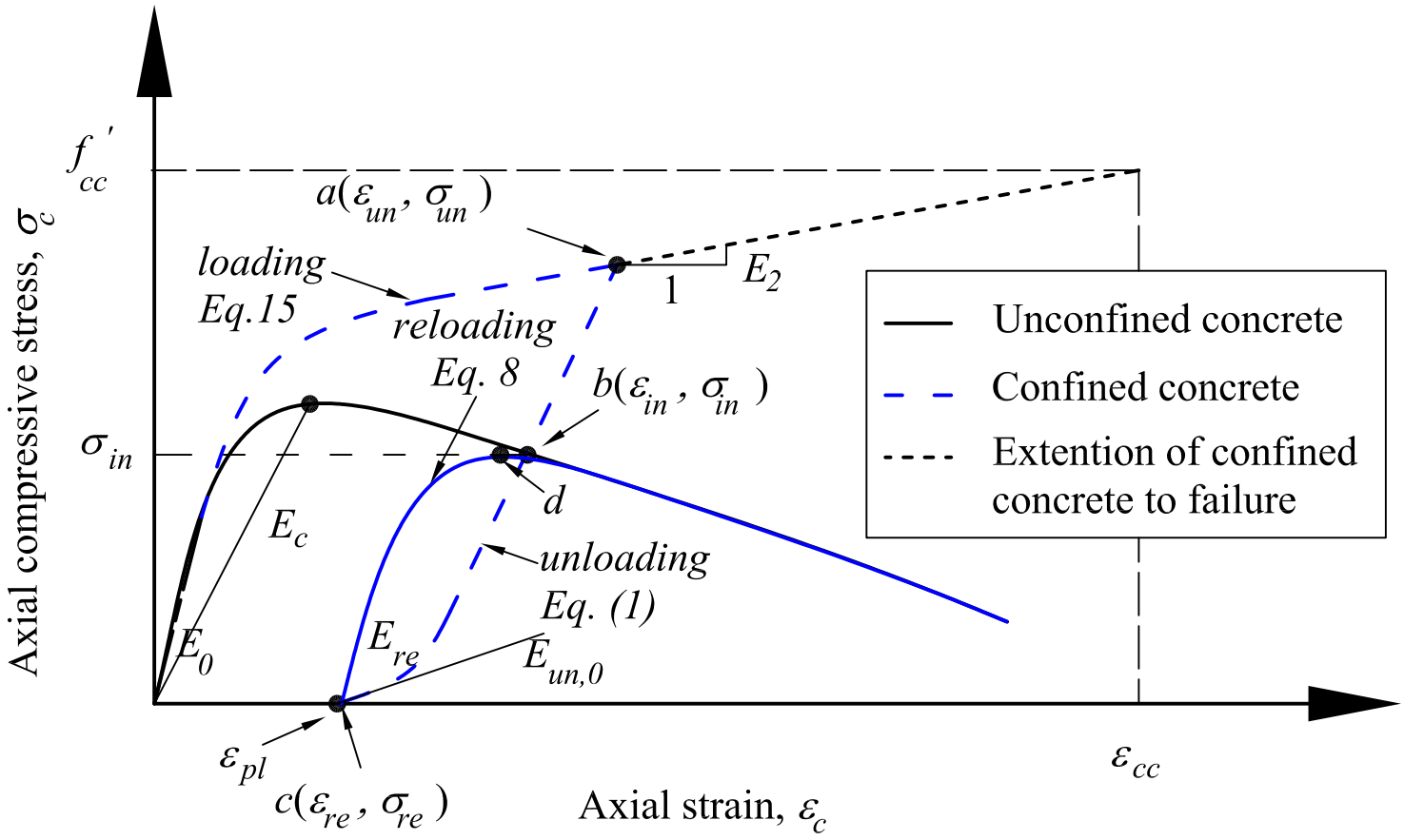
Axial compressive stress, σ_c
f'_{cc}
$a(\varepsilon_{un}, \sigma_{un})$
loading
Eq.15
reloading
Eq. 8
$b(\varepsilon_{in}, \sigma_{in})$
σ_{in}
E_2
1
E_c
E_0
E_{re}
$E_{un,0}$
d
unloading
Eq. (1)
ε_{pl}
$c(\varepsilon_{re}, \sigma_{re})$
Axial strain, ε_c
ε_{cc}
Unconfined concrete
Confined concrete
Extention of confined concrete to failure

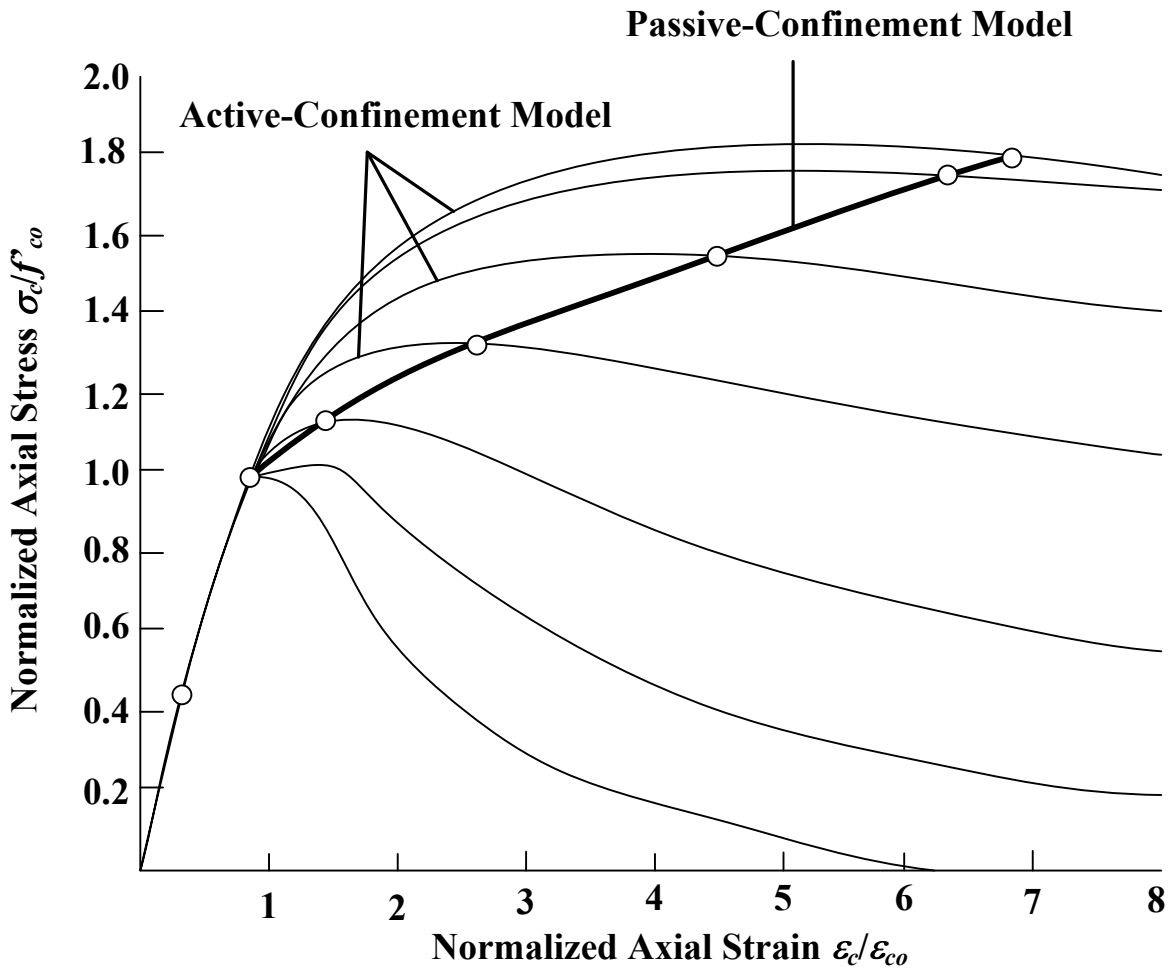
Passive-Confinement Model
Active-Confinement Model
Normalized Axial Stress σ_c/f'_{co}
2.0
1.8
1.6
1.4
1.2
1.0
0.8
0.6
0.4
0.2
1
2
3
4
5
6
7
8
Normalized Axial Strain $\varepsilon_c/\varepsilon_{co}$

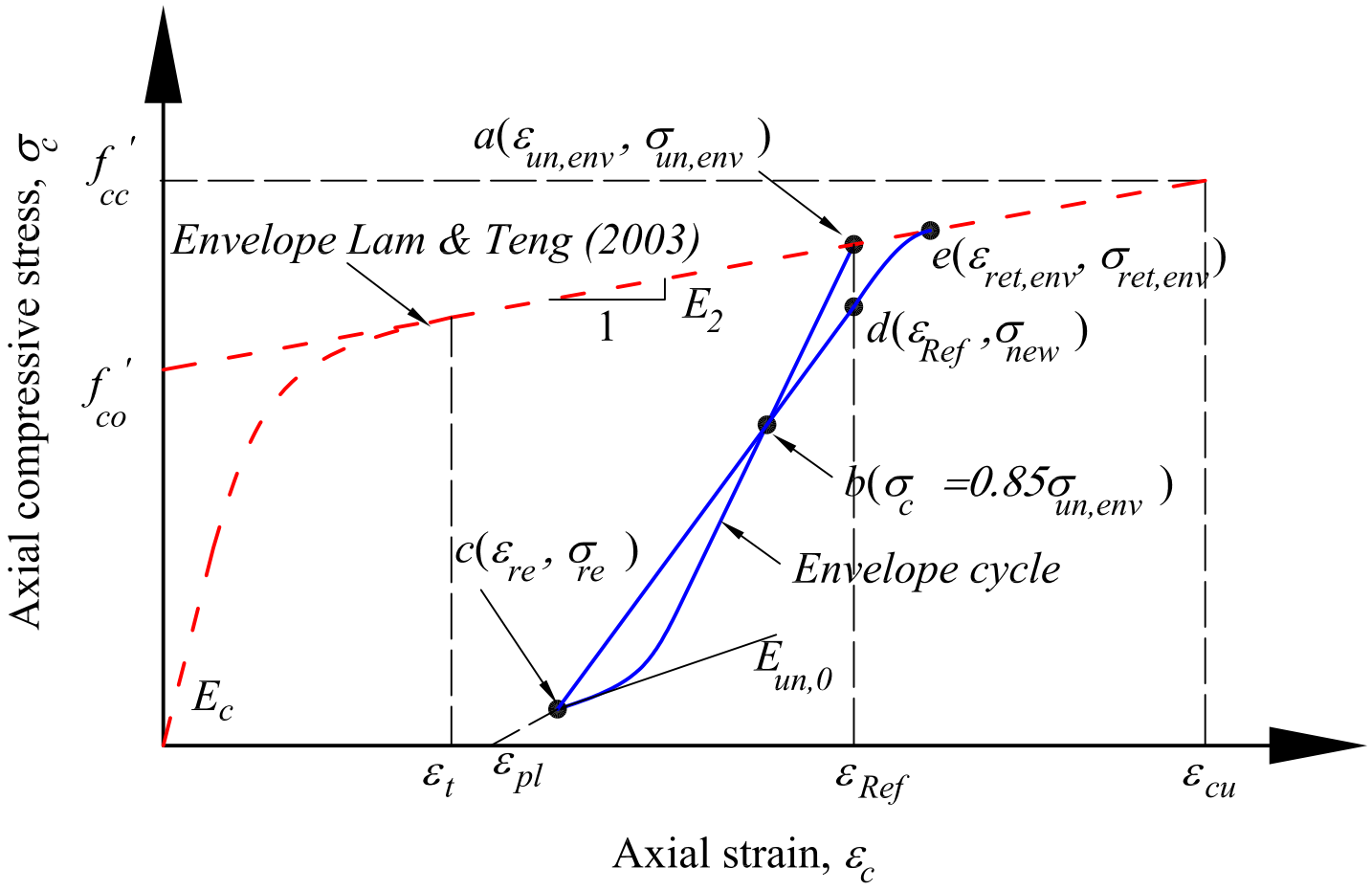
Axial compressive stress, σ_c
f_{cc}'
f_{co}'
$a(\varepsilon_{un,env}, \sigma_{un,env})$
Envelope Lam & Teng (2003)
1
E_2
$e(\varepsilon_{ret,env}, \sigma_{ret,env})$
$d(\varepsilon_{Ref}, \sigma_{new})$
$b(\sigma_c = 0.85\sigma_{un,env})$
$c(\varepsilon_{re}, \sigma_{re})$
Envelope cycle
$E_{un,0}$
E_c
ε_t
ε_{pl}
ε_{Ref}
ε_{cu}
Axial strain, ε_c

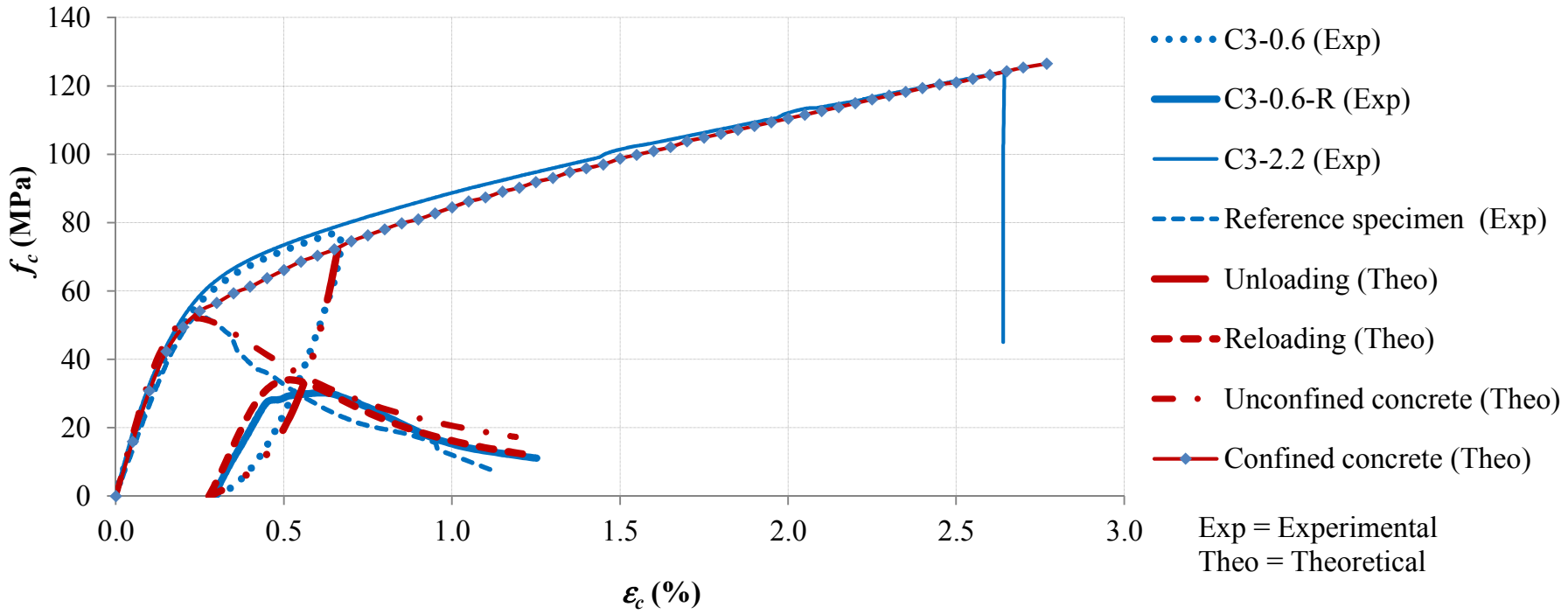
140
120
100
80
60
40
20
0
0.0
0.5
1.0
1.5
2.0
2.5
3.0
f_c (MPa)
ε_c (%)
C3-0.6 (Exp)
C3-0.6-R (Exp)
C3-2.2 (Exp)
Reference specimen (Exp)
Unloading (Theo)
Reloading (Theo)
Unconfined concrete (Theo)
Confined concrete (Theo)
Exp = Experimental
Theo = Theoretical

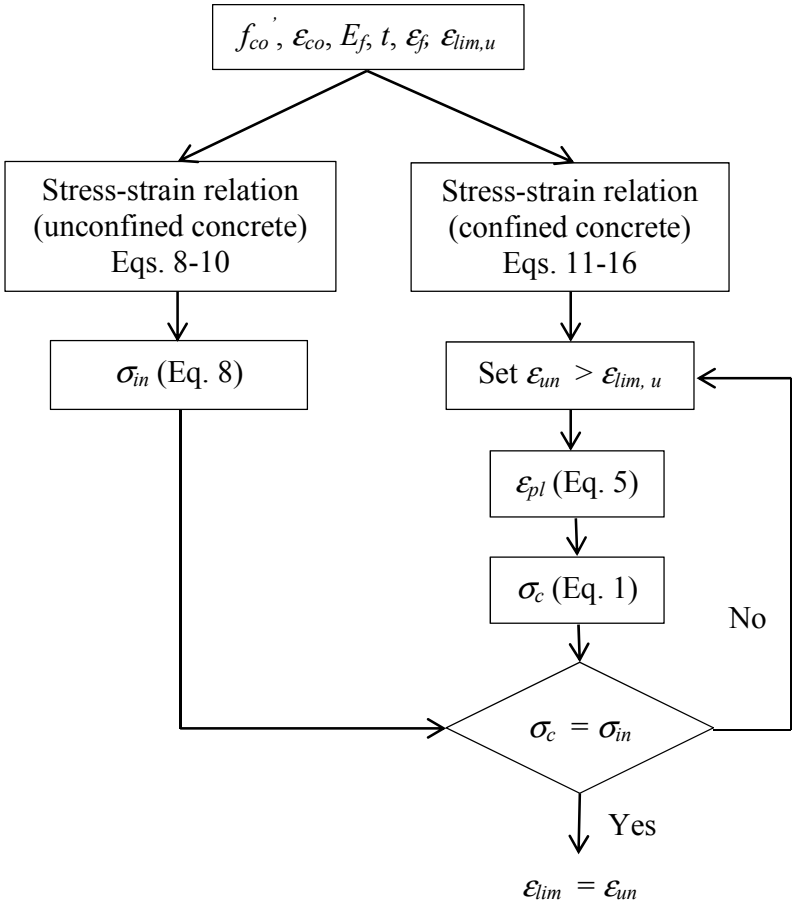
f_{co}', ε_{co}, E_f, t, ε_f, $\varepsilon_{lim,u}$
Stress-strain relation (unconfined concrete) Eqs. 8-10
Stress-strain relation (confined concrete) Eqs. 11-16
σ_{in} (Eq. 8)
Set $\varepsilon_{un} > \varepsilon_{lim,u}$
ε_{pl} (Eq. 5)
σ_c (Eq. 1)
No
$\sigma_c = \sigma_{in}$
Yes
$\varepsilon_{lim} = \varepsilon_{un}$

6 CIRCULARIZING SQUARE COLUMNS TO CIRCULAR COLUMNS

6.1 Circularizing by Normal Strength Concrete

Summary

This study investigates three methods of strengthening existing reinforced square concrete columns under different loading conditions. Four groups of sixteen reinforced concrete square columns were made from normal strength concrete. Reinforcement was kept at minimum ratio, simulating columns which need retrofitting. Columns of the first group were reference columns (Group N) while the corners of the second group columns (Group RF) were rounded and wrapped with three layers of Carbon Fiber Reinforced Polymers (CFRP). The sides of the columns of the third group (Group CF) were bonded with four pieces of concrete with a segmental circular shape, thus changing the cross section of the column from a square to a circle before each column was wrapped with three layers of CFRP. The columns of the last group (Group CS) were modified as the third group to result in a circular cross section, but were confined with steel straps. Results from the study showed that all confinement methods increased the capacity and ductility of columns. In particular, segmental circular concrete covers dramatically reduced the stress concentration at the corners and increased confinement efficacy. The Interaction (*P-M)* diagrams of experimental results and theoretical analysis all confirmed high performance of groups RF and CF.

Citation

This paper was published in Journal of Composites for Construction with the following citation:

Hadi, M.N.S., Pham, T.M., and Lei, X. (2013). "New Method of Strengthening Reinforced Concrete Square Columns by Circularizing and Wrapping with Fiber-Reinforced Polymer or Steel Straps." *Journal of Composites for Construction,* 17(2), 229-238.

New Method of Strengthening Reinforced Concrete Square Columns by Circularizing and Wrapping with Fiber-Reinforced Polymer or Steel Straps

Muhammad N. S. Hadi, M.ASCE[1]; Thong M. Pham[2]; and Xu Lei[3]

Abstract: This study investigates three methods of strengthening existing reinforced square concrete columns under different loading conditions. Four groups of sixteen reinforced concrete square columns were made from normal-strength concrete. Reinforcement was kept at minimum ratio, simulating columns that need retrofitting. Columns of the first group were reference columns (Group N), while the corners of the second group columns (Group RF) were rounded and wrapped with three layers of carbon-fiber-reinforced polymers (CFRPs). The sides of the columns of the third group (Group CF) were bonded with four pieces of concrete with a segmental circular shape, thus changing the cross section of the column from a square to a circle before each column was wrapped with three layers of CFRP. The columns of the last group (fourth) were modified as the third group to result in a circular cross section, but were confined with steel straps. Results from the study showed that all confinement methods increased the capacity and ductility of columns. In particular, segmental circular concrete covers dramatically reduced the stress concentration at the corners and increased confinement efficacy. The interaction (P–M) diagrams of experimental results and theoretical analysis all confirmed high performance of groups RF and CF. **DOI: 10.1061/(ASCE)CC.1943-5614.0000335.**

CE Database subject headings: Fiber reinforced polymer; Eccentric loads; Reinforced concrete; Concrete columns; Experimentation.

Author keywords: Square columns; Steel straps; P–M interaction diagram.

Introduction

Retrofitting existing columns in bridges and buildings has become an indispensable requirement in recent decades. Application of fiber-reinforced polymers (FRPs) has been used to strengthen existing reinforced concrete (RC) columns. This use of FRP has been shown to increase the strength, stiffness, and ductility of the strengthened columns. The behavior of FRP-confined concrete has been previously investigated through both experimental tests and theoretical methods (Lam and Teng 2003; Hadi 2006a, b; Hadi 2007a, b; Wu and Zhou 2010; Csuka and Kollár 2012; Hadi and Widiarsa 2012). These studies simulated stress-strain models for FRP-confined concrete, particularly circular columns under concentric load. These theoretical models were found to correlate well with experimental data. Based on the models and experimental results, it is evident that the efficacy of FRP confinement of a circular column is higher than that of a square column. In such cases, stress concentration at the corners of the square column and the effective area of the confined section led to a decrease in FRP efficacy. Therefore, it was found that converting a square column to a circular one will increase the effectiveness of FRP confinement.

Most of the existing columns are square or rectangular in cross sections. However, early research studies indicated that FRP-confined square or rectangular columns with sharp corners provide little enhancement in their load-carrying capacity, while confinement effectiveness increases proportionally with an increase in the corner radius (Wu and Zhou 2010). Meanwhile, curvature of the corners could cause stress concentration (Al-Salloum 2007). Therefore, changing a square column to a circular column may minimize the stress concentration, which was an objective of this study.

The knowledge of eccentric load effects on FRP-confined concrete columns is considerably less than that of concentric load effects. It is known that an eccentric load causes a pronounceable varied distribution of the confinement stress (Csuka and Kollár 2012), thus possibly leading to pockets of less confined parts of the cross section. As a result, the effectiveness of FRP in concentrically loaded columns is much higher than eccentrically loaded columns (Li and Hadi 2003; Hadi and Li 2004; Hadi 2006a, b; Hadi 2007a, b). To further investigate the effects of FRP confinement, this study focuses on retrofitting structural members by comparing three different approaches of strengthening.

Built structures sometimes are required to be retrofitted in cases involving change of the use of the structures, change of design codes, or construction errors. As most structures are built using normal-strength concrete, the experiments of this study emulate that by utilizing normal-strength concrete. This study investigates the technique of changing the cross section of a RC column from a square to a circle and compares the use of two wrapping materials, namely, carbon-fiber-reinforced polymer (CFRP) and steel straps.

[1]Associate Professor, School of Civil, Mining and Environmental Engineering, Univ. of Wollongong, New South Wales 2522, Australia (corresponding author). E-mail: mhadi@uow.edu.au

[2]Ph.D. Student, School of Civil, Mining and Environmental Engineering, Univ. of Wollongong, New South Wales 2522, Australia. E-mail: mtp027@uowmail.edu.au

[3]ME Research Student, School of Civil, Mining and Environmental Engineering, Univ. of Wollongong, New South Wales 2522, Australia. E-mail: xl158@uowmail.edu.au

Note. This manuscript was submitted on February 13, 2012; approved on September 21, 2012; published online on September 23, 2012. Discussion period open until September 1, 2013; separate discussions must be submitted for individual papers. This paper is part of the ***Journal of Composites for Construction***, Vol. 17, No. 2, April 1, 2013. © ASCE, ISSN 1090-0268/2013/2-229-238/$25.00.

Theoretical Consideration

Confinement Model

Triaxial compressive stress provided by confinement delays expansion and damage propagation by restricting crack growth and decreasing the dilation ratio of concrete. When the stress in concrete approaches the uniaxial strength, the volume starts to increase due to progressive internal fracturing and the concrete bears the transverse reinforcement, at which point the concrete becomes confined (Kent and Park 1971). This study uses a FRP-confined concrete model to determine the compressive strength of FRP-confined concrete which was proposed by Lam and Teng (2003) as follows:

$$\frac{f'_{cc}}{f'_{co}} = 1 + 3.3\frac{f_{l,a}}{f'_{co}} \tag{1}$$

where f'_{cc} and f'_{co} = compressive strength of confined and unconfined concrete, respectively; and $f_{l,a}$ = effective confining pressure, which can be estimated by the following equation:

$$f_{l,a} = k_e\frac{2f_{\text{frp}}t}{d} \tag{2}$$

where f_{frp} and t = rupture stress and the thickness of FRP, respectively; d = diameter of a column; and k_e = FRP efficiency factor which was defined by Harries and Carey (2003) and then taken as 0.586 by Lam and Teng (2003). This model was used for calculating the strength of full-CFRP-wrapped circular columns.

For steel straps–confined columns, the model proposed by Mander et al. (1988) was used in this study to calculate the confined strength of the specimens as follows:

$$f'_{cc} = f'_{co}\left(-1.254 + 2.254\sqrt{1 + \frac{7.94f_{l,a}}{f'_{co}}} - 2\frac{f_{l,a}}{f'_{co}}\right) \tag{3}$$

Similar to the model of FRP-confined columns, the confinement pressure $f_{l,a}$ can be calculated as follows:

$$f_{l,a} = k_s\frac{2f_{st}t}{d} \tag{4}$$

where f_{st} and t = yield strength and the thickness of steel straps, respectively; d = diameter of the column; and k_s = confinement efficiency factor for steel straps as shown in Fig. 1. This factor was modified to suit the case of steel straps confinement in this study as follows:

$$k_s = \frac{A_e}{A} = \frac{(1 - \frac{s}{2d})^2}{1 - \rho} \tag{5}$$

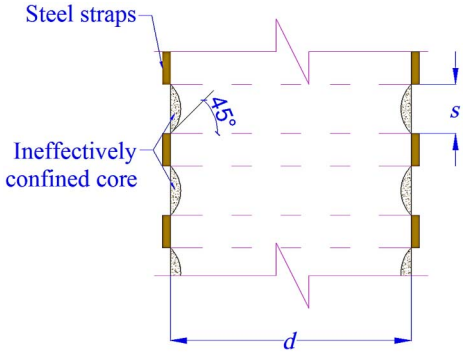

Fig. 1. Effective core for steel straps–confined columns

where ρ = ratio of longitudinal reinforcement and s = vertical spacing between steel straps.

A continuous curve of the stress-strain model proposed by Popovics (1973) was used to express the compressive stress in concrete in terms of the strain:

$$f_c = \frac{f'_{cc}xr}{r - 1 + x^r} \tag{6}$$

$$x = \frac{\varepsilon_c}{\varepsilon_{cc}} \tag{7}$$

$$r = \frac{E_c}{E_c - E_{\text{sec}}} \tag{8}$$

$$E_{\text{sec}} = \frac{f'_{cc}}{\varepsilon_{cc}} \tag{9}$$

where ε_c = compressive strain of concrete corresponding to axial stress f_c; ε_{co} = strain of unconfined concrete corresponding to the maximum stress, which can be taken as 0.002; and ε_{cc} = compression strain of confined concrete at the peak stress, which can be calculated from ACI 440.2R-08 [American Concrete Institute (ACI) 2008].

The elastic modulus of unconfined concrete, E_c, can be calculated using the equation given by AS 3600 [Australian Standard (AS) 2009]

$$f'_{co} \le 40\text{ MPa}, \qquad E_c = \rho^{1.5}\left(0.043\sqrt{f'_{co}}\right)\text{ MPa} \tag{10}$$

$$f'_{co} > 40\text{ MPa}, \qquad E_c = \rho^{1.5}\left(0.024\sqrt{f'_{co}} + 0.12\right)\text{ MPa} \tag{11}$$

where ρ = density of concrete, which can be taken as 2,400 kg/m^3 for normal-weight concrete.

Ductility

Ductility is the ability of a material to deform plastically without fracturing. In this study, the ductility of concrete columns was calculated using two methods, which were based on two different definitions (Hadi 2009). For the first method, the ductility (λ) is calculated as the ratio of the deflection at the 85% postultimate load (δ_u) divided by yield deflection (δ_y), which can be written as follows:

$$\lambda = \frac{\delta_u}{\delta_y} \tag{12}$$

For the second method, the ductility is calculated as the ratio of A_2 divided by A_1, which is written as follows:

$$\lambda = \frac{A_2}{A_1} \tag{13}$$

where A_1 and A_2 = area under the axial load-deflection curve up to the yield load and the 85% postultimate load, respectively. In both cases, the yield deflection is assumed to be the deflection at the limit of the elastic behavior, which was based on the definition by Pessiki and Pieroni (1997).

Interaction Diagram

An axial load-bending moment (P–M) interaction diagram is a continuous curve used to determine the axial load (P) and bending

J. Compos. Constr. 2013.17:229-238.

moment (M) of a given RC column cross section. Each point on this curve includes two components, namely, the value of the axial loading and the corresponding bending moment. In this study, an experimental interaction diagram was drawn based on four points: (1) a pure axial load of the column under a concentric load, (2) two points of eccentric loads of 15 and 25 mm in which the axial loads were recorded from the testing machine and the bending moments were calculated by Eq. (14), and (3) a pure bending moment observed from the four-point loading test

$$M = P_{\max}(e + \delta) \tag{14}$$

where $P_{\max}$ = ultimate axial load; e = eccentricity of loading; and δ = lateral deflection at the ultimate load.

In order to draw a theoretical interaction diagram (P–M), the confined concrete models shown in the preceding sections were utilized and two methods were derived. The compressive strength of the confined concrete was estimated by the models as mentioned in the preceding sections. An equivalent stress block was used to transfer nonuniform compressive-confined concrete stresses to rectangular distribution of stresses as recommended by AS 3600 (AS 2009).

For the first method, the centroid of a compressive concrete region for a circular cross section was calculated by Fig. 2 and Eqs. (15) (Case 1) and (16) (Case 2). The interaction diagram was drawn by this methodology as equivalent computation

$$y = \frac{4R(\sin\theta)^3}{3(2\theta - \sin 2\theta)} \tag{15}$$

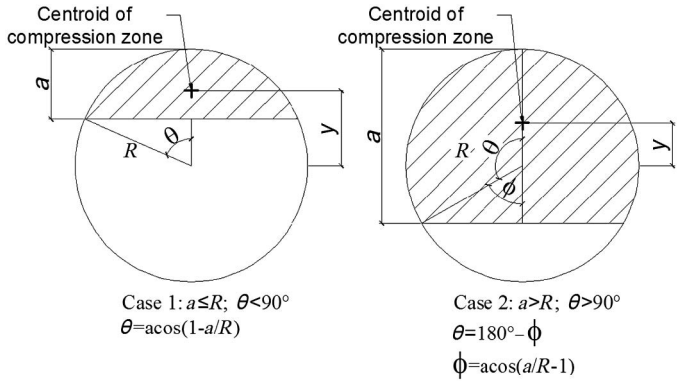

Fig. 2. Centroid of compression zone of the column

$$y = \frac{2R(\sin\phi)^3}{3(\pi - \phi + \sin\phi\cos\phi)} \tag{16}$$

where y, R, ϕ, and θ are shown in Fig. 2.

For the second method, interaction diagrams were drawn as described by Yazici and Hadi (2009). The cross section of the column is assumed to contain parallel finite strips, which are small enough to attain accurate precision, yet large enough for easy calculations. In this paper, the width of strips was taken as 5 mm as shown in Fig. 3, where α = rectangular stress block parameter (AS 2009). This parameter is used to change the nonlinear stress distribution in the compressive concrete to a uniform stress distribution.

Experimental Program

Design of Experiments

A total of 16 square RC columns, classified into four groups, were cast and tested at the High Bay Laboratory of the University of Wollongong. The dimensions of the columns were 150×150 mm^2 in cross section and 800 mm in length. The first group (Group N) was considered as a reference group with no external confinement or any modification of the section. The second group (Group RF columns) was cast to have 20-mm round corners that were horizontally wrapped with three layers of CFRP (75 mm in width). The third and fourth groups, Groups CF and CS, were bonded with four segmental circular concrete covers to modify the shapes of the cross sections from square to circular. Columns of Group CF were horizontally wrapped with three layers of CFRP, while columns of Group CS were confined with steel straps (19.1 mm in width) at 30-mm spacing. From each group the first column was concentrically loaded, while the second and the third columns were subjected to eccentric loading at 15 and 25 mm, respectively. The fourth specimen was tested under four-point loading as a beam to observe the flexural behavior.

The notation of the specimens consists of two parts: the first part is N-, RF-, CF-, and CS- that states the name of the group to which the specimens belong (normal, round corners with FRP, circular with FRP, and circular with steel straps). The second part indicates the loading conditions. For instance, 0 means concentric load, F is flexural loading, 15 and 25 mean loading at 15 and 25 mm eccentricity, respectively. Table 1 shows the test matrix of the experiments.

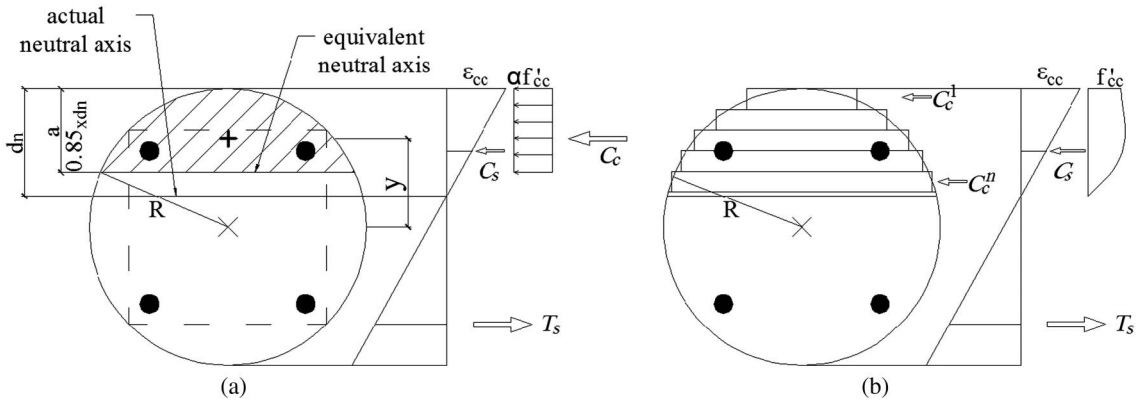

Fig. 3. Stress-strain analysis for computing P–M diagram: (a) equivalent method; (b) small strips method

J. Compos. Constr. 2013.17:229-238.

Table 1. Test Matrix

Specimens	Modification	Internal reinforcement	External reinforcement	Eccentricity
N-0	None	4N12 R6@120	None	0
N-15				15
N-25				25
N-F				Flexural
RF-0	20-mm round corners	4N12 R6@120	Three layers of CFRP	0
RF-15				15
RF-25				25
RF-F				Flexural
CF-0	Concrete covers	4N12 R6@120	Three layers of CFRP	0
CF-15				15
CF-25				25
CF-F				Flexural
CS-0	Concrete covers	4N12 R6@120	Steel straps	0
CS-15				15
CS-25				25
CS-F				Flexural

The nominal compressive strength of concrete used was 32 MPa. The internal reinforcement of each of the specimens consists of 4N12 (12-mm deformed bars with 500-MPa nominal tensile strength) as longitudinal bars and R6 plain bars (6-mm plain bars with 250-MPa nominal tensile strength) tied at 120-mm spacing. Fig. 4 shows the cross sections of the specimens.

Loading System

For testing of specimens, a special loading head system was used to apply the required eccentric loads as illustrated by Hadi and Widiarsa (2012). The loading head contained two main parts: a 25-mm thick steel plate [see Fig. 5(a)] sitting on top of the column, and a circular roller loading [see Fig. 5(b)] welded on another 25-mm thick steel plate with a specific distance which equals to the eccentricity, offset from the center line of the plate. A pair

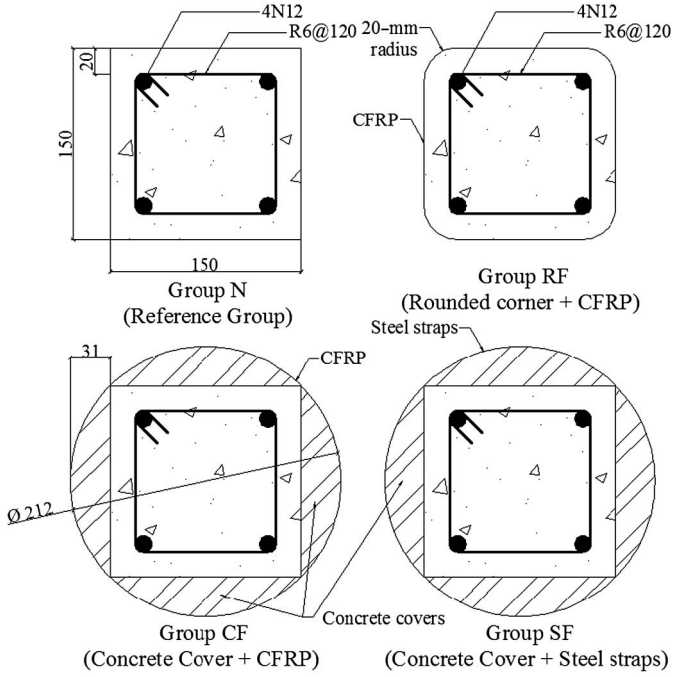

Fig. 4. Plan view of specimens

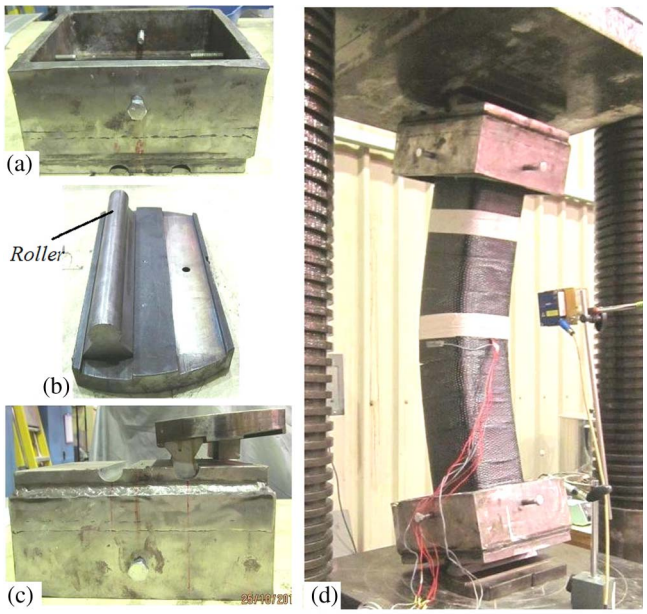

Fig. 5. Eccentric loading system: (a) loading head; (b) loading roller; (c) a pair of loading head; and (d) whole loading system

of two plates is placed as shown in Fig. 5(c). The details of the eccentric loading system are depicted in Fig. 5(d), which shows the configuration of the loading plates.

Specimen Construction

Normal-strength ready-mixed concrete was supplied by a local supplier. Two formworks made from plywood were used to construct the core specimens and the segmental circular concrete covers (Fig. 6). For the segmental circles, a box of 34 rectangular segments having a dimension of 51 × 170 mm^2 was built. Next, a section mold of foam was added to each rectangular segment in order to create a mold for the concrete cover [Figs. 6 and 7(a)]. Each segmental circular concrete cover had a chord of 150 mm (equal to the side length of the core column section) and the height of the segment was 31 mm. After 28 days, any foam pieces attached to the concrete surface covers were removed and surface ground to ensure smooth contact when bonding with FRP or steel straps.

For Groups CF and CS, each specimen was bonded with four segmental circular concrete covers using microsphere blend, mixed together with epoxy resin at 2:1 ratio [Fig. 7(b)]. The epoxy resin has a tensile strength of 54 MPa, tensile modulus of 2.8 GPa, and 3.4% tensile elongation (WEST SYSTEM n.d. 2012). After that, Group CF specimens were wrapped with three layers of CFRP and left to dry for 7 days as specified by the supplier. For the Group CS specimens, steel straps were installed.

The adhesive used was a mixture of epoxy resin and hardener at 5:1 ratio. Before the first layer of CFRP was attached, the adhesive was spread onto the surface of the column and CFRP was attached onto the surface. After the first ring, the adhesive was spread onto the surface of the first layer of CFRP and the second layer was continuously bonded. The third layer of CFRP was applied in a similar manner, ensuring that 100-mm overlap was maintained. The main fiber orientation was perpendicular to the longitudinal axis of the column. The steel straps were installed by a bending tool (Product No. C00169), which was supplied by Blackwoods (2012).

J. Compos. Constr. 2013.17:229-238.

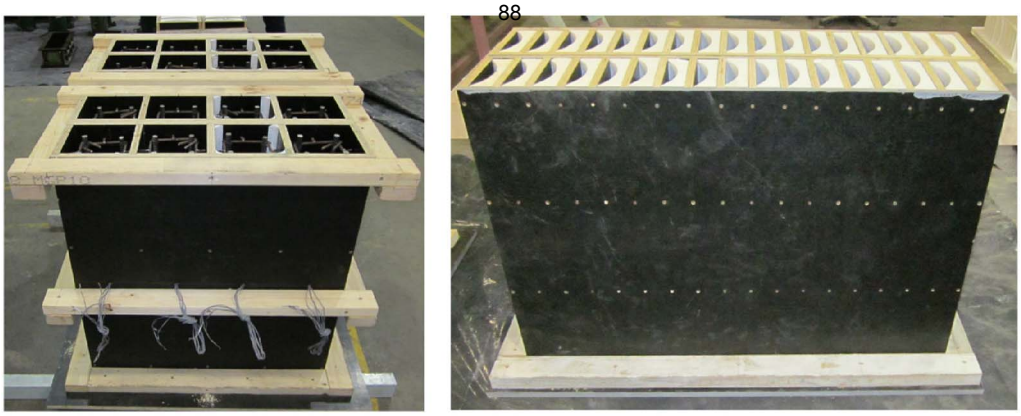

(a) (b)

Fig. 6. Formworks: (a) core columns and (b) concrete covers

(a) (b)

Fig. 7. Segmental circular concrete covers and modified section columns: (a) concrete covers and (b) bonded specimens

Preliminary Tests

Compression tests at 28 days showed that the average compressive strength of the concrete was 27 MPa. To determine the material properties of CFRP, which was used as the confining material, the CFRP flat coupon tests were conducted according to ASTM D7565 (ASTM 2010). The average width of the test coupons was 28 mm and the average maximum tensile force per unit width was 1,972 N/mm. The strain at the average maximum tensile force and the average elastic modulus were 0.024 mm/mm and 82 kN/mm, respectively. Even though the thickness of CFRP is not generally reported in accordance with ASTM D7565 (ASTM 2010), the average thickness of three CFRP layers was measured at 1.2 mm. The tensile strength of CFRP was 1,461 MPa in accordance with ASTM 3039 (ASTM 2008). Three specimens of N12-deformed bars and R6 plain bars (length: 250 mm) were prepared and tested in accordance with AS 1391 (AS 2007). The tests revealed that the average tensile strength of N12 and R6 is 568 and 478 MPa, respectively. Three coupons of steel straps, which were used in confining the columns in Group CS, were prepared and tested according to ASTM D3953 (ASTM 2007). The tensile strength of the steel straps was 434 MPa.

Column Tests

The Denison 5,000-kN testing machine was used for testing all the specimens. The columns were capped with high-strength plaster at both ends to ensure full contact between the loading heads and the column. The first loading head was placed on the flat steel plate and the column was then seated vertically upon it. Calibration was then performed to ensure that the columns were placed at the center of the testing machine. For the flexural tests, two four-point loading systems were used. The square four-point loading frame by Hadi and Widiarsa (2012) was used for Specimens N-F and RF-F, while the circular four-point loading frame by Yazici and Hadi (2009) was used for Specimens CF-F and CS-F.

Strain gauges, which were placed at midheight of the specimens to investigate the actual strain of FRP, were connected to a data logger to record the data every 2 s. In order to measure the lateral deflection for the eccentrically loaded columns and the deflection for the flexural tests, a laser triangulation was used and connected to the data logger as well. For the column tests, the laser triangulation was set up at midheight of the column, and for the beam tests, the laser triangulation was placed on a hole, which is located at midspan of the bottom loading plate. The tests were conducted as deflection controlled with a rate of 0.3–0.5 mm/min.

J. Compos. Constr. 2013.17:229-238.

Table 2. Results of Specimens Tested under Concentric Loading

Specimens	N-0	RF-0	CF-0	CS-0
Yield load (kN)	707	796	1,478	1,060
Corresponding axial deflection (mm)	1.31	1.85	2.01	1.85
Ultimate load (kN)	717	1,564	2,907	1,116
Corresponding axial deflection (mm)	1.46	22.76	13.35	2.68
Ductility (Method 1)[a]	1.41	13.42	6.98	1.88
Ductility (Method 2)[a]	1.71	32.41	16.94	2.77

[a]See the "Ductility" section for the definition of the methods.

Experimental Results

Behavior of Specimens under Concentric Load

The first specimen in each group was tested under concentric loading. Results are given in Table 2 with the axial load-deflection diagrams shown in Fig. 8. Specimen N-0 failed by concrete spalling on the surface and buckling of the longitudinal reinforcement. Specimens RF-0 and CF-0 failed by rupture of CFRP at midheight of the specimen, as shown in Fig. 9(a). The concrete of the whole section at midheight was completely crushed but was restrained by CFRP. As a consequence, aggregates of Specimens RF-0 and CF-0 were completely separated from each other, which were different from the concrete of Specimens N-0 and CS-0. For Specimen RF-0, the applied load was gradually increased to 1,542 kN, after which a loud cracking sound could be heard when one ring of CFRP ruptured, and the load immediately dropped to 1,194 kN. Subsequently, a small part of a CFRP ring ruptured, which led to a slow decrease of the compressive load. Moreover, the load of Specimen CF-0 dropped faster than that of Specimen RF-0. That load was witnessed by a sudden drop from 2,924 to 928 kN (68%). At that time, a very loud sound was heard from two rings of CFRP rupturing simultaneously. Specimen CS-0 failed by ruptures of straps and crushing of the concrete at the upper height.

In Fig. 6, Specimens N-0 and RF-0 demonstrated identical behavior during the first stage of the diagram, that is, the concrete was not crushed. The same response was recorded from Specimens CF-0 and CS-0. However, the slopes of the load-deflection diagrams of Specimens CF-0 and CS-0 were higher than that of Specimens N-0 and RF-0 because the area of the cross sections of the former was bigger than the latter. After reaching the yield load, the loads of Specimens CF-0 and RF-0 were gradually increased to the postultimate load, which was higher than the yield load, at which point it was considered that the specimens were effectively confined. In other words, the loads of Specimens N-0 and CS-0 decreased after the yield load.

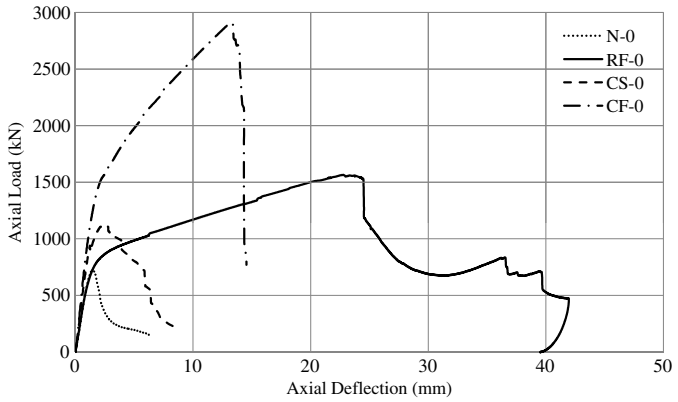

Fig. 8. Axial load-deflection diagram for concentric loading tests

Fig. 9. Failure modes: (a) Specimen CF-0 and (b) Specimen CS-15

Behavior of Specimens under Eccentric Load

The second and third specimens in each group were subjected to 15 and 25 mm of eccentric loading, respectively. Tables 3 and 4 depict the results of eccentric loading tests, while Figs. 10 and 11 demonstrate the axial load-deflection graphs of the eccentrically loaded specimens. During loading, Specimens N-15 and N-25 had their covers spalled off and the concrete crushed in the compression region. The longitudinal steels buckled in the compression region of Specimen N-15. Specimen RF-15 failed by the concrete crushing in the compression region while cracking of the specimen in the tension region was observed between two rings of CFRP at midheight. Specimen RF-25 failed by the same means as Specimen RF-15 except the rupture of the longitudinal steels in the tension region led to a complete collapse of the specimen. Interestingly, no CFRP rupture was observed in either of these cases.

For Groups CF and CS, the specimens failed by rupture of the confinement materials at midheight and crushing concrete in the compression region [Fig. 9(b)]. Cracks were observed in the tension region at the early stage. All specimens reached the ultimate load and then decreased considerably due to ruptures of CFRP rings or steel straps, which created a loud sound. Take Specimen

Table 3. Results of Specimens Tested under Eccentric Loading

Specimens	N-15	RF-15	CF-15	CS-15
Yield load (kN)	563	635	1,202	905
Corresponding axial deflection (mm)	1.24	1.58	2.02	1.55
Ultimate load (kN)	579	686	1,489	917
Corresponding axial deflection (mm)	1.36	2.31	6.50	1.97
Corresponding lateral deflection (mm)	2.34	5.42	19.50	3.19
Ductility (Method 1)[a]	1.63	5.22	4.82	3.23
Ductility (Method 2)[a]	1.53	7.89	8.62	1.96

Note: $e = 15$ mm.
[a]See the "Ductility" section for the definition of the methods.

J. Compos. Constr. 2013.17:229-238.

Table 4. Results of Specimens Tested under Eccentric Loading

Specimens	N-25	RF-25	CF-25	CS-25
Yield load (kN)	414	515	1,011	766
Corresponding axial deflection (mm)	0.96	1.68	1.69	1.40
Ultimate load (kN)	427	562	1,170	766
Corresponding axial deflection (mm)	1.08	2.91	6.12	1.40
Corresponding lateral deflection (mm)	2.33	8.10	21.75	1.69
Ductility (Method 1)[a]	1.33	4.73	5.11	2.03
Ductility (Method 2)[a]	1.78	7.32	9.25	2.48

Note: $e = 25$ mm.
[a]See the "Ductility" section for the definition of the methods.

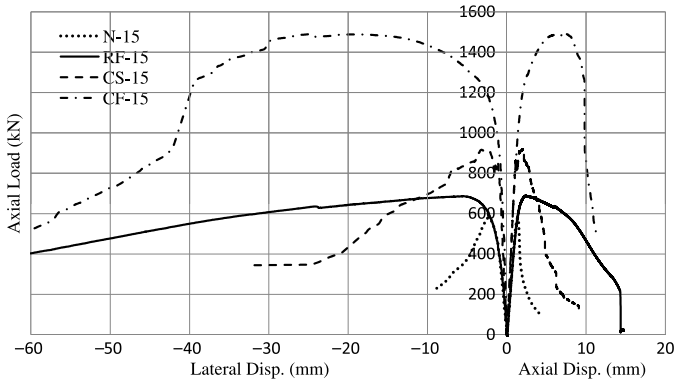

Fig. 10. Axial load-deflection diagram for eccentric loading tests ($e = 15$ mm)

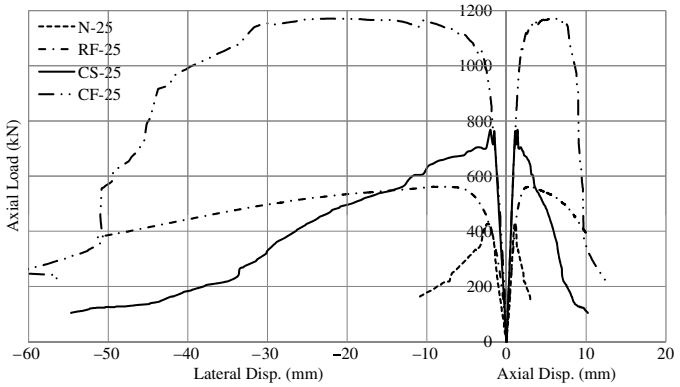

Fig. 11. Axial load-deflection diagram for eccentric loading tests ($e = 25$ mm)

CF-25 as a typical example: the specimen reached the ultimate load of 1,170 kN, then a small cracking sound was heard and the applied load dropped to 1,082 kN. Consequently, some continuously small cracking sounds and a loud sound were heard during which the applied load of the specimen dropped to 386 kN (67%). Moreover, the specimens confined with steel straps showed a strange response at the ultimate load. For example, Specimen RF-25 reached the ultimate load then a small sound was heard. Immediately, the applied load dropped from 763 to 723 kN and increased again with the same slope of load-axial deflection curve as the first stage to the ultimate load at 766 kN. This response can be explained as the specimen rearranged the structure of the core, concrete covers, and steel straps to work together during the next stage.

As can be seen in Figs. 10 and 11, the specimens with the same section behaved in a similar manner during the first stage of the diagram when concrete was not crushed. As a result, specimens in Groups CF and CS showed the same slope of curve in the load-axial deflection diagram while the applied load of the specimens in Groups N and RF increased at the same rate. Furthermore, the behavior of the specimens under eccentric load was different from that under concentric load after the yield loads. After reaching the yield loads, the confined specimens under concentric load kept raising toward the ultimate loads with other slopes of the load-axial deflection diagrams, which belonged to the ascending branch. In other words, the confined specimens of Groups CF and CS under eccentric load soared directly to the ultimate loads from the value of zero and then failed shortly by rupture of the confinement materials. It can be clearly seen that the confined specimens showed the ascending branch under concentric load but the descending branch under eccentric load. A summary of the confinement efficacy can be seen in Tables 3 and 4.

Flexural Behavior

The last specimen in each group was tested under four-point loading as a beam. Table 5 summarizes the test results and Fig. 12 demonstrates the load-midspan deflection graphs.

Specimen N-F failed by debonding of concrete and longitudinal steels at the ends. Specimens RF-F and CF-F failed by huge deflections, which resulted from a very big crack width and long cracks in the tension region between CFRP rings at the midspan and at the ends of the beams, respectively. The load-midspan deflection diagrams of Specimens RF-F and CF-F are divided into two stages with two different slopes of the diagram as mentioned in the concentric behavior. The same behavior of Specimen CS-F was observed when it failed, but one steel strap ruptured at the biggest crack near the ends. All confinement specimens took a long way to reach the ultimate load, which denotes that their ductility was very high.

Table 5. Results of Specimens in Flexural Tests

Specimens	N-F	RF-F	CF-F	CS-F
Yield load (kN)	74	108	149	160
Corresponding midspan deflection (mm)	2.34	4.82	4.78	5.94
Ultimate load (kN)	81	158	254	160
Corresponding midspan deflection (mm)	3.48	35.75	30.4	5.94
Ductility (Method 1)[a]	2.34	8.41	9.54	3.57

[a]See the "Ductility" section for the definition of the methods.

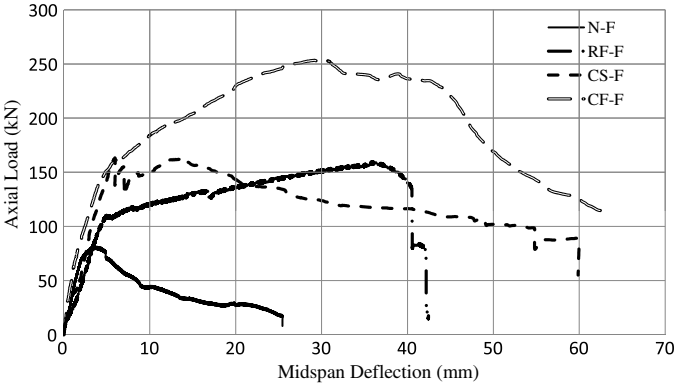

Fig. 12. Load-midspan deflection diagram for specimens under flexural tests

J. Compos. Constr. 2013.17:229-238.

Analysis and Discussion

The nominal average axial stress of the specimens under concentric load was calculated by dividing the axial load by the cross-sectional area of the specimens. The axial stress-strain curves are presented in Fig. 13. The slope of the postpeak curve of Specimen CF-0 is higher than that of Specimen RF-0. Thus, it can be seen that the most effective confinement occurred in Specimen CF-0, followed by Specimen RF-0. No confinement effect could be found in Specimen CS-0. All the results of this study were plotted in the same axial load-bending moment diagrams to clarify the effective confinement of these methods as shown in Fig. 12. The confinement efficiency was compared with the corresponding value of Group N. In case of Groups CF and CS, the concrete of covers and core columns worked together until failure. No debonding between core square columns and segmental circular concrete covers was found.

To evaluate the efficiency of these methods, Table 6 and Fig. 14 reveal that Groups RF and CF show the same trend, for which the increment of the columns' capacity under concentric load is 63% higher than that of both eccentric load and flexural behavior. It can be concluded that CFRP confinement is beneficial for concentrically loaded specimens. For instance, the highest increase of ultimate load is 402% for Specimen CF-0. Table 6 also shows that the efficacy of Group CF is two times higher than Group RF. Compared with the corresponding columns of Group N, furthermore, the columns of Group CS depict the same efficiency for concentric, eccentric load, and flexural behavior, which is approximately 70% of the capacity increases. In other words, the relative ineffective confinement of Group CS may have been caused by the confinement ratio (f_l/f'_{co}), which was approximately 0.05 < 0.08 according to ACI 440.2R-08 (ACI 2008).

Theoretical Verification

The aforementioned confinement models were adopted to carry out the interaction diagrams, which were used to verify the experimental results. The *P–M* diagram of circular-section specimen is calculated by two methods, which are the equivalent method and the small strips method. For the equivalent method, the compressive force in the compression zone of concrete can be represented by a force placed at the centroid, which is calculated using Eqs. (15) and (16). In addition, the small strips method divides the section into many small strips and the compressive stress of concrete is calculated using Eq. (6).

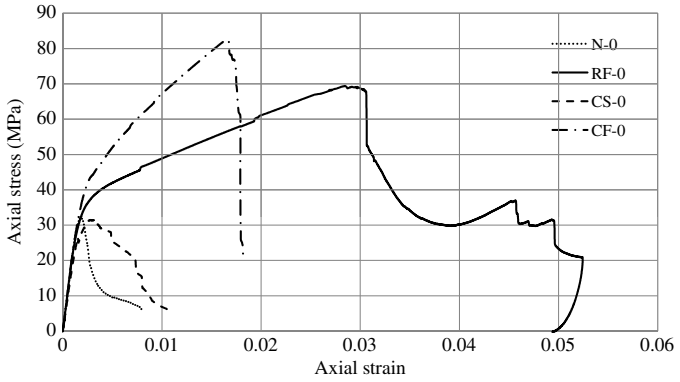

Fig. 13. Axial stress-strain diagrams for concentric loading tests

Table 6. Summary of Confinement Efficiency

Group	Load/increment	$e = 0$	$e = 15$	$e = 25$	Flexural
N	Applied load (kN)	724	579	427	89
RF	Applied load (kN)	1,562	686	562	131
	Increment (%)	216	118	132	147
CF	Applied load (kN)	2,907	1,490	1,171	254
	Increment (%)	402	257	274	285
CS	Applied load (kN)	1,116	917	766	163
	Increment (%)	154	158	179	183

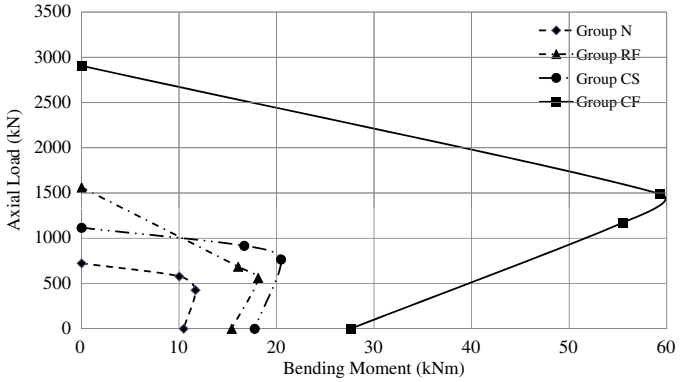

Fig. 14. Experimental *P–M* diagrams

The effect of the eccentricity on the axial load of Group CF is much more sensitive than Group CS. When the applied load changes from a concentric load to an eccentric one of 15 mm, the decrease of the axial load of Group CF is 48% (from 2,907 to 1,490 kN) compared with 19% (from 1,160 to 945 kN) of Group CS (see Fig. 15). Besides, this strengthening method is very effective for Group RF under concentric load (see Fig. 16).

In order to calculate the *P–M* diagram of Group RF, the actual strain of CFRP that was obtained from the strain gauges attached on the surface of CFRP was used. In such a case, the coefficient k_e in Eq. (2) was set to 1. For concentric loading, Specimen RF-0 was damaged by rupture of CFRP, while Specimens RF-15 and RF-25 failed by crushing of concrete. Therefore, the strain of CFRP of these specimens obtained (0.0071 and 0.0053 for Specimens RF-15 and RF-25, respectively) from the actual reading of strain gauges is used to estimate the actual strength of CFRP. Fig. 16 compares the experimental and analytical values of Groups N and RF, which have the similar cross-sectional areas. In Fig. 16, there is a considerable gap (29.4%) between the theoretical analysis and the experimental values for Group RF.

During the test period, standard 100-mm cylinders were tested to check the actual compressive strength of concrete. The average

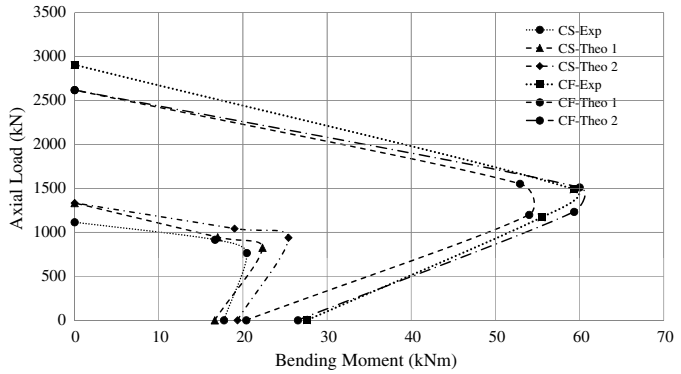

Fig. 15. Comparison of theoretical and experimental *P–M* diagrams (Groups CF and CS)

J. Compos. Constr. 2013.17:229-238.

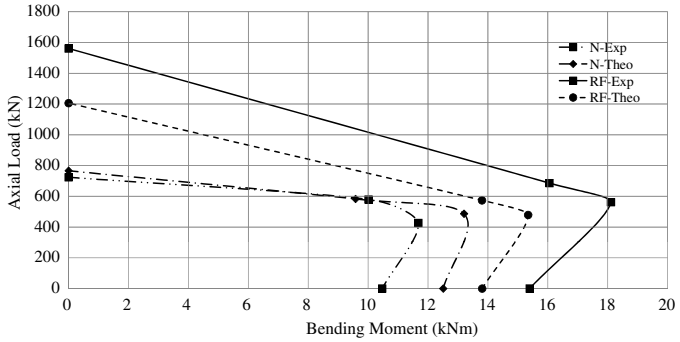

Fig. 16. Comparison of theoretical and experimental *P–M* diagrams (Groups N and RF)

compressive strength of cylinders was 43 MPa, which can be verified by tracing it to the actual axial load of Specimen CF-0. A review of the *P–M* diagrams of Groups CF and CS reveals comparable experimental and analytical results with only a 10% difference. Two different methods were employed to draw *P–M* diagrams for the circular specimens in this paper. Fig. 15 indicates that the second analytical method emulates the experimental results closer than the first analytical method. However, the first analytical method results in a graph, which is similar to that of the experimental results.

Conclusions

From the experimental results and the theoretical analyses, the following conclusions can be drawn:

1. Strengthening a column with segmental circular concrete covers and wrapping with CFRP as in Group CF is successful. The experiments indicate that the whole section of the specimen acts as a whole until failure (no debonding). The whole modified section was strengthened by the confinement materials.
2. All confined specimens showed higher load-carrying capacity compared with the unconfined specimens. Among the three groups that were externally confined, Group CF achieved the highest load-carrying capacity followed by Group CS. This enhancement is mainly because the segmental circular concrete covers considerably increase the cross-sectional area of the specimens.
3. Group CF significantly outperformed Groups CS and RF. The main reason for the outstanding performance is largely due to the reduction of stress concentration in the corners of square specimens by bonding segmental circular concrete covers. The bonding of segmental circular concrete covers significantly increases the confinement efficacy and thus the load-carrying capacity.
4. For CFRP-confined specimens in Groups RF and CF, the descending branch of the load-deflection diagrams after ultimate load can be witnessed for eccentric loading tests, while the ascending branch was achieved from concentrically loaded specimens. This phenomenon indicates that eccentricity decreases the confinement efficiency of CFRP.
5. The procedure used to calculate the interaction diagram provides satisfactory estimates of the ultimate load and of the bending moment of reinforced circular concrete specimens confined with CFRP and steel straps.

Finally, the idea of modifying the cross-sectional area from a square to a circle by the circularization process proved to be effective in maximizing the load-carrying capacity of the CFRP-confined concrete columns. It is evident that the efficiency of the CFRP confinement of the circularized columns was higher than that of the columns with round corners. This method can be considered as an effective and efficient method in strengthening columns in existing buildings and bridges.

Acknowledgments

The authors would like to acknowledge Ph.D. Scholar Mr. Ida Bagus Rai Widiarsa, who designed the loading heads that were used in the experimental program, and Mr. Frank Crabtree, technical officer at the High Bay Laboratory, who constructed the loading heads. Furthermore, the contribution of Mr. Fernando Escribano, the main technical officer of this study, is appreciated. Finally, the second author would like to acknowledge the Vietnamese Government for the support of his full Ph.D. scholarship.

References

Al-Salloum, Y. A. (2007). "Influence of edge sharpness on the strength of square concrete columns confined with FRP composite laminates." *Compos., Part B*, 38(5–6), 640–650.

American Concrete Institute (ACI). (2008). "Guide for the design and construction of externally bonded FRP systems for strengthening concrete structures." *440.2R-08*, Farmington Hills, MI.

ASTM. (2007). "Standard specification for strapping, flat steel and seals." *D3953:2007*, West Conshohocken, PA.

ASTM. (2008). "Standard test method for tensile properties of polymer matrix composite materials." *3039:2008*, West Conshohocken, PA.

ASTM. (2010). "Standard test methods for determining tensile properties of fiber reinforced polymer matrix composites used for strengthening civil structures." *D7565:2010*, West Conshohocken, PA.

Australian Standard (AS). (2007). "Metallic materials—Tensile testing at ambient temperature." *1391:2007*, Sydney, NSW, Australia.

Australian Standard (AS). (2009). "Concrete structures." *3600:2009*, Sydney, NSW, Australia.

Blackwoods. (2012). "TOOL BAND-IT C001 (0426501)." ⟨http://www.blackwoods.com.au/PartDetail.aspx?part_no=04246501⟩ (Jun. 15, 2012).

Csuka, B., and Kollár, L. P. (2012). "Analysis of FRP confined columns under eccentric loading." *Compos. Struct.*, 94(3), 1106–1116.

Hadi, M. N. S. (2006a). "Behaviour of FRP wrapped normal strength concrete columns under eccentric loading." *Compos. Struct.*, 72(4), 503–511.

Hadi, M. N. S. (2006b). "Comparative study of eccentrically loaded FRP wrapped columns." *Compos. Struct.*, 74(2), 127–135.

Hadi, M. N. S. (2007a). "Behaviour of FRP strengthened concrete columns under eccentric compression loading." *Compos. Struct.*, 77(1), 92–96.

Hadi, M. N. S. (2007b). "The behaviour of FRP wrapped HSC columns under different eccentric loads." *Compos. Struct.*, 78(4), 560–566.

Hadi, M. N. S. (2009). "Behaviour of eccentric loading of FRP confined fibre steel reinforced concrete columns." *Constr. Build. Mater.*, 23(2), 1102–1108.

Hadi, M. N. S., and Li, J. (2004). "External reinforcement of high strength concrete columns." *Compos. Struct.*, 65(3–4), 279–287.

Hadi, M. N. S., and Widiarsa, I. B. R. (2012). "Axial and flexural performance of square RC columns wrapped with CFRP under eccentric loading." *J. Compos. Constr.*, 16(6), 640–649.

Harries, K. A., and Carey, S. A. (2003). "Shape and "gap" effects on the behavior of variably confined concrete." *Cem. Concr. Res.*, 33(6), 881–890.

Kent, D. C., and Park, R. (1971). "Flexural members with confined concrete." *J. Struct. Div.*, 97(ST7), 1969–1990.

J. Compos. Constr. 2013.17:229-238.

Lam, L., and Teng, J. G. (2003). "Design-oriented stress-strain model for FRP-confined concrete." *Constr. Build. Mater.*, 17(6–7), 471–489.

Li, J., and Hadi, M. N. S. (2003). "Behaviour of externally confined high-strength concrete columns under eccentric loading." *Compos. Struct.*, 62(2), 145–153.

Mander, J. B., Park, R., and Priestley, M. J. N. (1988). "Theoretical stress-strain model for confined concrete." *J. Struct. Eng.*, 114(8), 1804–1826.

Pessiki, S., and Pieroni, A. (1997). "Axial load behavior of large-scale spirally-reinforced high-strength concrete columns." *ACI Struct. J.*, 94(3), 304–314.

Popovics, S. (1973). "Numerical approach to the complete stress-strain curve of concrete." *Cem. Concr. Res.*, 3(5), 583–599.

West System. (2012). "Epoxy resins and hardeners—Physical properties." ⟨http://www.westsystem.com/ss/typical-physical-properties⟩ (Jun. 15, 2012).

Wu, Y. F., and Zhou, Y. W. (2010). "Unified strength model based on Hoek-Brown failure criterion for circular and square concrete columns confined by FRP." *J. Compos. Constr.*, 14(2), 175–184.

Yazici, V., and Hadi, M. N. S. (2009). "Axial load-bending moment diagrams of carbon FRP wrapped hollow core reinforced concrete columns." *J. Compos. Constr.*, 13(4), 262–268.

6.2 Circularizing by High Strength Concrete

Summary

A technique called circularization where segmental circular concrete covers made of different concrete strengths (40 MPa, 80 MPa and 100 MPa) was used to change a square column to a circular column. The applicability of the circularization method was experimentally studied for a wide range of concrete strengths (from 40 MPa to 100 MPa). The behaviour of the strengthened specimens under different loading conditions including concentric loading, eccentric loading (25 mm and 50 mm) and flexural bending was investigated. The experimental results demonstrate that using high strength concrete (HSC) for the additional covers to strengthen existing square reinforced concrete (RC) columns provides higher load-carrying capacity than covers made of normal strength concrete. The HSC covers and the concrete cores worked as a composite material to failure. The FRP strain at peak load was observed for the purpose of estimating the specimens' capacity. The distribution of FRP strain around the circumference of the column section was also reported.

Citation

This paper was published in Construction and Building Materials with the following citation:

Pham, T.M., Doan, L.V., and Hadi, M.N.S. (2013). "Strengthening square reinforced concrete columns by circularization and FRP confinement." *Construction and Building Materials*, 49(0), 490-499.

7 CONCLUSIONS

7.1 Introduction

The confinement mechanism of FRP-confined concrete columns has been investigated in this study. A few models were proposed to predict the compressive strength and strain of confined concrete. These models were made to provide a better understanding of the confinement mechanism and more accurate predictions than existing models. Additionally, a new practical method was introduced to strengthen existing square reinforced concrete columns by circularisation and FRP confinement. From the results of the theoretical and experimental studies, some conclusions are drawn in the sections below.

7.2 FRP-confined Circular Columns

The confinement mechanism of FRP-confined circular concrete columns has been investigated in this study. Based on the experimental results in the literature, the effect of the jacket stiffness has been demonstrated and confirmed. The proposed model for FRP-confined circular normal- and high-strength concrete shows good performance. From the results of this study, some concluding remarks can be made as follows:

a. In order to calculate the compressive strength of FRP-confined circular columns, the ratio between the FRP thickness and the column diameter should be taken into account. When this parameter is considered, only a unified equation is used to calculate the compressive strength of confined concrete with varied FRP types, which have significant difference in the jacket stiffness.

b. The proposed strength model could estimate the compressive strength of confined concrete with unconfined concrete strength ranging between 15 MPa and 170 MPa.

c. The relationship between the energy absorption of the column and the energy absorbed by the jacket is developed. This relationship showed that only a portion of the energy absorbed by the column is transferred to rupture the FRP jacket.

d. This study confirms that using energy method could estimate well the compressive strain of FRP-confined concrete as compared to experimental results. The applicability of the energy-based strain model covers seven types of FRP.

7.3 FRP-confined Rectangular/Square Columns

The stress concentration at the four corners of the columns' section has been analysed and discussed. This study assumed that the confining stress is transmitted to the concrete at the four corners of the section. The proposed models to calculate the compressive strength and strain of FRP-confined rectangular or square concrete columns show good correlation with the experimental results. Based on the proposed models and discussions, the following conclusions are drawn:

a. The "membrane hypothesis" was utilized to analyse the behaviour of FRP-confined rectangular columns. The confining pressure of confined columns is concentrated at the corners of the section. In order to comply with the "membrane hypothesis", the corners of the sections should be rounded to have a radius being at least twenty times greater than the nominal FRP thickness.

b. A new ratio reflecting the non-uniform confining pressure was proposed, which is the ratio of the corners and the perimeter of the whole section. This ratio is different from the common shape factor that simulates a similar sense.

c. The corner effect ratio (k_c) accounts for the effects of the non-uniform confining pressure around rectangular sections. It was used to distribute equally the confining pressure at corners of rectangular sections to the whole circumference of the sections.

d. The actual rupture strain of FRP at corners of the sections depends on the ratio of the corner radius and the length of the shorter side in addition to the confinement stiffness ratio. An equation was proposed to calculate the actual rupture strain of FRP.

e. A greater corner radius of a rectangular or square section provides double benefits. This greater corner radius firstly increases the corner effect ratio,

which means that the confinement effect is improved. Secondly, the greater corner radius results in higher rupture strain of the FRP jacket.

f. The limit of FRP amount to obtain sufficient confinement was proposed. This limit is based not only on the ratio of the corner radius and the length of the shorter side but also the confinement stiffness ratio.

7.4 Application of ANN

ANN has been used to predict the compressive strength and strain of FRP-confined rectangular or square columns. The performance of the proposed ANN-based models is excellent as compared to other existing models. In addition, this study uses ANN not only to calculate the compressive strength and strain but also to generate simple-form equations from a trained ANN. The subsequent conclusions were drawn based on the proposed models and discussions:

a. The accuracy of the proposed ANN-based models significantly increases as compared to other existing models. The average absolute error (AAE) of the proposed ANN-based models is approximately 5% while the AAE of other existing models is around 10% and 30% for strength models and strain models, respectively.

b. A new method was proposed to generate predictive simple-form equations from trained ANN-based models. The proposed simple equations predict the compressive strength and strain with small errors as compared to other models.

c. From the results of ANN-based models, the corner radius of the section significantly affects the compressive strength but marginally affects the compressive strain of FRP-confined rectangular or square concrete columns.

7.5 Maximum Usable Strain of FRP-Confined Concrete

The progressive failure of FRP-confined concrete was investigated based on the failure of the concrete cores. The residual strengths of the concrete cores were determined experimentally and theoretically at many axial strain levels. The findings are summarized as follows:

a. The residual strengths of the concrete cores were reduced more than 56% at the axial strain 1% of FRP-confined concrete.

b. A model was proposed to estimate the residual strength of the concrete cores of a FRP-confined concrete column at a certain axial strain.

c. The maximum usable strain of FRP-confined concrete is much smaller than the value of 1% proposed by ACI 440-2R (2008).

7.6 Circularization Technique

A practical technique, namely circularization technique, was introduced to strengthen existing square reinforced concrete columns. The square columns were circularised and then wrapped with a number of FRP layers to improve its axial capacity. The applicability of the proposed technique was verified with two types of confinement materials including FRP jacket and steel straps. The use of normal strength concrete and high strength concrete is also verified. From the experimental results and discussions, the following concluding remarks are drawn:

a. Strengthening a column with segmental circular concrete covers and wrapping with CFRP is successful. The experiments indicate that the whole section of the specimen acts as a whole until failure (no debonding). The whole modified section was strengthened by the confinement materials.

b. The columns circularised and wrapped with FRP significantly outperformed the square columns wrapped with FRP. The main reason for the outstanding performance is largely due to the reduction of stress concentration at the corners of square specimens by bonding segmental circular concrete covers. The bonding of segmental circular concrete covers significantly increases the confinement efficacy and thus the load carrying capacity.

c. For CFRP-confined specimens, the descending branch of the load – axial deflection diagrams after ultimate load can be witnessed for eccentric loading tests while the ascending branch was achieved from concentrically loaded specimens. This phenomenon indicates that eccentricity decreases the confinement efficiency of CFRP.

d. The procedure used to calculate the interaction diagram provides satisfactory estimates of the ultimate load and of the bending moment of reinforced circular concrete specimens confined with CFRP and steel straps.

e. Two concrete components including the original concrete core and the additional concrete covers worked as a composite material to failure under pure axial load, flexure, and eccentric loads. The bonding of two components observed after testing was perfect bond. Thus, it is concluded that the proposed technique is able to improve the capacity of a noncircular column.

f. The ductility of the strengthened columns significantly increased compared to the reference columns since FRP has the same full confinement effect on the tested columns as on a conventional original circular column.

g. The applicability of the proposed technique was verified by a variety of concrete strength up to 100 MPa. The experiments demonstrated that this technique could be used for not only normal strength concrete but also high strength concrete. Bonding high strength concrete covers to the column core with low concrete strength was successfully confirmed.

h. The FRP strain was recorded during the loading process. The rupture strain of FRP on the concentrically loaded columns was around 0.7 of the ultimate strain from flat coupon tests. The FRP strain at the peak load of the eccentrically loaded columns was much smaller than the rupture strain at the ultimate load. The measured FRP strain at the peak load was approximately 0.34 of the ultimate strain from flat coupon tests. This value should be used to estimate the capacity of a FRP-confined concrete column under eccentric loads.

7.7 Further Research

Based on the conclusions of this study, the following future research areas are recommended:

a. For FRP-confined circular columns, the behaviour of specimens under concentric loads has been extensively examined but not that under eccentric loads. Thus the behaviour of specimens under eccentric loads needs to be

investigated, specially, the distribution of the FRP jacket around the perimeter of the section.

b. For FRP-confined rectangular or square columns, the actual rupture strain of the FRP jacket that depends on the jacket thickness, the corner radius, and the unconfined concrete strength need to be examined.

c. For FRP-confined concrete, more studies should focus on predicting the axial strain of the confined concrete in order to improve the accuracy of existing strain models.

REFERENCES

ACI 318-11 (2011). *Building Code Requirements for Structural Concrete and Commentary*. Farmington Hills, Michigan, USA, American Concrete Institute (ACI).

ACI 440.2R-08. (2008). "Guide for the Design and Construction of Externally Bonded FRP Systems for Strengthening Concrete Structures." *440.2R-08*, Farmington Hills, MI.

Adeli, H., and Park, H.S. (1995). "Counterpropagation neural networks in structural engineering." *Journal of structural engineering-ASCE*, 121(8), 1205-1212.

Ahmad, S.H., Khaloo, A.R., and Irshaid, A. (1991). "Behavior of Concrete Spirally Condined by Fiberglass Filaments." *Magazine of Concrete Research*, 43(156), 143-148.

Aire, C., Gettu, R., Casas, J.R., Marques, S., and Marques, D. (2010). "Concrete laterally confined with fibre-reinforced polymers (FRP): experimental study and theoretical model." *Materiales de Construccion*, 60(297), 19-31.

Al-Salloum, Y.A. (2007). "Influence of edge sharpness on the strength of square concrete columns confined with FRP composite laminates." *Composites Part B: Engineering*, 38(5), 640-650.

Almusallam, T.H. (2007). "Behavior of normal and high-strength concrete cylinders confined with E-glass/epoxy composite laminates." *Composites Part B: Engineering*, 38(5), 629-639.

American Concrete Institute (ACI). (2002). "Guide for the design and construction of externally bonded FRP systems for strengthening concrete structures." *440.2R-02*, Farmington Hills, MI.

ASTM. (2010). "Standard test method for tensile properties of fiber reinforced polymer matrix composites used for strengthening of civil structures." *D7565:2010*, West Conshohocken, PA.

Au, C., and Buyukozturk, O. (2005). "Effect of fiber orientation and ply mix on fiber reinforced polymer-confined concrete." *Journal of Composites for Construction*, 9(5), 397-407.

Australian Standard-1545. (1976). "Methods for the Calibration and Grading of Extenometers." *1545-1976*, Homebush, NSW 2140.

Australian Standard (AS). (2009). "Concrete structures." *3600:2009*, Sydney, NSW, Australia.

Bakis, C.E., Bank, L.C., Brown, V.L., Cosenza, E., Davalos, J.F., Lesko, J.J., Machida, A., Rizkalla, S.H., and Triantafillou, T.C. (2002). "Fiber-Reinforced Polymer Composites for Construction---State-of-the-Art Review." *Journal of Composites for Construction*, 6(2), 73-87.

Bank, L.C. (2006). *Composites for construction: structural design with FRP materials*. Hoboken, N.J, John Wiley & Sons.

Bank, L.C. (2013). "Progressive Failure and Ductility of FRP Composites for Construction: Review." *Journal of Composites for Construction*, 17(3), 406-419.

Benzaid, R., Mesbah, H., and Chikh, N.E. (2010). "FRP-confined Concrete Cylinders: Axial Compression Experiments and Strength Model." *Journal of Reinforced Plastics and Composites,* 29(16), 2469-2488.

Berthet, J.F., Ferrier, E., and Hamelin, P. (2005). "Compressive behavior of concrete externally confined by composite jackets. Part A: experimental study." *Construction and Building Materials,* 19(3), 223-232.

Berthet, J.F., Ferrier, E., and Hamelin, P. (2006). "Compressive behavior of concrete externally confined by composite jackets: Part B: modeling." *Construction and Building Materials,* 20(5), 338-347.

Bisby, L.A., Dent, A.J.S., and Green, M.F. (2005). "Comparison of confinement models for fiber-reinforced polymer-wrapped concrete." *ACI Structural Journal,* 102(1), 62-72.

Calladine, C.R. (1983). *Theory of shell structures*. Cambridge, Cambridge University Press.

Carey, S.A., and Harries, K.A. (2005). "Axial Behavior and Modeling of Confined Small-, Medium-, and Large-Scale Circular Sections with Carbon Fiber-Reinforced Polymer Jackets." *ACI Structural Journal,* 102(4), 596-596.

Chaallal, O., Hassan, M., and Shahawy, M. (2003a). "Confinement model for axially loaded short rectangular columns strengthened with fiber-reinforced polymer wrapping." *ACI Structural Journal,* 100(2), 215-221.

Chaallal, O., Shahawy, M., and Hassan, M. (2003b). "Performance of axially loaded short rectangular columns strengthened with carbon fiber-reinforced polymer wrapping." *Journal of Composites for Construction,* 7(3), 200-208.

Chen, H.M., Tsai, K.H., Qi, G.Z., Yang, J.C.S., and Amini, F. (1995). "Neural-network for structural control." *Journal of Computing in Civil Engineering,* 9(2), 168-176.

Concrete Society (2012). *Design guidance for strengthening concrete structures using fibre composite materials*. Camberley, Concrete Society.

Csuka, B., and Kollár, L.P. (2012). "Analysis of FRP confined columns under eccentric loading." *Composite Structures,* 94(3), 1106-1116.

Cui, C., and Sheikh, S.A. (2010a). "Analytical Model for Circular Normal- and High-Strength Concrete Columns Confined with FRP." *Journal of Composites for Construction,* 14(5), 562-572.

Cui, C., and Sheikh, S.A. (2010b). "Experimental Study of Normal- and High-Strength Concrete Confined with Fiber-Reinforced Polymers." *Journal of Composites for Construction,* 14(5), 553-561.

Cusson, D., and Paultre, P. (1995). "Stress-Strain Model for Confined High-Strength Concrete." *Journal of Structural Engineering,* 121(3), 468-477.

De Lorenzis, L., and Tepfers, R. (2003). "Comparative Study of Models on Confinement of Concrete Cylinders with Fiber-Reinforced Polymer Composites." *Journal of Composites for Construction,* 7(3), 219-237.

Doan, L.V., Lei, X., Pham, T.M., and Hadi, M.N.S. (2013). Confinement Effect of FRP and Transverse Steel on Retrofitting Square Concrete Columns. *The 4th Asia-Pacific Conference on FRP in Structures* (1-6), Melbourne, Victoria, Australia.

Eid, R., Roy, N., and Paultre, P. (2009). "Normal- and High-Strength Concrete Circular Elements Wrapped with FRP Composites." *Journal of Composites for Construction,* 13(2), 113-124.

Elkordy, M.F., Chang, K.C., and Lee, G.C. (1993). "Neural Networks Trained by Analytically Simulated Damage States." *Journal of Computing in Civil Engineering,* 7(2), 130-145.

Flood, I., and Kartam, N. (1994). "Neural Networks in Civil Engineering. I: Principles and Understanding." *Journal of Computing in Civil Engineering,* 8(2), 131-148.

Green, M.F., Bisby, L.A., Fam, A.Z., and Kodur, V.K.R. (2006). "FRP confined concrete columns: Behaviour under extreme conditions." *Cement and Concrete Composites,* 28(10), 928-937.

Hadi, M.N.S. (2003). "Neural networks applications in concrete structures." *Computers & Structures,* 81(6), 373-381.

Hadi, M.N.S. (2006a). "Behaviour of FRP wrapped normal strength concrete columns under eccentric loading." *Composite Structures,* 72(4), 503-511.

Hadi, M.N.S. (2006b). "Comparative study of eccentrically loaded FRP wrapped columns." *Composite Structures,* 74(2), 127-135.

Hadi, M.N.S. (2007a). "Behaviour of FRP strengthened concrete columns under eccentric compression loading." *Composite Structures,* 77(1), 92-96.

Hadi, M.N.S. (2007b). "The behaviour of FRP wrapped HSC columns under different eccentric loads." *Composite Structures,* 78(4), 560-566.

Hadi, M.N.S. (2009). "Behaviour of eccentric loading of FRP confined fibre steel reinforced concrete columns." *Construction and Building Materials,* 23(2), 1102-1108.

Hadi, M.N.S., and Li, J. (2004). "External reinforcement of high strength concrete columns." *Composite Structures,* 65(3-4), 279-287.

Hadi, M.N.S., Pham, T.M., and Lei, X. (2013). "New Method of Strengthening Reinforced Concrete Square Columns by Circularizing and Wrapping with Fiber-Reinforced Polymer or Steel Straps." *Journal of Composites for Construction,* 17(2), 229-238.

Hadi, M.N.S., and Widiarsa, I.B.R. (2012). "Axial and Flexural Performance of Square RC Columns Wrapped with CFRP under Eccentric Loading." *Journal of Composites for Construction,* 16(6), 640-649.

Hajela, P., and Berke, L. (1991). "Neurobiological computational models in structural analysis and design." *Computers and Structures,* 41(4), 657-667.

Harajli, M.H., Hantouche, E., and Soudki, K. (2006). "Stress-strain model for fiber-reinforced polymer jacketed concrete columns." *ACI Structural Journal,* 103(5), 672-682.

Harries, K.A., and Carey, S.A. (2003). "Shape and “gap” effects on the behavior of variably confined concrete." *Cement and Concrete Research,* 33(6), 881-890.

Hoek, E., and Brown, E.T. (1980). "Empirical Strength Criterion for Rock Masses." *Journal of the Geotechnical Engineering Division,* 106(Compendex), 1013-1035.

Hornik, K., Stinchcombe, M., and White, H. (1989). "Multilayer feedforward networks are universal approximators." *Neural Networks,* 2(5), 359-366.

Ilki, A., and Kumbasar, N. (2003). "Compressive behaviour of carbon fibre composite jacketed concrete with circular and non-circular cross-sections." *Journal of earthquake Engineering,* 7(3), 381-406.

Ilki, A., Peker, O., Karamuk, E., Demir, C., and Kumbasar, N. (2008). "FRP retrofit of low and medium strength circular and rectangular reinforced concrete columns." *Journal of Materials in Civil Engineering,* 20(2), 169-188.

Jalal, M., and Ramezanianpour, A.A. (2012). "Strength enhancement modeling of concrete cylinders confined with CFRP composites using artificial neural networks." *Composites Part B: Engineering,* 43(8), 2990-3000.

Jiang, T., and Teng, J.G. (2007). "Analysis-oriented stress-strain models for FRP-confined concrete." *Engineering Structures,* 29(11), 2968-2986.

Karabinis, A., Rousakis, T., and Manolitsi, G. (2008). "3D Finite-Element Analysis of Substandard RC Columns Strengthened by Fiber-Reinforced Polymer Sheets." *Journal of Composites for Construction,* 12(5), 531-540.

Karabinis, A.I., and Rousakis, T.C. (2002). "Concrete confined by FRP material: a plasticity approach." *Engineering Structures,* 24(7), 923-932.

Karbhari, V.M., and Gao, Y. (1997). "Composite Jacketed Concrete under Uniaxial Compression Verification of Simple Design Equations." *Journal of Materials in Civil Engineering,* 9(4), 185-193.

Kent, D.C., and Park, R. (1971). "Flexural Members with Confined Concrete." *Proceedings, ASCE,* 97(ST7), 1969-1990.

Khalili, H.H., and Fardis, M.N. (1982). "FRP-encased concrete as a structural material." *Magazine of Concrete Research,* 34(121), 191-202.

Kim, Y.Y., Kapania, R.K., Johnson, E.R., Palmer, M.E., Kwon, T.K., Hong, C.U., and Kim, N.G. (2006). "Dynamic analysis and structural optimization of a fiber optic sensor using neural networks." *Journal of Mechanical Science and Technology,* 20(2), 251-261.

Lam, L., and Teng, J.G. (2003a). "Design-oriented stress-strain model for FRP-confined concrete." *Construction and Building Materials,* 17(6-7), 471-489.

Lam, L., and Teng, J.G. (2003b). "Design-oriented stress-strain model for FRP-confined concrete in rectangular columns." *Journal of Reinforced Plastics and Composites,* 22(13), 1149-1186.

Lam, L., and Teng, J.G. (2004). "Ultimate condition of fiber reinforced polymer-confined concrete." *Journal of Composites for Construction,* 8(6), 539-548.

Lam, L., and Teng, J.G. (2009). "Stress–strain model for FRP-confined concrete under cyclic axial compression." *Engineering Structures,* 31(2), 308-321.

Lam, L., Teng, J.G., Cheung, C.H., and Xiao, Y. (2006). "FRP-confined concrete under axial cyclic compression." *Cement and Concrete Composites,* 28(10), 949-958.

Lee, C.-S., Hegemier, G.A., and Phillippi, D.J. (2010a). "Analytical Model for Fiber-Reinforced Polymer-Jacketed Square Concrete Columns in Axial Compression." *ACI Structural Journal,* 107(2), 208-208-217.

Lee, C.S., and Hegemier, G.A. (2009). "Model of FRP-Confined Concrete Cylinders in Axial Compression." *Journal of Composites for Construction,* 13(5), 442-454.

Lee, J., Y., Yi, C., K., Jeong, H., S., Kim, S., W., and Kim, J., K. (2010b). "Compressive Response of Concrete Confined with Steel Spirals and FRP Composites." *Journal of Composite Materials,* 44(4), 481-504.

Lei, X., Pham, T.M., and Hadi, M.N.S. (2012a). Behaviour of CFRP wrapped square RC columns under eccentric loading. *Australasian Structural Engineering Conference* (pp. 1-8), Australia: Engineers Australia.

Lei, X., Pham, T.M., and Hadi, M.N.S. (2012b). Comparative behaviour of FRP confined square concrete columns under eccentric loading. *6th International Conference on Bridge Maintenance, Safety and Management, IABMAS 2012* (pp. 1207-1214), The Netherlands: CRC Press/Balkema.

Li, J., and Hadi, M.N.S. (2003). "Behaviour of externally confined high-strength concrete columns under eccentric loading." *Composite Structures,* 62(2), 145-153.

Li, Y.-F., Lin, C.-T., and Sung, Y.-Y. (2003). "A constitutive model for concrete confined with carbon fiber reinforced plastics." *Mechanics of Materials,* 35(3), 603-619.

Lim, J.C., and Ozbakkaloglu, T. (2014). "Confinement Model for FRP-Confined High-Strength Concrete." *Journal of Composites for Construction,* doi:10.1061/(ASCE)CC.1943-5614.0000376.

Lin, H.-J., and Liao, C.-I. (2004). "Compressive strength of reinforced concrete column confined by composite material." *Composite Structures,* 65(2), 239-250.

Lin, H., J., and Chen, C., T. (2001). "Strength of Concrete Cylinder Confined by Composite Materials." *Journal of Reinforced Plastics and Composites,* 20(18), 1577-1600.

Lu, G., and Yu, T.X. (2003). *Energy absorption of structures and materials*. Boca Raton, Woodhead Publishing.

MacGregor, J.G. (2005). *Reinforced concrete: mechanics and design*. Upper Saddle River, N.J, Prentice Hall.

Mandal, S., Hoskin, A., and Fam, A. (2005). "Influence of concrete strength on confinement effectiveness of fiber-reinforced polymer circular jackets." *ACI Structural Journal,* 102(3), 383-392.

Mander, J.B., Park, R., and Priestley, M.J.N. (1988). "Theoretical Stress-Strain Model for Confined Concrete." *Journal of Structural Engineering,* 114(8), 1804-1826.

Masia, M.J., Gale, T.N., and Shrive, N.G. (2004). "Size effects in axially loaded square-section concrete prisms strengthened using carbon fibre reinforced polymer wrapping." *Canadian Journal of Civil Engineering,* 31(1), 1-1.

Masri, S.F., Chassiakos, A.G., and Caughey, T.K. (1992). "Structure-unknown non-linear dynamic systems: identification through neural networks." *Smart Materials and Structures*, 1(Journal Article), 45.

MATLAB, R2012b. The Math Works, Inc.: Natick, MA.

Matthys, S., Toutanji, H., Audenaert, K., and Taerwe, L. (2005). "Axial load behavior of large-scale columns confined with fiber-reinforced polymer composites." *ACI Structural Journal*, 102(2), 258-267.

Matthys, S., Toutanji, H., and Taerwe, L. (2006). "Stress-strain behavior of large-scale circular columns confined with FRP composites." *Journal of Structural Engineering*, 132(1), 123-133.

Mirmiran, A., Shahawy, M., Samaan, M., Echary, H.E., Mastrapa, J.C., and Pico, O. (1998). "Effect of Column Parameters on FRP-Confined Concrete." *Journal of Composites for Construction*, 2(4), 175-185.

Mirmiran, A., and Shahawy, R. (1997). "Behavior of concrete columns confined by fiber composites." *Journal of Structural Engineering*, 123(5), 583-590.

Miyauchi, K., Inoue, I., Kuroda, T., and Kobayashi, A. (1999). "Strengthening effects of concrete column with carbon fiber sheet." *Transactions of the Japan Concrete Institute*, 21, 143-150.

Naderpour, H., Kheyroddin, A., and Amiri, G.G. (2010). "Prediction of FRP-confined compressive strength of concrete using artificial neural networks." *Composite Structures*, 92(12), 2817-2829.

Nanni, A., and Bradford, N.M. (1995). "FRP jacketed concrete under uniaxial compression." *Construction and Building Materials*, 9(2), 115-124.

Ozbakkaloglu, T., and Lim, J.C. (2013). "Axial compressive behavior of FRP-confined concrete: Experimental test database and a new design-oriented model." *Composites Part B: Engineering*, 55(0), 607-634.

Ozbakkaloglu, T., Lim, J.C., and Vincent, T. (2013). "FRP-confined concrete in circular sections: Review and assessment of stress–strain models." *Engineering Structures*, 49(0), 1068-1088.

Parvin, A., and Wang, W. (2001). "Behavior of FRP Jacketed Concrete Columns under Eccentric Loading." *Journal of Composites for Construction*, 5(3), 146-152.

Perera, R., Arteaga, A., and Diego, A.D. (2010a). "Artificial intelligence techniques for prediction of the capacity of RC beams strengthened in shear with external FRP reinforcement." *Composite Structures*, 92(5), 1169-1175.

Perera, R., Barchín, M., Arteaga, A., and Diego, A.D. (2010b). "Prediction of the ultimate strength of reinforced concrete beams FRP-strengthened in shear using neural networks." *Composites Part B: Engineering*, 41(4), 287-298.

Pessiki, S., Harries, K.A., Kestner, J.T., Sause, R., and Ricles, J.M. (2001). "Axial behavior of reinforced concrete columns confined with FRP jackets." *Journal of Composites for Construction*, 5(4), 237-245.

Pessiki, S., and Pieroni, A. (1997). "Axial load behavior of large-scale spirally-reinforced high-strength concrete columns." *ACI Structural Journal*, 94(3), 304-314.

Pham, T.M., Doan, L.V., and Hadi, M.N.S. (2013a). Behavior of Modified RC Columns Retrofitted with CFRP. *Understanding Concrete* (1-10), Gold Coast, Queensland, Australia.

Pham, T.M., Doan, L.V., and Hadi, M.N.S. (2013b). "Strengthening square reinforced concrete columns by circularisation and FRP confinement." *Construction and Building Materials,* 49(0), 490-499.

Pham, T.M., Doan, L.V., and Hadi, M.N.S. (2013c). Strengthening Square Reinforced Concrete Columns by Shape Modification and CFRP. *Structures Congress 2013***:** 2602-2613.

Pham, T.M., and Hadi, M.N.S. (2013a). "Predicting Stress and Strain of FRP Confined Rectangular Columns Using Artificial Neural Networks. I: Model Building." *Journal of Composites for Construction,* (Under review).

Pham, T.M., and Hadi, M.N.S. (2013b). Retrofitting square reinforced columns using FRP and precasr concrete segments. *First International Confenrence on Concrete Sustainability* (1020-1025), Tokyo, Japan.

Pham, T.M., and Hadi, M.N.S. (2013c). "Strain Estimation of CFRP Confined Concrete Columns Using Energy Approach." *Journal of Composites for Construction,* 17(6), 04013001.

Pham, T.M., and Hadi, M.N.S. (2014a). "Predicting Stress and Strain of FRP Confined Rectangular/Square Columns Using Artificial Neural Networks." *Journal of Composites for Construction,* (Accepted).

Pham, T.M., and Hadi, M.N.S. (2014b). "Stress Prediction Model for FRP Confined Rectangular Concrete Columns with Rounded Corners." *Journal of Composites for Construction,* 18(1), 04013019.

Pham, T.M., Lei, X., and Hadi, M.N.S. (2013d). Effect of eccentric load on retrofitted reinforced concrete columns confined with FRP. *22nd Australasian Conference on the Mechanics of Structures and Materials (ACMSM22)* (139-144): London: Taylor & Francis Group.

Popovics, S. (1973). "Numerical Approach to The Complete Stress-Strain Curve of Concrete." *Cement and Concrete Research,* 3(5), 583-599.

Priestley, M.J.N., and Seible, F. (1995). "Design of seismic retrofit measures for concrete and masonry structures." *Construction and Building Materials,* 9(6), 365-377.

Priestley, M.J.N., Seible, F., and Calvi, G.M. (1996). *Seismic design and retrofit of bridges*. New York, Wiley.

Richart, F.E., Brandtzaeg, A., and Brown, R.L. (1928). "A study of the failure of concrete under combined compressive stress." *Bulletin 1985, Univ. of Illinois Engineering Experimental Station, Champaign, III.*

Richart, F.E., Brandtzaeg, A., and Brown, R.L. (1929). "The failure of plain and spirally reinforced concrete in compression." *Bulletin 1990, Univ. of Illinois Engineering Experimental Station, Champaign, III.*

Rochette, P., and Labossière, P. (2000). "Axial Testing of Rectangular Column Models Confined with Composites." *Journal of Composites for Construction,* 4(3), 129-136.

Rousakis, T., and Karabinis, A. (2012). "Adequately FRP confined reinforced concrete columns under axial compressive monotonic or cyclic loading." *Materials and Structures,* 45(7), 957-975.

Rousakis, T., Rakitzis, T., and Karabinis, A. (2012a). "Design-Oriented Strength Model for FRP-Confined Concrete Members." *Journal of Composites for Construction,* 16(6), 615-625.

Rousakis, T., Rakitzis, T., and Karabinis, A. (2012b). Empirical Modelling of Failure Strains of Uniformly FRP Confined Concrete Columns. *The 6th International Conference on FRP Composites in Civil Engineering - CICE 2012*, Rome.

Rousakis, T.C., Karabinis, A.I., and Kiousis, P.D. (2007). "FRP-confined concrete members: Axial compression experiments and plasticity modelling." *Engineering Structures,* 29(7), 1343-1353.

Saadatmanesh, H., Ehsani, M.R., and Jin, L. (1997). "Seismic retrofitting of rectangular bridge columns with composite straps." *Earthquake Spectra,* 13(2), 281-304.

Saenz, N., and Pantelides, C. (2006). "Short and Medium Term Durability Evaluation of FRP-Confined Circular Concrete." *Journal of Composites for Construction,* 10(3), 244-253.

Samaan, M., Mirmiran, A., and Shahawy, M. (1998). "Model of concrete confined by fiber composites." *Journal of Structural Engineering,* 124(9), 1025-1031.

Sargin, M., Ghosh, S.K., and Handa, V.K. (1971). "Effects of lateral reinforcement upon the strength and deformation properties of concrete." *Magazine of Concrete Research,* 23(Compendex), 99-110.

Shao, Y., Zhu, Z., and Mirmiran, A. (2006). "Cyclic modeling of FRP-confined concrete with improved ductility." *Cement and Concrete Composites,* 28(10), 959-968.

Shehata, I.A.E.M., Carneiro, L.A.V., and Shehata, L.C.D. (2002). "Strength of short concrete columns confined with CFRP sheets." *Materials and Structures,* 35(1), 50-58.

Silva, M.A.G., and Rodrigues, C.C. (2006). "Size and Relative Stiffness Effects on Compressive Failure of Concrete Columns Wrapped with Glass FRP." *Journal of Materials in Civil Engineering,* 18(3), 334-342.

Smith, S.T., Kim, S.J., and Zhang, H.W. (2010). "Behavior and Effectiveness of FRP Wrap in the Confinement of Large Concrete Cylinders." *Journal of Composites for Construction,* 14(5), 573-582.

Spoelstra, M.R., and Monti, G. (1999). "FRP-Confined Concrete Model." *Journal of Composites for Construction,* 3(3), 143.

Tamuzs, V., Valdmanis, V., Tepfers, R., and Gylltoft, K. (2008). "Stability analysis of CFRP-wrapped concrete columns strengthened with external longitudinal CFRP sheets." *Mechanics of Composite Materials,* 44(3), 199-208.

Tao, Z., Yu, Q., and Zhong, Y.Z. (2008). "Compressive behaviour of CFRP-confined rectangular concrete columns." *Magazine of Concrete Research,* 60(10), 735-745.

Tasdemir, M.A., Tasdemir, C., Akyüz, S., Jefferson, A.D., Lydon, F.D., and Barr, B.I.G. (1998). "Evaluation of strains at peak stresses in concrete: A three-phase composite model approach." *Cement and Concrete Composites,* 20(4), 301-318.

Teng, J.G., Huang, Y.L., Lam, L., and Ye, L.P. (2007). "Theoretical model for fiber-reinforced polymer-confined concrete." *Journal of Composites for Construction,* 11(2), 201-210.

Teng, J.G., Jiang, T., Lam, L., and Luo, Y.Z. (2009). "Refinement of a Design-Oriented Stress-Strain Model for FRP-Confined Concrete." *Journal of Composites for Construction,* 13(4), 269-278.

Theriault, M., Neale, K.W., and Claude, S. (2004). "Fiber-Reinforced Polymer-Confined Circular Concrete Columns: Investigation of Size and Slenderness Effects." *Journal of Composites for Construction,* 8(4), 323-331.

Toutanji, H., Han, M., Gilbert, J., and Matthys, S. (2010). "Behavior of Large-Scale Rectangular Columns Confined with FRP Composites." *Journal of Composites for Construction,* 14(1), 62-71.

Toutanji, H.A. (1999). "Stress-strain characteristics of concrete columns externally confined with advanced fiber composite sheets." *ACI Materials Journal,* 96(3), 397-404.

Upadhyaya, B.R., and Eryurek, E. (1992). "Application of neural networks for sensor validation and plant monitoring." *Nuclear Technology,* 97(2), 170-176.

Valdmanis, V., De Lorenzis, L., Rousakis, T., and Tepfers, R. (2007). "Behaviour and capacity of CFRP-confined concrete cyliners subjected to monotonic and cyclic axial compressive load." *Structural Concrete,* 8(4), 187-190.

Wang, L.M., and Wu, Y.F. (2008). "Effect of corner radius on the performance of CFRP-confined square concrete columns: Test." *Engineering Structures,* 30(2), 493-505.

Wang, Z.Y., Wang, D.Y., Smith, S.T., and Lu, D.G. (2012a). "CFRP-Confined Square RC Columns. I: Experimental Investigation." *Journal of Composites for Construction,* 16(2), 150-160.

Wang, Z.Y., Wang, D.Y., Smith, S.T., and Lu, D.G. (2012b). "CFRP-Confined Square RC Columns. II: Cyclic Axial Compression Stress-Strain Model." *Journal of Composites for Construction,* 16(2), 161-170.

WEST SYSTEM n.d. (2012). "Epoxy resins and hardeners - Physical properties." <http://www.westsystem.com/ss/typical-physical-properties> (Jun. 15, 2012).

Wolff, C., Bastid, P., and Bunsell, A.R. (1994). "Relation of energy absorption of composite structures to material strength." *Composites Engineering,* 4(2), 195-218.

Wong, Y.L., Yu, T., Teng, J.G., and Dong, S.L. (2008). "Behavior of FRP-confined concrete in annular section columns." *Composites Part B: Engineering,* 39(3), 451-466.

Wu, G., Wu, Z.S., Lu, Z.T., and Ando, Y.B. (2008). "Structural Performance of Concrete Confined with Hybrid FRP Composites." *Journal of Reinforced Plastics and Composites,* 27(12), 1323-1348.

Wu, H.L., Wang, Y.F., Yu, L., and Li, X.R. (2009). "Experimental and Computational Studies on High-Strength Concrete Circular Columns Confined by Aramid Fiber-Reinforced Polymer Sheets." *Journal of Composites for Construction,* 13(2), 125-134.

Wu, X., Ghaboussi, J., and Garrett, J.H. (1992). "Use of neural networks in detection of structural damage." *Computers and Structures,* 42(4), 649-659.

Wu, Y.F., Liu, T., and Oehlers, D.J. (2006). "Fundamental principles that govern retrofitting of reinforced concrete columns by steel and FRP jacketing." *Advances in Structural Engineering,* 9(4), 507-533.

Wu, Y.F., and Wang, L.M. (2009). "Unified Strength Model for Square and Circular Concrete Columns Confined by External Jacket." *Journal of Structural Engineering,* 135(3), 253-261.

Wu, Y.F., and Wei, Y.Y. (2010). "Effect of cross-sectional aspect ratio on the strength of CFRP-confined rectangular concrete columns." *Engineering Structures,* 32(1), 32-45.

Wu, Y.F., and Zhou, Y.W. (2010). "Unified Strength Model Based on Hoek-Brown Failure Criterion for Circular and Square Concrete Columns Confined by FRP." *Journal of Composites for Construction,* 14(2), 175-184.

Xiao, Q.G., Teng, J.G., and Yu, T. (2010). "Behavior and Modeling of Confined High-Strength Concrete." *Journal of Composites for Construction,* 14(3), 249-259.

Xiao, Y., and Wu, H. (2000). "Compressive behavior of concrete confined by carbon fiber composite jackets." *Journal of Materials in Civil Engineering,* 12(2), 139-146.

Yan, Z.H., and Pantelides, C.P. (2006). "Fiber-reinforced polymer jacketed and shape-modified compression members: II - Model." *ACI Structural Journal,* 103(6), 894-903.

Yan, Z.H., Pantelides, C.P., and Reaveley, L.D. (2006). "Fiber-reinforced polymer jacketed and shape-modified compression members: I - Experimental behavior." *ACI Structural Journal,* 103(6), 885-893.

Yazici, V., and Hadi, M.N.S. (2009). "Axial Load-Bending Moment Diagrams of Carbon FRP Wrapped Hollow Core Reinforced Concrete Columns." *Journal of Composites for Construction,* 13(4), 262-268.

Yazici, V., and Hadi, M.N.S. (2012). "Normalized Confinement Stiffness Approach for Modeling FRP-Confined Concrete." *Journal of Composites for Construction,* 16(5), 520-528.

Youssef, M.N., Feng, M.Q., and Mosallam, A.S. (2007). "Stress–strain model for concrete confined by FRP composites." *Composites Part B: Engineering,* 38(5), 614-628.

Zhang, S., Ye, L., and Mai, Y.W. (2000). "A study on polymer composite strengthening systems for concrete columns." *Applied Composite Materials,* 7(2-3), 125-138.